FATE OF CHLORINE IN INDOOR SWIMMING POOLS:
A NUMERICAL MODELLING APPROACH

by

Pedram Mahinpour

M.Sc., The University of Leeds, 2010

A THESIS SUBMITTED IN PARTIAL FULFILLMENT OF

THE REQUIREMENTS FOR THE DEGREE OF

MASTER OF APPLIED SCIENCE

in

THE COLLEGE OF GRADUATE STUDIES

(Mechanical Engineering)

THE UNIVERSITY OF BRITISH COLUMBIA

(Okanagan)

October 2014

Abstract

Swimming is one of the most popular recreational activities around the world. The interactions and activities of bathers during swimming may introduce contaminants which can lead to serious infections and health issues. There are a number of different techniques currently used to improve the sanitation in swimming pools. Some of the disinfectants commonly used in swimming pools include chlorine ozone and UV radiation. Chlorination is popular because it is simple, affordable and has residuals, but there is evidence that it may pose risks to human health as chlorine reacts with organic and inorganic matter in the water which generates disinfection by-products (DBPs). Extensive research has been performed on the kinetics of DBPs formation, and on the fate of chlorine in swimming pools. However, the effects of hydraulics in swimming pools have not been given the same level of attention. This thesis focuses on examining the fate of chlorine based on hydraulic behaviour in swimming pools. In this research, numerical simulations have been performed using computational fluid dynamics (CFD).

Three different scenarios have been studied to estimate the effects of inlet size on the distribution of chlorine in indoor swimming pools. The spatial distribution of chlorine and the mixing rates for chlorine are known to be significantly affected by the inlet size. In all three selected scenarios, after a period of two hours, the average concentration of chlorine in the swimming pool reached a constant level of approximately 60% of the maximum injected concentration. The simulation results suggest that, while the mass flow rate is constant, a smaller inlet size provides better mixing rates. The chemical reaction of chlorine with ammonia has been examined using random releases to mimic urine release in swimming pools. The results show that significant amounts of ammonia may not react with chlorine. This can be explained by the high stoichiometric ratio of the reacting components. Chlorine available for the reaction was found to be far less than the required amount. This research contributes towards improved understanding of the chlorination process in swimming pools. This research guides an improved indoor swimming pool design that can ensure better chlorine distribution and reduced DBPs formation, and thereby reduced human health risks.

Table of Contents

List of Tables

List of Figures

List of Abbreviations

CDC	U.S. Centre for Disease Control
CEL	CFX Expression Language
CFD	computational fluid dynamics
CSTR	completely stirred tank reactor
DBPs	disinfection by-products
DNS	Direct Numerical Solution
EDC	Eddy Dissipation Concept
FAC	Free Available Chlorine
HAA	Haloacetic acids
HAN	Haloacetonitrile
HOCl	hypochlorous acid
IDDF	Integrated Disinfection Design Framework
LES	Large Eddy Simulation
MCA	monochloramine
RANS	Reynolds-averaged Navier-Stokes methods
RNG	Re-Normalization Group
RTD	Residence Time Distribution
THM	Trihalomethanes
UV	Ultraviolet radiation

Acknowledgements

I would like to express my deep gratitude to my supervisor, Prof. Rehan Sadiq, not only for his technical advice but also for his inspiration and support through difficult times. Without his caring attention it would have been much more difficult for me to achieve my academic goals. I would also like to thank my colleague, Ms. Roberta Dyck, for her kind help and valuable advice throughout my research, and my friend and colleague Mohammad Rezainia who motivated me through thoughtful advices in long hours of discussion.

Many thanks also to my mother and father, for their generous and ongoing support. Finally, I am deeply grateful for the indescribable patience of my wife, Mania. Without her support I could never have accomplished this undertaking.

Chapter 1: Introduction

1.1 Background

Swimming is one of the most popular recreational activities around the world. Statistics Canada (2013) categorized swimming among the top ten favourite activities in Canada. However, the interactions and activities of bathers during swimming may introduce contaminants into the pool including microorganisms (e.g., viruses, bacteria, and protozoa), which can lead to serious infections. A number of prevention techniques are commonly used to improve the sanitation in swimming pools and the most common disinfectants include chlorine, UV radiation, and ozone.

Chlorination is a widely used method for disinfecting drinking water and approximately 90% of Canada's water supply system is treated in this way (Health Canada, 2009). Chlorination has long been used as a popular disinfection method for swimming pools as well, due to its affordability and the simplicity of chlorine application. Nevertheless, chlorination may pose some risks to human health. In the process of disinfection, reactions with organic and inorganic matter in the water can generate disinfection by-products (DBPs) that may pose health risks. Numerous studies on DBPs formation have reported an adverse impact on human health (Erdinger, et al., 2004; Bernard et al., 2006; Nemery, Hoet, & Nowack, 2002). One of the major challenges in the treatment of swimming pool water is the necessity to reduce the introduction and production of organic compounds in order to reduce the formation of DBPs.

The efficiency of chlorination depends on several factors, including the concentration of organic matter, pH levels, temperature of the water, and the residual concentration of chlorine (National Collaborating Centre for Environmental Health [NCCEH] 2014). To maximize the efficiency of chlorination, and to minimize the generation of DBPs, an understanding of the disinfection process is crucial. Most of the research that examines the formation and fate of DBPs in swimming pools proceeds on the assumption that the pool acts as a completely stirred tank reactor (CSTR) (Cloteaux, Gérardin, & Midoux, 2013; Dyck, Sadiq, Rodriguez, Simard, & Tardiff, 2011). A CSTR is an ideal reactor where reactants and products are well mixed and uniformly distributed throughout the domain. In the case of a swimming pool, essentially a large reactor, the assumption about this hydraulic behaviour can be misleading. Realistically, the

concentration and distribution of chemical components is expected to be dependent on the hydraulic characteristics of the pool, characteristics which are not uniform and more closely resemble plug flow conditions.

1.2   Research motivation

In order to maximize the efficiency of chlorination, the concentration of chlorine should be maintained at adequate levels with a uniform distribution throughout the swimming pool. A common method for analyzing hydraulics in chemical reactors is the Residence Time Distribution (RTD) which predicts the length of time for a particle to exit the outlet after its entry from the inlet. The RTD method assumes that concentration at the outlet is the same as the domain, and it ignores the spatial distribution of the particles. As with any non-ideal reactor, the hydraulic characteristics of swimming pools may play a significant role in determining the path of the particles.

In some studies (e.g., Cloteaux et al., 2013), the RTD method has been combined with computational fluid dynamics (CFD) simulation to model the hydraulic behaviour of the swimming pool (Angeloudis, Stoesser, & Falconer, 2014). Since the RTD method is based on particle tracking, the Lagrangian method is applied to estimate the time lapse. This method raises two important issues for chlorination: First, chlorine is soluble in water and is therefore a continuous fluid rather than one that is segregated into particles; this indicates that the Lagrangian method may be an inappropriate way to measure the reaction. Second, with respect to the distribution of chlorine, while the concentration of chlorine at the outlets can be equal to the average concentration in the domain, the spatial and temporal concentration of chlorine is not uniform. For a non-ideal reactor like a swimming pool, the hydraulic characteristics of the domain are expected to dictate the distribution and concentration of chlorine and, consequently, the formation and distribution of DBPs.

Computational fluid dynamics can provide insight about the domain in ways that may not be possible through experimental and pilot investigations. A few studies have reported on the hydraulic behaviour of swimming pools and its effect on the chlorination process (Liu & Ducoste, 2006; Cloteaux et al., 2013). However, to our knowledge, there are no studies that have examined the spatial and temporal distribution of chlorine.

2

The primary motivation for this research is to simulate fluid behaviour numerically, and determine the fate of chlorination in a typical indoor swimming pool. These results will help engineers enhance the efficiency of the disinfection process, and thereby improve the design and operation of swimming pools. These results will also contribute to the development of best management practices and guidelines for indoor swimming pools in public places. Furthermore, there is not a universal agreement for required level of chlorine in swimming pools and each country follows different guidelines. These results will help to find a better understanding on distribution and fate of chlorine, hence improve guidelines on required optimum level of free chlorine.

1.3   Research objectives and methodology

The primary objective of this research is to better understand the fate of chlorine and associated DBPs using hydraulic and kinetic modelling through CFD approach, with an ultimate aim of optimizing the design of swimming pools. This study uses the Eulerian approach to simulate the distribution and fate of chlorine for a "typical indoor swimming pool."

The problem has been divided into two stages: First, to study the effects of inlet size on the distribution of chlorine and second, to predict the behaviour of chemical reactions between chlorine and ammonia during one *turnover* period, i.e., the time required to re-circulate the entire pool water one time. Nitrogen compounds, especially urea, are precursor for chloramines (Schmalz, Frimmel, & Zwiener, 2011). All of the scenarios were solved under transient conditions. However, for the sake of simplicity in this study, only ammonia and chlorine were introduced as reaction partners or reactants. All simulations were performed under transient conditions. To simulate the chemical reaction, the Eddy Dissipation Concept (EDC) was applied. This method considers the hydraulic behaviour (turbulence) of flow and chemical reaction kinetics at the same time. Furthermore, to make the simulation closer to real-world operating conditions in the swimming pool, ten vertical cylinders were placed in the domain at random locations to represent swimmers and simulate the effect of their motion on the mixing rate in the pool. CFX solver software from the ANSYS package version 14.5 (ANSYS 2012) was used for the 3D modelling. These research results will help improve the design of chlorination delivery

systems in swimming pools, and assist in the development of best management practices for indoor public pools.

In risk assessment of swimming pools different uncertainties may arise. One source of uncertainty may be the multiplicity of chemical reactions that occur in the pool water. Each reaction can be affected by swimming pool conditions –such as water temperature, pH, turnover period and etc._- as well as presence of different chemical components that are introduced by bathers and may vary significantly from pool to another. In order to reduce source of uncertainties in this study only the chemical reaction between ammonia and chlorine has been considered. This will help to isolate generation of chloramines from other source of reactions and helps to study fate of chlorine due to this specific chemical reaction.

1.4 Thesis outline

This thesis is organized into five chapters. Chapter 1 introduced the research problem; Chapter 2 provides a brief review of the literature as it concerns the chlorination process, DBPs formation, and CFD modelling; Chapter 3 outlines the problem and describes the proposed methodology of this research; Chapter 4 outlines and discusses the results for the different simulation scenarios; Chapter 5 presents the conclusions, offers recommendations for future research as it relates to the design of swimming pool design, and also addresses best management practices for the maintenance and operation of swimming pools.

Chapter 2: Literature Review

2.1   Chlorination and related disinfection by-products (DBPs)

A wide range of contaminants, including microorganisms, can be found in swimming pools. These contaminants enter into the system through swimmers or source water, and some of the microorganisms (pathogens) can lead to serious infections (Florentin, Hautemaniere, & Hartemann, 2011; Weaver et al., 2009). Disinfection is required to inactivate the pathogens and thereby to prevent a potential hazard to swimmers. Chlorination, one of the common methods for disinfecting swimming pools, is a process that involves adding chlorine gas, sodium, calcium, or lithium hypochlorite to the water to form hypochlorous acid (HOCl), which is a very strong disinfectant. HOCl then dissociates in the water as follows:

$$\underset{\text{(hypochlorous acid)}}{\text{HOCl}} \leftrightarrow \underset{\text{(hydrogen ion)}}{\text{H}^+} + \underset{\text{(hypochlorite ion)}}{\text{OCl}^-} \qquad \textbf{Reaction 2.1}$$
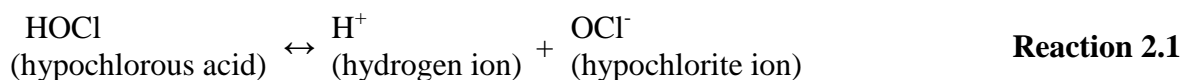
The rate of dissociation of HOCl depends on the pH levels as well as the temperature of the water. The rate of dissociation increases at a higher pH and, since HOCl is a stronger disinfectant than the hypochlorite ion, it is advisable to maintain pH at lower levels. The World Health Organization [WHO] (2006) advises that pH levels should be in the range 7.2-7.8.

The mixture of hypochlorite ions (OCl^-) and hypochlorous acid (HOCl) is known as the Free Available Chlorine (FAC). Ammonia (NH_3) is a contaminant that can be introduced into swimming pools by way of perspiration and urine from bathers and the reaction between chlorine and ammonia generates chloramines (combined chlorine). The concentration of free chlorine gradually decreases as it reacts with contaminants and other chemicals. To maintain an adequate capacity, the hypochlorous acid needs to be added constantly. There is no universal agreement about the optimum level of free chlorine, although various ranges have been recommended in different jurisdictions (WHO, 2006). Table 2.1 (below) sets out the Canadian guidelines (Health Canada, 2006) for free chlorine concentration in various jurisdictions (following from the National Collaborating Centre for Environmental Health [NCCEH]—an amount which varies from 0.5 to 5 *mg/L* from province to province. In some provinces, the recommended level of free chlorine is as high as 10 *mg/L* to be administered at least once a day in the absence of swimmers

(NCCEH, 2014). Periodic increase of the chlorine concentration up to 10 *mg/L* results in complete disinfection and reduces the potential for side effects. The U.S. Centre for Disease Control (CDC, 2012) recommends 2-4 ppm (*mg/L*) with a maximum concentration of 5 ppm (*mg/L*) when bathers are present.

Table 2.1: Recommended chlorine concentration in indoor swimming pools in various jurisdictions within Canada (modified after NCCEH 2014).

Province/Territory	Free Available Chlorine (ppm, mg/L)	Combined Available Chlorine (ppm, mg/L)
British Columbia	Min. 0.5 if ≤ 30°C ; Min. 1.5 if > 30°C	Less than 1.0
Ontario	Min. 0.5; Min 1.0 if cyanuric acid is used	None
Saskatchewan	Min. 2.0	None
Yukon Territory	Min. 0.5 if ≤ 30°C; Min 1.0 if > 30°C	< 1.0
Nunavut	Show a residual as close to 1.2 as possible, should fall between 1.0 and 1.5 inclusive	Less than 2.5
Northwest Territories	Show a residual as close to 1.2 as possible, should fall between 1.0 and 1.5 inclusive	Less than 2.5 < 0.5
Newfoundland & Labrador	[0.5-1.5] Should not be greater than 5 when bathers present	Less than 0.5
Alberta	Min. 1.0 if ≤ 30°C; Min. 2.0 if > 30°C	None
Prince Edward Island	[1.0-3.0]	None
Quebec	[0.8-2.0]	Less than 0.5
Manitoba	[1.0-5.0]	Less than 1.5
New Brunswick	No guideline or legislation accessed	None
Nova Scotia	[1.0-2.0]	Not legislated

Although chlorination is effective and widely used, the reaction between chlorine and organic compounds released from bathers results in the production of undesirable DBPs (Rook, 1977). More than 600 DBPs have been identified in drinking water, and some of these are also commonly found in swimming pools (Zwiener et al., 2007; Richardson, Plewa, Wagner, Schoeny, & DeMarini, 2007; Richardson et al., 2010). A number of studies indicate that chlorination in swimming pools has the potential for adverse effects on human health, including asthma and respiratory ailments (Bernard, Nickmilder, & Voisin, 2008; Bernard, Carbonnelle, de Burbure, Michel, & Nickmilder, 2006; Levesque et al., 2006). Concentrations of DBPs are highly dependent on pool conditions, which tend to vary from one study to another. These variable conditions include the type of organics, water temperature, pH levels, and the rate of water exchange (Zwiener et al., 2007; Chowdhury, Al-Hooshani, & Karanfil, 2014). In general, major classes of DBPs due to chlorination are as follows: Trihalomethanes (THMs), Haloacetonitrile (HAN), and Haloacetic acids (HAA). See Table 2.2 (Sadiq & Rodriguez, 2004).

Chloramines are chemicals that may be produced when the hypochlorous acid reacts with nitrogen compounds such as ammonia (Jafvert & Valentine, 1992; Vikesland et al., 2001; Qiang & Adams, 2004). Although some chloramines can be used for disinfection of drinking water, they are also formed during chlorine disinfection in swimming pools due to nitrogenous compounds introduced by swimmers (Lian, Yue, Li and Blatchley, 2014; Richardson, 2010; Weng and Blatchley 2011; Weaver et al.2009). While the use of the term "disinfection byproduct" when referring to chloramines is less common in drinking water because it is also used as a disinfectant, many researchers in swimming pool water quality consider them to be disinfection byproducts in swimming pools (Lian, Yue, Li and Blatchley, 2014; Richardson, 2010; Weng and Blatchley 2011; Weaver et al.2009; Catto et al., 2012; Chowdhury, Alhooshani, Karanfil; 2014; Florentin, Hautemanière, Hartemann, 2011). Nitrogen trichloramine particularly has been linked with a number of undesirable health symptoms in bathers (such as asthma) (WHO, 2006; Carbonnelle et al., 2002; Thickett, McCoach, Gerber, Sadhra, & Burge, 2002; Bernard et al., 2003). This research has focused on the generation of chloramines, discussed in detail in the following section.

Table 2.2: Important groups of DBPs produced using different types of disinfectants.
(modified after Sadiq & Rodriguez, 2004)

Class of DBP's	Common Example	Chlorine	Ozone	ClO$_2$	Chloramines
Trihalomethanes (THM)	Chloroform	✔	✔		✔
Other Haloalkanes		✔			
Haloalkenes		✔			
Haloacetic Acids (HAA)	Chloroacetic Acid	✔			✔
Haloaromatic Acids		✔			
Other Halomonocarboxylic acids		✔			✔
Unsaturated Halocarboxylic acids		✔			✔
Halodicarboxylic acids		✔			✔
Halotricarboxylic acids		✔			
MX and analogues		✔		✔	✔
Other halofuranones		✔			
Haloketones		✔	✔	✔	
Haloacetonitrile (HAN)	Chloroacetonitrile	✔	✔		
Other halonitrile	Cyanogen Chloride	✔			✔
Haloaldehyde	Chloro hydrate	✔			✔
Haloalcohols		✔			✔
Phenols	2-Chlorophenol	✔	✔		
Halonitromethane	Chloropicrin	✔			
Inorganic Compounds	Bromated, hypobromite		✔	✔	
Aliphatic aldehyde	Formaldehyde	✔	✔	✔	
Other aldehydes		✔	✔	✔	
Ketones (aliphatic and aromatic)	Acetone	✔	✔	✔	
Carboxylic Acids	Acetic acid	✔	✔	✔	
Aromatic Acids	Benzoic acid	✔	✔	✔	
Aldo and ketoacids			✔	✔	
Hydroxy acids		✔	✔		
Other		✔	✔	✔	✔

2.2   Chloramines

There has been extensive research to examine the chemical reactions related to the formation of chloramines. Chloramines include monochloramine (NH$_2$Cl), dichloramine (NHCl$_2$), and trichloramine (NCl$_3$) all of which can be generated from reaction of chlorine and nitrogen

compounds in swimming pools. Impurities that contain nitrogen can be introduced into swimming pools by urine from bathers. Urea, a nitrogen compound, is a major constituent of urine; the other nitrogen compounds in urine include ammonia, ammonia acids, creatinine, and uric acid (White, 1986).

Schmalz et al. (2011) investigated formation of trichloramine in swimming pools as a DBP of the reaction between hypochlorous acid and urea. Research indicates that this DBP may lead to a number of health risks (e.g., asthma) in bathers (WHO, 2006; Carbonnelle et al., 2002; Thickett et al., 2002; Bernard et al., 2003). This research focused specifically on the formation of chloramines, which is discussed in detail in the following section. Schmalz et al. (2002) examined hypochlorous acid reactions but ignored the intermediate reactions (Reaction 2.2):

urea + HOCl → NCl_3 **Reaction 2.2**

A pseudo first order reaction rate constant was determined to be 4.58×10^{-6} s^{-1}, where the concentrations of urea and hypochlorous were 3.3×10^{-5} *mol/L* and 1.13×10^{-5} *mol/L*, respectively (Cl/N = 0.17; pH = 6.9; T = 30°C). Schmalz et al. (2011) found that only 4% of the urea nitrogen was converted into trichloramine, taking 75 hours to consume all of the chlorine available for the reaction. They also proposed that, under real conditions in swimming pools, where the ratio of available chlorine to nitrogen (Cl/N) is 0.15, less than 1% of the urea nitrogen is converted into trichloramine and noted that no significant decrease in the urea concentration would occur. Their results were in line with those of Blatchley and Cheng (2010). In other words, although urea can react with hypochlorous acid, it reacts too slowly to contribute significantly to the generation of chloramines within one turn-over period.

Urine also contains ammonia (NH_3), another nitrogen compound that can be found in swimming pools. Numerous studies have looked at reaction between ammonia and trichloramine. A number of these were summarized by Jafvert and Valentine (1992), and by Vikesland, Ozekin, & Valentine (2001). Table 2.2 below shows the reaction stoichiometry and related rate coefficients (Jafvert & Valentine, 1992; Vikesland et al., 2001). The chemical reactions shown in Table 2.3 can be simplified as follows (Qiang & Adams, 2004):

$$\text{HOCl} + \text{NH}_3 \rightarrow \text{NH}_2\text{Cl} + \text{H}_2\text{O} \qquad \textbf{Reaction 2.3}$$

$$\text{HOCl} + \text{NH}_2\text{Cl} \rightarrow \text{NHCl}_2 + \text{H}_2\text{O} \qquad \textbf{Reaction 2.4}$$

$$\text{HOCl} + \text{NHCl}_2 \rightarrow \text{NCl}_3 + \text{H}_2\text{O} \qquad \textbf{Reaction 2.5}$$

These three competitive reactions lead to the formation of trichloramine. The reaction rate constants for each of the above reactions have been studied by different researchers with some variation in the results. For instance, Qiang and Adams (2004) looked at the rate constant of monochloramine formation (Reaction 2.2) and found the Arrhenius relation to be $k_{[HOCl][NH3]} = 5.40 \times 10^9 \exp(-2237/T)$, while Isaac and Morris (1983) proposed $k_{[HOCl][NH3]} = 6.6 \times 10^8 \exp(-1510/T)$.

Qiang and Adams (2004) studied the mechanism of Reaction 2.2 (above) with respect to the formation of monochloramine (NH_2Cl) and recorded the following intermediate reactions:

$$\text{HOCl} + \text{NH}_4^+ \rightarrow \text{NH}_2\text{Cl} + \text{H}_2\text{O} + \text{H}^+ \qquad \textbf{Reaction 2.6}$$

$$\text{OCl}^- + \text{NH}_3 \rightarrow \text{NH}_2\text{Cl} + \text{OH}^- \qquad \textbf{Reaction 2.7}$$

$$\text{OCl}^- + \text{NH}_4^+ \rightarrow \text{NH}_2\text{Cl} + \text{H}_2\text{O} \qquad \textbf{Reaction 2.8}$$
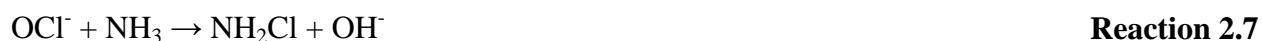
They proposed that the reactivity of NH_4^+ is negligible and can be ignored. Reaction 2.3 was studied by Deborde and Von Gunten (2008), based on a study by Isaac and Morris (1983); the second order reaction rate of monochloramine and hypochlorous acid was found to be 2.7×10^2 M^{-1} s^{-1}. Despite the conflicting results for the reaction rates, it was agreed that the reaction rate of Reaction 2.3, 2.4, and 2.5 is much faster than Reaction 2.2. This suggests that ammonia has a significantly higher contribution to the generation of NCl_3 in comparison with urea in short term, i.e. one turn-over period.

Table 2.3: Chloramine reaction model (modified after Jafvert and Valentine, 1992).

Reaction Stoichiometry	Rate Expressions	Rate Coefficients/Equilibrium (T=25°C)
1. $HOCl+NH_3 \rightarrow NH_2Cl+H_2O$	$K[HOCl][NH_3]$	$K = 1.5 \times 10^{10} \, M^{-1}h^{-1}$
2. $NH_2Cl+H_2O \rightarrow HOCl+NH_3$	$K[NH_2Cl]$	$K = 7.6 \times 10^{-2} \, M^{-1}h^{-1}$
3. $HOCl+NH_2Cl \rightarrow NHCl_2+H_2O$	$K[HOCl][NH_2Cl]$	$K = 1.0 \times 10^6 \, M^{-1}h^{-1}$
4. $NHCl_2+H_2O \rightarrow HOCl+NH_2Cl$	$K[NHCl_2]$	$K = 2.37 \times 10^{-3} \, h^{-1}$
5. $NH_2Cl+NH_2Cl \rightarrow NHCl_2+NH_3$	$K[NHCl]^2$	$K = k[H^+]+k[H_2CO_3] +k[HCO_3^-]$ $k[H+] = 2.5 \times 10^7 \, M^{-2}h^{-1}$ $k[H_2CO_3] = 2.7 \times 10^3 \, M^{-2}h^{-1}$ $k[HCO_3^-] = 2.95 \times 7.2 \, M^{-2}h^{-1}$
6. $NHCl_2+NH_3 \rightarrow NH_2Cl+NH_2Cl$	$K[NHCl_2][NH_3][H^+]$	$K = 2.16 \times 10^8 \, M^{-1}h^{-1}$
7. $NHCl_2+H_2O \rightarrow I^a$	$K[NHCl_2][OH^-]$	$K = 4 \times 10^5 \, M^{-1}h^{-1}$
8. $I+NHCl_2 \rightarrow HOCl+products^b$	$K[I][NHCl_2]$	$K = 1.0 \times 10^8 \, M^{-1}h^{-1}$
9. $I+NH_2Cl \rightarrow products$	$K[I][NH_2Cl]$	$K = 3.0 \times 10^7 \, M^{-1}h^{-1}$
10. $NH_2Cl+NHCl_2 \rightarrow products$	$K[NH_2Cl][NHCl_2]$	$K = 55.0 \, M^{-1}h^{-1}$
11. $HOCl+NHCl_2 \rightarrow NCl_3+H_2O$	$K[NHCl_2][HOCl]$	$K = 2.16 \times 10^{10}[CO_3^{2-}]+3.24 \times 10^8[OCl^-] + 1.18 \times 10^{13}[OH^-]$
12. $NHCl_2+NCl_3+2H_2O \rightarrow 2HOCl$ + products	$K[NHCl_2][NCl_3][OH^-]$	$K = 2.0 \times 10^{14} \, M^{-2}h^{-1}$
13. $NH_2Cl+NCl_3+H_2O \rightarrow HOCl$ + products	$K[NH_2Cl][NCl_3][OH^-]$	$K = 5.0 \times 10^{12} \, M^{-2}h^{-1}$
14. $NHCl_2+2HOCl+H_2O \rightarrow NO_3^- +5H^+ +4Cl^-$	$K[NHCl_2][OCl^-]$	$K = 8.3 \times 10^5 \, M^{-1}h^{-1}$

a: I is the unidentified monochloramine auto-decomposition intermediate
b: products may include N_2, H_2O, Cl^-, H^+, NO_2^-

Another key factor in the formation of trichloramine is the ratio of the concentration of FAC to nitrogen (Qiang & Adams, 2004; Schmalz et al., 2011). The weighted ratio of ammonia, nitrogen, and FAC can generally be used to predict the risk of trihalomethanes and haloacetic acid formation (Qiang & Adams, 2004).

All of the above studies considered reactions under the conditions of a CSTR, where reactants are assumed to be well mixed and homogenously distributed. However, this assumption may not be based on the real conditions in swimming pools where a higher concentration of chlorine is introduced by way of inlets that feed into the domain of the pool. As the concentrated chlorine moves through the domain and mixes with the pool water the concentration gradually decreases. Meanwhile, when high concentrations of ammonia react with chlorine, all of the chlorine reacts with only a portion of the ammonia. As the ammonia continues mixing with the water, it reacts only with that part of the chlorine which the ammonia contacts. In other words, the concentration of free chlorine may vary to a high extent spatially, depending on the hydraulic behaviour of the pool water and the available mixing rate. Thus, chemical reactions on the molecular scale are governed by the large scale fluid motion in the swimming pool. This study proposes that, to thoroughly understand the process of disinfection, a comprehensive investigation of the fluid behaviour of swimming pool water is necessary. Precise studies—using CFD—are required in order to model the chemical reactions in the turbulent flow characteristic of swimming pools.

2.3   Computational fluid dynamics (CFD)

Equations to describe fluid motion were originally proposed in the 1840s by Claude-Louis Navier and George Gabriel Stokes. Up until now, no analytical solution has been found for the Navier-Stokes equations. However, more recently, advances in computer science have provided a way of solving these equations numerically by way of computational fluid dynamics (CFD).

CFD has been identified as a tool with the potential to improve the design and efficiency of water purification and treatment units. Greene, Farouk, and Haas (2004) used CFD to study various chlorination processes. They compared their results to the more traditional methods for analyzing these processes, particularly the Integrated Disinfection Design Framework (IDDF). They argued that the IDDF method assumes the reactor (swimming pool) to be an ideal macrofluid in which the components are well mixed, and they pointed out that this assumption was misleading, especially with respect to the large fluid domain of the swimming pool. They also argued that the IDDF is not capable of taking the structure of the reactor into account and proposed that CFD simulations can overcome these issues due to their capability for applying the Navier-Stokes equations to more precisely predict the flow at any point in the domain.

2.3.1 Governing equations

The governing equations that describe the flow in a swimming pool, include the continuity equation, the Navier-Stokes equations (momentum equations), and the energy equation. These equations can be derived by taking into account the conservation laws of physics over a volume of fluid. The general differential equation for the conservation of linear momentum is as follows:

$$\frac{\partial}{\partial t}(\rho V) + \nabla \cdot (\rho V V) = \rho g + \nabla \cdot \sigma_{ij} \qquad \textbf{Equation 2.1}$$

where ρ is density, g is gravity, σ_{ij} is shear stress tensor, and V is the velocity vector. For a Newtonian fluid, where the shear stress and velocity gradient have a linear relationship, it can be stated as follows:

$$\tau_{ij} = \mu \left(\frac{\partial v_i}{\partial x_j} + \frac{\partial v_j}{\partial x_i} \right) \qquad \textbf{Equation 2.2}$$

where μ is the shear viscosity, x is the spatial coordinate, v is velocity, and τ_{ij} is the viscous stress tensor or deviatoric stress tensor. Combining the above equation with thermodynamic pressure (P), the total shear stress tensor (σ_{ij}) is defined as follows:

$$\sigma_{ij} = -P\delta_{ij} + \mu \left(\frac{\partial v_i}{\partial x_j} + \frac{\partial v_j}{\partial x_i} \right) \qquad \textbf{Equation 2.3}$$

where δ_{ij} is 1, if $i = j$ and zero otherwise. Inserting Equation 2.3 into Equation 2.1, the general equation for Newtonian incompressible flow with constant viscosity (known as the Navier-Stokes equation) can be written as follows:

$$\rho \frac{D \vec{V}}{D t} = -\vec{\nabla} P + \rho \vec{g} + \mu \nabla^2 \vec{V} \qquad \textbf{Equation 2.4}$$

In Equation 2.4, we have four unknowns, and three components of velocity and pressure. To solve this equation, another equation is required—a continuity equation. For an incompressible fluid, the continuity equation is as follows:

$$\frac{\partial u}{\partial x} + \frac{\partial v}{\partial y} + \frac{\partial w}{\partial z} = 0 \qquad \textbf{Equation 2.5}$$

In cases where there are chemical reactions, an axillary equation is required in order to model the mass fraction of chemical components. The transport (conservation) equation for reacting species i, is as follows:

$$\frac{\partial c_i}{\partial t} + u_j \frac{\partial c_i}{\partial x_j} = D \frac{\partial^2 c_i}{\partial x_j^2} + r_i$$

Equation 2.6

In this equation, c_i is the species concentration. In this case, the first and second terms on the left side of the equation correspond to the rate of change of mass fraction and flux due to convection by the flow field. The first term on the right side corresponds to diffusion, where D is molecular diffusivity, and r_i is the rate of generation of the species c_i.

2.3.2 Turbulence

Fluid motions are categorized as either laminar or turbulent flow. Laminar flow refers to a fluid motion that is smooth and follows an orderly pattern, while turbulent flow is highly disordered and includes vorticity in all length scales. There is no agreement on an exact definition for turbulence, but it can be defined as the region where properties of the fluid are chaotic and change rapidly. In particular, in turbulent flow, pressure and velocity change rapidly in time and space. Laminar and turbulent regimes can be distinguished by the Reynolds number (Wilcox, 1998). In real-world problems, most flows are turbulent. Turbulence modelling has been the subject of numerous investigations and different approaches have been proposed, according to the following categories:

- Direct Numerical Solution (DNS)
- Large Eddy Simulation (LES)
- Reynolds-averaged Navier-Stokes methods (RANS)

Some of these approaches are explained briefly below.

2.3.2.1   DNS and LES methods

Direct Numerical Simulation (DNS) solves the Navier-Stokes equation for unsteady motion of all scales. In this method, all of the fluid motion from the smallest to highest scales should be solved (Pope, 2000). Some attempts have been made to apply the DNS method to solve

multiphase flow. However, this method requires very small meshes and a high performance computing facility as yet unavailable for solving industrial problems. Instead, some simplifying assumptions can be made to solve the turbulent flow fields.

Turbulent flow contains eddies with different length scales. The behaviour of large-scale eddies depends on geometry and flow field, while small-scale eddies are independent from flow field and behave in a statistically similar way. In other words, small-scale eddies are isotropic and have universal behaviour. Based on this assumption, Large Eddy Simulation (LES) has been used to modify the DNS method, where the main assumption is that small-scale eddies always behaves in a similar and predictable way. Therefore, the unsteady features of turbulent flow are only resolved for large-scale eddies, and small-scale eddies are modelled by applying a spatial or temporal filtration to the Navier-Stokes equations (Pope, 2000; Sagaut, 2000). A few studies, including that conducted by Wang and Falconer (1998), have applied the LES method to simulate flow in drinking water treatment plants and conclude that, while this method is more accurate than other methods, the time and CPU costs are higher. Despite the accuracy of DNS, it only resolves the behaviour of large eddies and would not be of appropriate for the micromixing model (discussed below). Consequently, other methods were evaluated in order to find those most appropriate for turbulence modelling, including the Reynolds-averaged Navier-Stokes (RANS).

2.3.2.2   RANS methods

The RANS methods are based on the Reynolds decomposition, which proposes that turbulent flow quantities can be divided into two parts: a fluctuating part and a time-averaged part. For example, the velocity components can be described as follows:

$$u = \bar{u} + u'$$ <div style="text-align:right">**Equation 2.7a**</div>

$$v = \bar{v} + v'$$ <div style="text-align:right">**Equation 2.7b**</div>

$$w = \bar{w} + w'$$ <div style="text-align:right">**Equation 2.7c**</div>

where $\bar{u}$, $\bar{v}$, and $\bar{w}$ correspond to the averaged part; and u', v', and w' correspond to the fluctuating part.

When we insert Equations 2.8a-2.8c along with the pressure decomposition into the Navier-Stokes Equations, we have the following:

$$\rho \frac{\mathrm{D}\vec{V}}{\mathrm{D}t} = -\vec{\nabla}P + \rho\vec{g} + \mu\nabla^2\vec{V} + \rho\vec{\nabla}\cdot\left(\tau_{ij,\,turbulent}\right)$$
Equation 2.8

The last term on the right side of the equation above is the specific Reynolds stress tensor and is specified as follows:

$$\tau_{ij,\,turbulent} = -\begin{bmatrix} \overline{u'^2} & \overline{u'\,v'} & \overline{u'\,w'} \\ \overline{u'\,w'} & \overline{v'^2} & \overline{v'w'} \\ \overline{u'\,w'} & \overline{v'\,w'} & \overline{w'^2} \end{bmatrix}$$
Equation 2.9

Reynolds stress is symmetric and, consequently, the above matrix describes six unknowns (Cimbala & Cengel, 2006). In order to identify these unknowns a number of turbulence models have been proposed: one equation, two equation, algebraic, and Reynolds stress turbulence models. In particular, the two equation models, k-ε and k-ω, are popular (Versteeg & Malalasekera, 1995). Here, two additional transport equations must be solved simultaneously, along with the governing equations, in order to find k (turbulent kinetic energy), and ε (turbulent dissipation rate) or ω (specific dissipation), from which the specific Reynolds stress tensor can be defined. The k-ε model can be formulized in two ways: RNG and Standard k-ε. Liu and Ducoste (2006) studied the impact of turbulence models on the ability to predict chlorine decay by comparing standard k-ε, RNG k-ε, and k-ω. They found that the k-ε models were more accurate in comparison with the k-ω model. Their findings agreed with those of Wang and Falconer (1998). Since the RNG k-ε model can handle variation in the Reynolds number through the domain, Cloteaux et al. (2013) found it to be a suitable model for examining swimming pool turbulence. See Appendix A for a detailed discussion of the k-ε method.

2.3.3 Turbulent mixing and the eddy dissipation concept (EDC)

Turbulent flow is composed of "eddies" of different sizes. Inducing a high velocity stream into the domain creates a velocity gradient that produces large eddies. The large eddies lose energy as they break into smaller eddies, and this energy cascade down to the smaller eddies continues to

the stage where the small eddies are affected by molecular diffusion, and the viscosity acts to dissipate the turbulent energy.

The process of turbulent mixing can be divided into three levels: macromixing, mesomixing, and micromixing (Baldyga & Pohorecki, 1995). Mixing at the largest scale, i.e., the entire reactor is identified as macromixing, and this level of mixing dictates the mean distribution of concentration over the domain. In the macromixing process, large eddies (produced by the main stream flow) conduct fluid and define the environment for mesomixing and micromixing. The second level, mesomixing, is an intermediate stage between macromixing and micromixing. Mesomixing, which corresponds to the inertial-convective deformation of fluid, is followed by micromixing, which consists of viscous-convective deformation. Molecular diffusion is a dominant feature of the mixing process at this level, and this stage has a high impact on fast chemical reactions (Baldyga & Pohorecki, 1995; Bałdyga, Bourne, & Hearn,1997). In infinitely fast chemical reactions, mixing is localized between unmixed clumps and their surroundings, at a scale where viscosity and molecular diffusion are important. In such cases, the reaction rate is limited by the turbulence characteristics and should be expressed as a direct function of k and ε (Hannon, Hearn, & Marshall, 1998; Liu & Barkelew, 1986; Pohorecki & Bałdyga, 1983; Hjertager, Hjertager, & Solberg, 2002).

The Eddy Dissipation Concept (EDC) was originally proposed by Magnussen and Hjertager (1976) to describe combustion reactions by relating the reaction time scale to the local dissipation of turbulent eddies. Consider an irreversible reaction with an infinite reaction rate as follows:

Reaction 2.10

1kg A + *s kg* B → (*1+s*) *kg* C
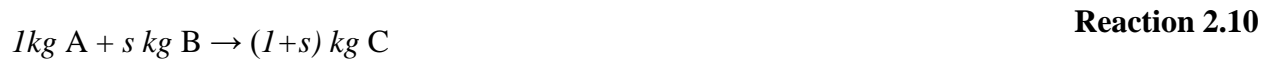
Replacing the concentration in Equation 2.7 by mass fraction, and adding turbulent diffusivity (D_T) to molecular diffusivity, the transport equation for species A can be written as follows:

$$\frac{\partial\left(\rho Y_A\right)}{\partial t} + u_j \frac{\partial\left(\rho Y_A\right)}{\partial x_j} = \frac{\partial}{\partial x_j}\left(D_{tot}\frac{\partial\left(\rho Y_A\right)}{\partial x_j}\right) + R_A$$

Equation 2.11

17

$$D_{tot} = D + D_T \qquad\qquad\qquad\qquad\qquad \textbf{Equation 2.12}$$

$$D_T = \frac{\mu_t}{\rho \, Sc_T} \qquad\qquad\qquad\qquad\qquad \textbf{Equation 2.13}$$

Sc_T is the turbulent Schmidt number. In the same way, the mass fraction of the mixture is:

$$\frac{\partial(\rho Y_M)}{\partial t} + u_j \frac{\partial(\rho Y_M)}{\partial x_j} = \frac{\partial}{\partial x_j}\left(D_{tot} \frac{\partial(\rho Y_M)}{\partial x_j} \right) \qquad \textbf{Equation 2.14}$$

For fast chemical reactions, according to the EDC model, the reaction rate is limited by micromixing and must be related to the rate of dissipation of turbulent kinetic energy. The reaction rate for species A, in its general form, can be expressed as (Magnussen & Hjertager, 1976):

$$R_A = -A \, \rho \, \frac{\varepsilon}{k} \, \min\left(Y_A, \frac{Y_B}{s}, \frac{Y_C}{1+s} \right) \qquad\qquad \textbf{Equation 2.15}$$

For liquid reactions, the dissipation of product C does not have to be considered. *A* is an empirical constant and varies from 1 to 5 with a nominal value of 2.5 (Liu & Ducoste, 2006); for liquid reactions the suggested value is 1 (Hjertager et al., 2002). The chemical reaction between chlorine and ammonia is instantaneous, with the micromixing stage having the dominant role. For these reasons, the EDC is used in this research to model the chemical reaction, and Equations 2.12 and 2.16 are modified for the purpose of this study (discussed below).

Chapter 3: Problem Formulation and Research Methodology

The CFD modelling process consists of three stages: pre-processing, solving, and post-processing (American Institute of Aeronautics and Astronautics [AIAA], 1998). The first step in the stage of pre-processing is to define the geometry, after which the geometry is to be segregated into smaller fragments called mesh (grid). This is followed by setting up the problem according to the following steps (National Aeronautics and Space Administration [NASA], 2008):

- flow conditions
- initial conditions
- marching strategy
- algorithms
- turbulence model
- chemistry model
- flux model
- boundary conditions

The next stage in the CFD modelling process is that of solving (iteration) during which the iterative convergence should be examined by monitoring the residuals. If the iterative residual does not converge, the problem set-up should be modified. The final stage, post-processing, involves the examination of grid convergence (mesh independency) and solution consistency, as well as looking at the results.

For transient cases, the problem should be set in terms of a steady state condition and, once the results are obtained, they should be applied as the initial condition for the transient problem. In addition, for turbulent cases, iteration should be continued to the point where turbulent kinetic energy (k) and turbulent dissipation are balanced. The solution algorithm for this study is illustrated in Figure 3.1.
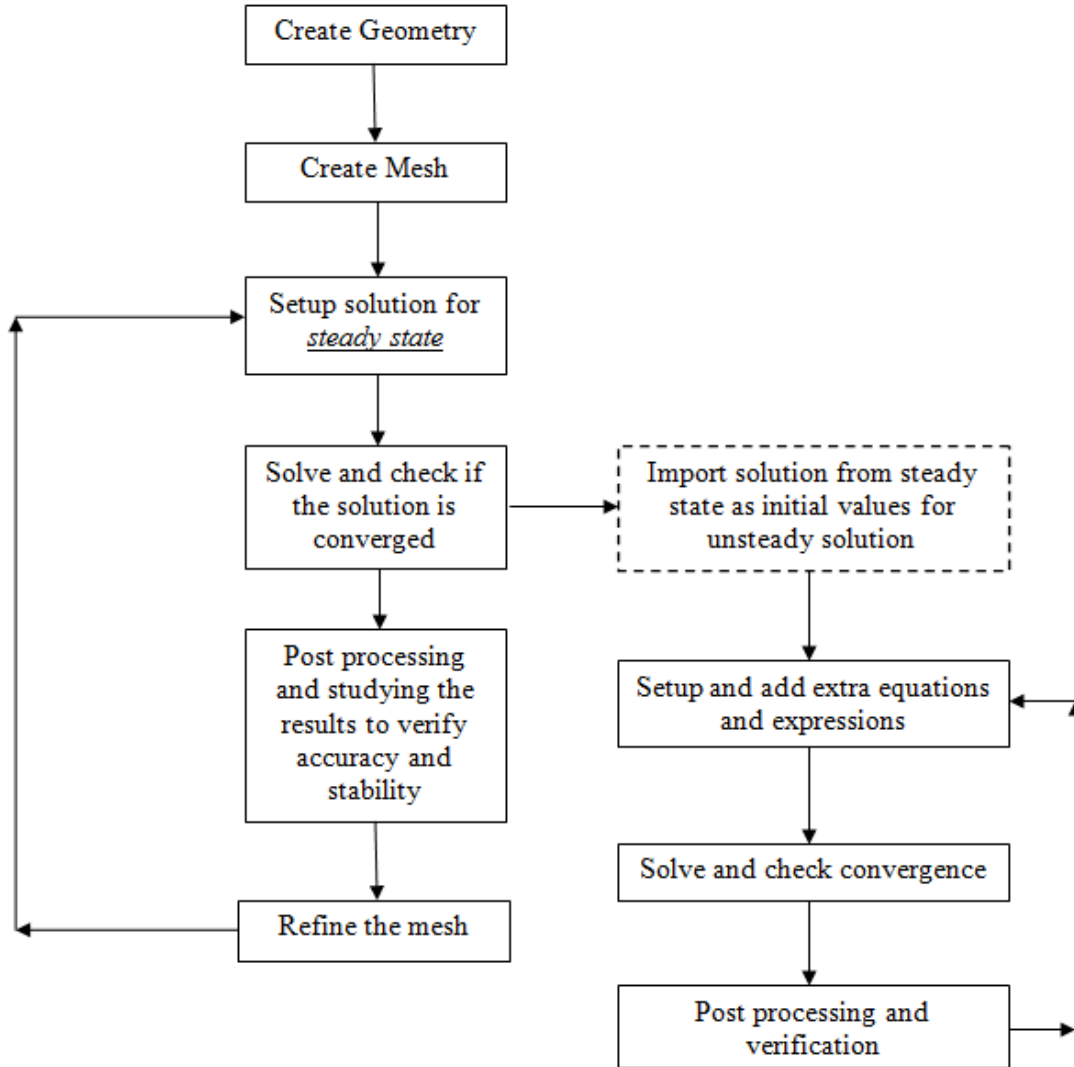
Figure 3.1: Solution algorithm proposed in this study

The main objective of this research is to predict the fate of hypochlorous acid in a typical indoor swimming pool in Canada. The simulations used in this research were divided into two parts. The simulations in the first part examined the effect of the inlet size on distribution of chlorine. The simulations in the second part examined the chemical reaction between ammonia and chlorine following a sudden injection of ammonia. The ANSYS package version 14.5 (ANSYS, 2012) was used to create the mesh and geometry, and the CFX solver was used to solve the problem.

In some cases, this problem has been solved using the FLUENT solver (another CFD solver available in the ANSYS package) in order to compare and validate the results. Maximum numerical residuals for all equations have been set to 10^{-6} in order to guarantee the convergence of solutions. Two different turbulence models (Standard and RNG k-ε) were used, and the results of each were compared in order to find the best approach for turbulence modelling. No significant difference was found in the outputs but, as noted above, the RNG model is generally recommended in the literature and, on this basis, the RNG model was chosen for this research. See Appendix A for details of the RNG model. In order to carry out the simulation for the chemical reaction, CFX Expression Language (CEL) was used to generate extra expressions (details following).

3.1   Geometry and dimensions

The dimensions of the swimming pool were chosen according to those of a "learning" swimming pool, common in British Columbia: 10 *m* (length) × 5 *m* (width) × 1 *m* (depth). British Columbia provides the following guidelines (British Columbia Ministry of Health, 2014):

- The velocity of water through the drains of any of the circulation systems must be less than 46 cm/s.
- Inlets should be submerged at least 61 cm below the average operating level.
- Surface skimming devices may be used in place of gutters to remove surface water from a pool if the pool has a surface area of 170 m^2 or less.
- At least one skimmer is required from each 42 *m^2* of surface area.

In order to maintain an acceptable water quality, all swimming pools should be designed to circulate water continuously. The flow rate depends on the type and condition of the swimming pool. For a public pool with a maximum water depth of 122 *cm* or less, a maximum turnover of two hours is recommended to completely re-circulate all the water.

To make this model more realistic, and to account for the effects of bathers on mixing, ten solid cylinders were placed in the domain (Figure 3.1) to represent swimmers. The distribution of cylinders was random, although they are assumed to be symmetric in order to make the validation easier. Since the geometry was symmetric the results were also symmetric, therefore it seemed appropriate to continue the modelling for just one half of the swimming pool (domain).

For each case, the mesh independence was examined separately. The number of total mesh nodes was changed from 49,972 to 934,110 in order to find the optimum mesh size. Approximately 420,000 meshes were required to obtain reliable results for all three scenarios. Table 3.1 shows changes in the outlet mass flow rate for different meshes.

Table 3.1: Mesh independency test

Number of Nodes	49,972	187,264	416,052	934,110
Outlet Mass Flow (*kg/s*)	0.59	0.566	0.501	0.502

3.2 Boundary conditions

3.2.1 Inlets

Two identical inlets were placed at opposite walls of the swimming pool. To study the effects of inlet size on distribution of chlorine, three different scenarios were considered. The boundary condition for the inlets in all scenarios was constant mass flow. Table 3.2 shows the properties of each scenario.

Table 3.2: Properties of inlets for all three scenarios.

Scenarios	Inlet Dimensions	Inlet mass flow (*kg/s*)	Mean velocity (*m/s*)
Scenario 1	$0.12\ m \times 0.12\ m$	3.4	0.22
Scenario 2	$0.15\ m \times 0.15\ m$	3.4	0.14
Scenario 3	$0.17\ m \times 0.17\ m$	3.4	0.11

In order to maintain the concentration of free chlorine at a certain level in the swimming pool, chlorine as chlorine gas, sodium, calcium, or lithium hypochlorite is added to the re-circulated (or fresh) water, and introduced into the pool from the inlets at a maximum allowed concentration of free chlorine. Therefore, an additional transport equation was used to simulate the distribution of chlorine (Equation 2.12). This helped to solve the exact concentration of hypochlorous acid at any location throughout the domain under an unsteady condition, without simplifications and without considering the domain as a black box. The transport equation,

presented in the previous chapter (Equation 2.12) can now be rewritten and should be solved simultaneously with other equations as follows:

$$\frac{\partial(\rho Y_A)}{\partial t} + u_j \frac{\partial(\rho Y_A)}{\partial x_j} = \frac{\partial}{\partial x_j}\left(\left(D + \frac{\mu_t}{\rho\, Sc_T}\right)\frac{\partial(\rho Y_A)}{\partial x_j}\right) + R_A \qquad \textbf{Equation 3.1}$$

The Turbulent Schmidt number (Sc_T) is equal to 0.9 for the purposes of this study, and the diffusion coefficient (D) for HOCl is calculated according to Chao (1969):

$$\log D = -a \times 10^3 \times \left(1/T\right) - b \qquad \textbf{Equation 3.2}$$

where a = 0.945, b = 1.72, and T is temperature.

3.2.2 Outlets

The outlets included four skimmers (with dimensions of 0.18 m × 0.09 m) at the top of the pool, and one drain at the bottom (with dimensions of 0.1 m × 0.1 m). The boundary conditions for all of the outlets were set as pressure outlets.

3.2.3 Symmetric and wall conditions

To reduce the CPU time, only half of the domain was modelled, and therefore a symmetric boundary condition was applied at the cross-section. The upper surface of the pool was considered as a free slip wall.

3.3   Chemical reactions

The reaction between hypochlorous acid and ammonia was simulated to mimic a sudden release of urine in a swimming pool. Initially, hypochlorous acid was introduced into the domain and iterations continued to the point where the average concentration of hypochlorous acid reached 3.9 mg/L. At this point, ammonia was injected into the domain for 21 seconds, while hypochlorous acid was introduced to the domain at the same rate as before. The duration of 21 seconds was chosen according to the rate that humans (and mammals) are known to empty their bladders (Yang, Pham, Choo, & Hu, 2013). Although urine consists of a number of different

components, this study used ammonia to represent urine. The following step function was defined in terms of CEL where H is the Heaviside function, t is time, and $c = 21$:

$$u_c = H(c - t)$$

<div align="right">**Equation 3.3**</div>

After the injection, iterations were continued for two hours (the time it takes for one turnover). The chemical reaction resulted in a decrease in the concentration of ammonia and hypochlorous acid and an increase in the concentration of chloramines. Hence, the source term in Equation 3.1 (the last term on the right side of this equation) was modified based on the EDC which considers the effects of turbulence and chemical kinetics at the same time. Since the chemical reaction rate is considered to be instantaneous, the reaction is limited by the characteristics of the turbulence and should be expressed as a function of the turbulent dissipation rate (ε) and the turbulent kinetic energy (k). Therefore, Equation 2.16 should be modified for each species in the domain. The source term for chlorine and ammonia can be modified as follows:

$$R_{HOCl} = -\rho A \left(\varepsilon / k \right) Min. (MF_{HOCl}, MF_{ammonia} \times i)$$

<div align="right">**Equation 3.4**</div>

$$R_{ammonia} = -\rho A \left(\varepsilon / k \right) Min. (\frac{MF_{HOCl}}{i}, MF_{ammonia})$$

<div align="right">**Equation 3.5**</div>

where ρ is density, i is the stoichiometry ratio, MF stands for mass fraction, and A is a constant between 1-4. For liquid phase reactions, A $= 1$ is recommended (Hjertager et al., 2002). The solution depends greatly on the values of turbulence kinetic energy and dissipation rate (ε/k). In order to enhance the accuracy, iterations for a single phase under an unsteady condition continued to the point where both k and ε were stabilized, and then extra equations were added to model the chemical reaction.

Due to computational limitations and the symmetry in the geometry, only one quarter of the swimming pool was identified as the domain for chemical reaction modelling.

3.4   Post-processing

After solving the problem in the CFX-solver, the results were post-processed for visualizations and quantitative analysis. Post-processing was done in CFX-post. In order to see the results for

each scenario, three planes were defined to illustrate the velocity and concentration contours for all scenarios so that the outputs illustrated on these planes. To compare the results for each scenario, plane 1 (Figure 3.2.a) was placed on the ZX plane at an elevation of 0.45 m to capture the Inlet contours. Plane 2 (Figure 3.2.b) shows the results on the water surface, and plane 3 (Figure 3.2.c) shows the intersection of the domain on the YX plane.
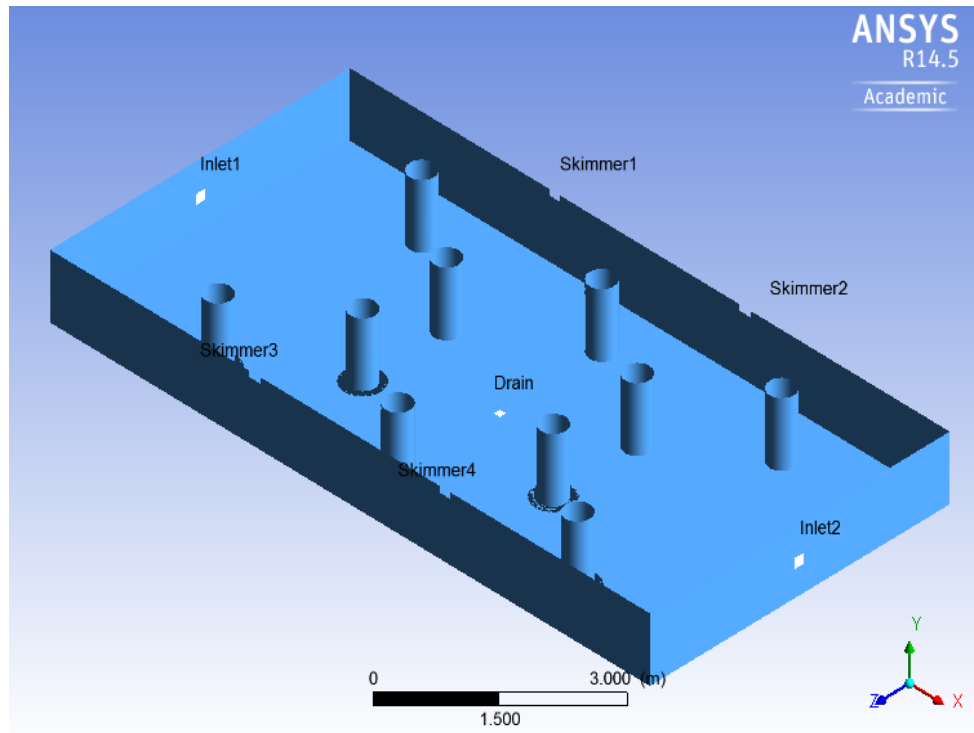
Figure 3.2: Geometry of a common indoor swimming pool
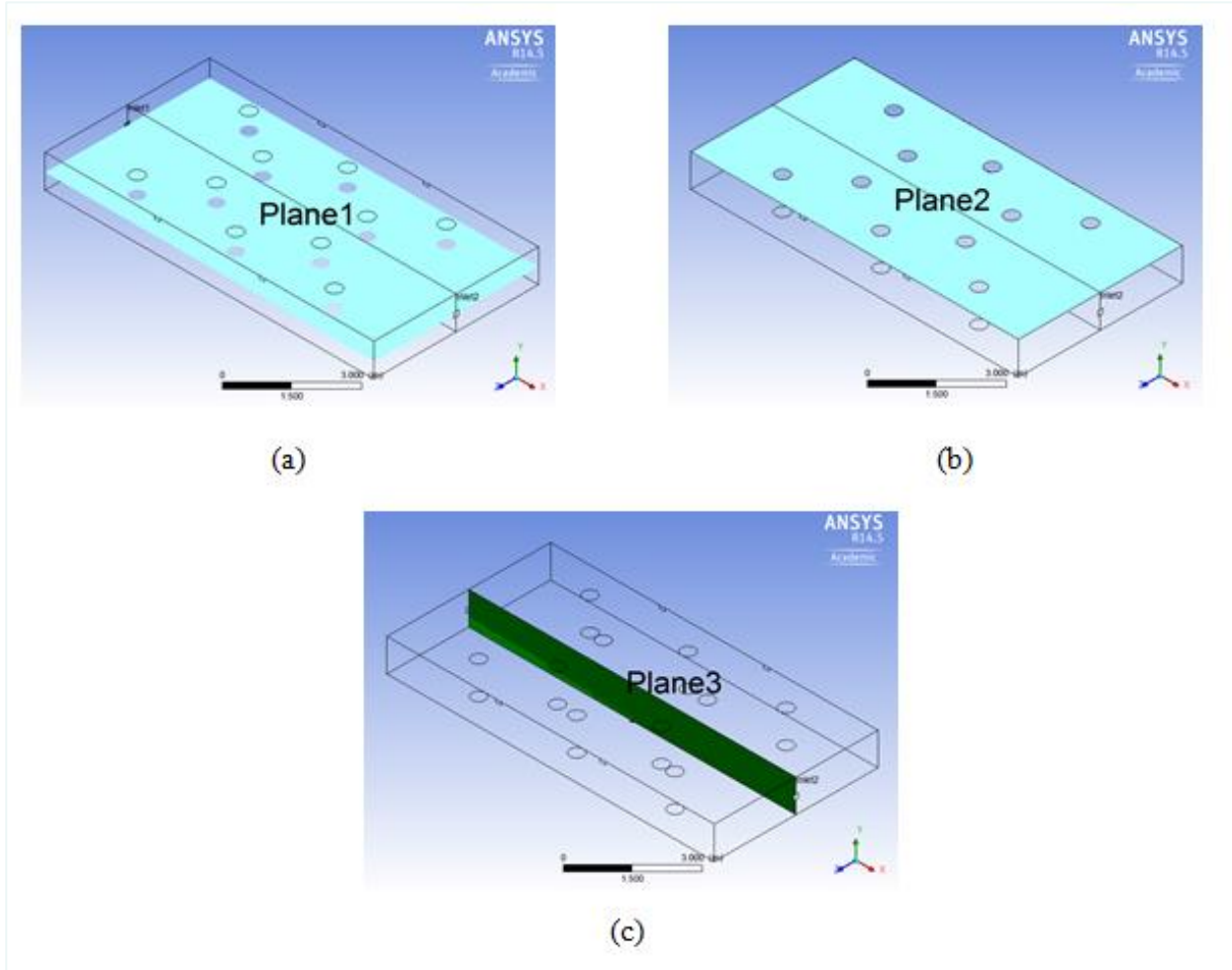
Figure 3.3: Plane 1, 2, and 3 (a) plane 1 on mid-surface parallel to the free surface, at elevation of y = 0.45 m; (b) plane 2 on surface y = 1 m; (c) plane 3 perpendicular to free surface at the middle of the swimming pool at z = 2.5 m.

Results are verified against experimental studies. In the next chapter, results are presented and discussed with details based on the above formulations and methods.

Chapter 4: Results and Discussion

The hydraulic behavior in an indoor swimming pool was examined for three different inlet sizes in order to determine the impact of inlet size on the distribution of chlorine. The basic assumption for each scenario was provided in Chapter 3. The mass flow rate through each inlet was kept constant at 3.4 *kg/s* for all three scenarios, i.e., at a turnover rate of two hours. Since the mass flow rate is kept at constant rate, the mean velocity is decreases as the size of the inlet increases. Hypochlorous acid was introduced into the domain at a concentration of 5 *mg/L*. In reality, part of the hypochlorous acid dissociates in water and forms hypochlorite ion, which would have its own reactions to form chloramines; however, to simplify the model, here we assume that the free chlorine represents concentration of hypochlorous acid. Loss of chlorine due to the chemical reaction is ignored in the first three scenarios. In these three scenarios initial chlorine in the pool is taken to be zero and average concentration of gradually increases. In order to define the mixing rate, an average ratio of *(ε/k)* at the inlets and for the entire domain was calculated. Detailed results for each scenario are presented in the following sections.

4.1   Impact of inlet size

4.1.1 Scenario 1

In the first scenario, the dimension of the inlets was set at 0.12 *m* × 0.12 *m*. The maximum velocity in the domain close to inlets was 0.247 *m/s* —the point at which re-circulated water and chlorine was injected into the pool. The velocity was close to zero at specific spots near the cylinders. Velocity contours at planes 1, 2, and 3 are shown in Figures 4.1, 4.2, and 4.3. Figures 4.4 and 4.5 demonstrate stream lines that start from the inlets and find their way out at the skimmers or drain. As expected, the density of stream lines at some points was significantly higher than the rest of the domain, which highlight the dead zones.
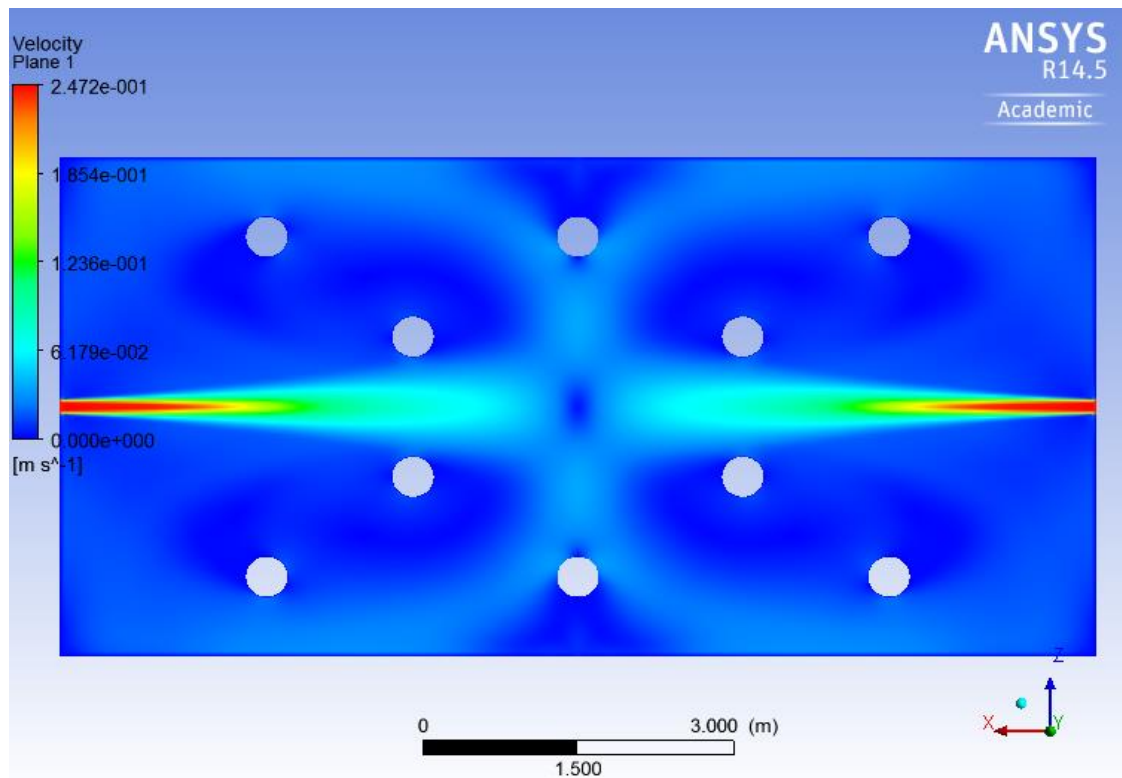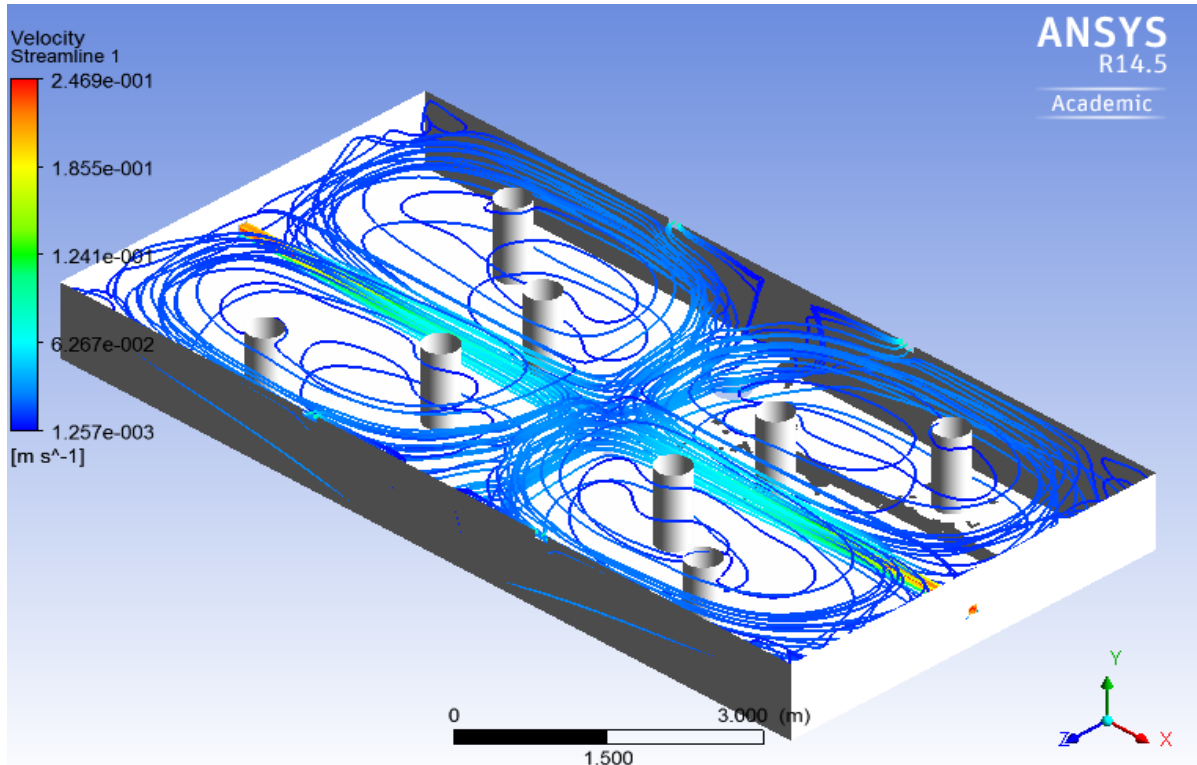
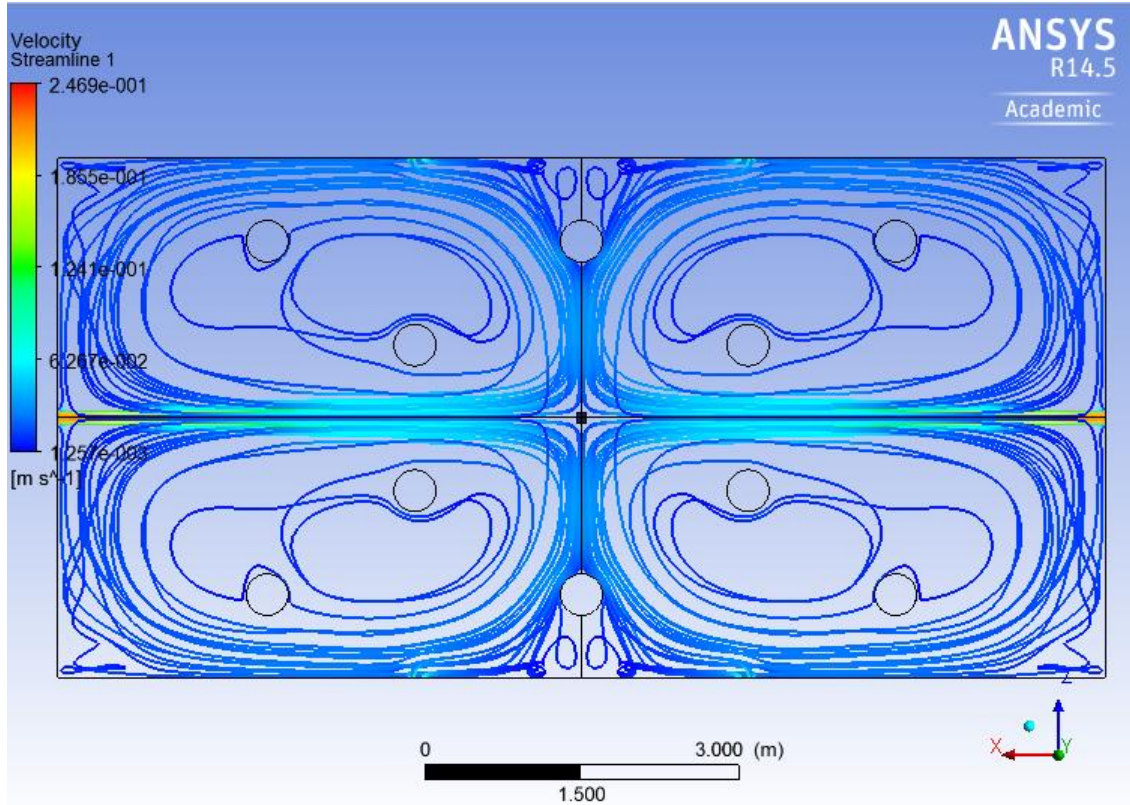**Figure 4.1:** Velocity contours on plane 1 (elevation of y = 0.45 m); top view.
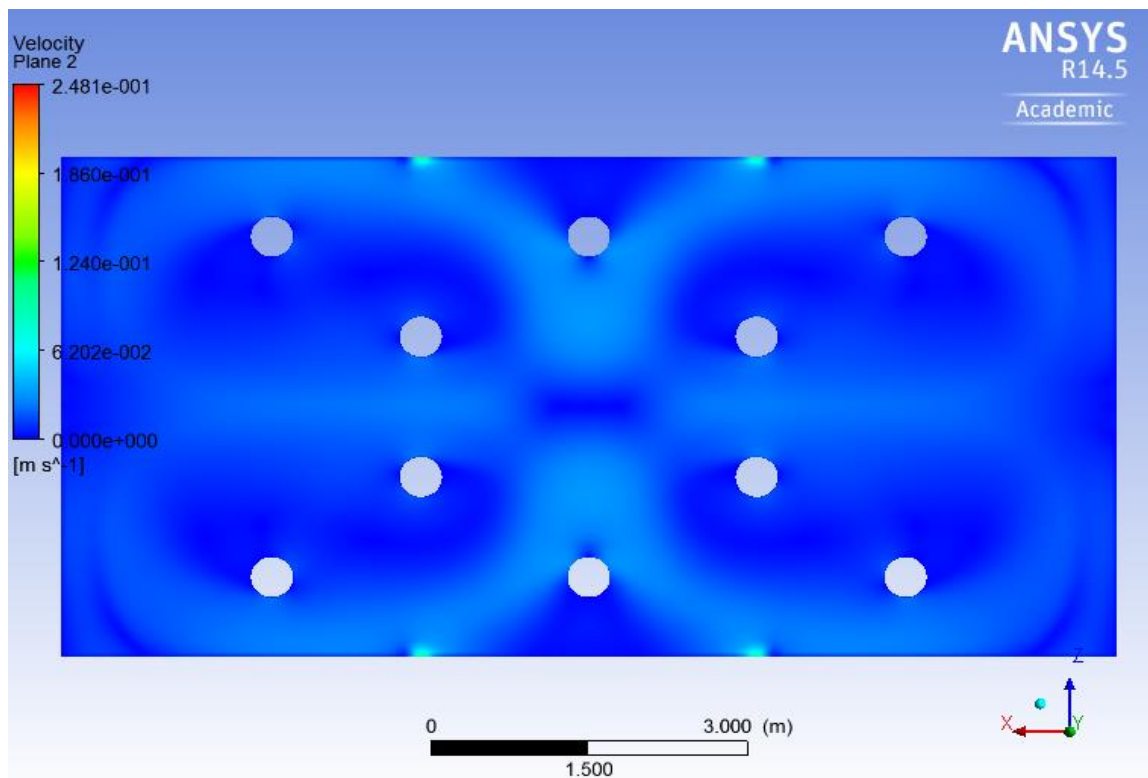
Figure 4.2: Velocity contours on plane 2 (elevation of y = 1 m); top view.

28
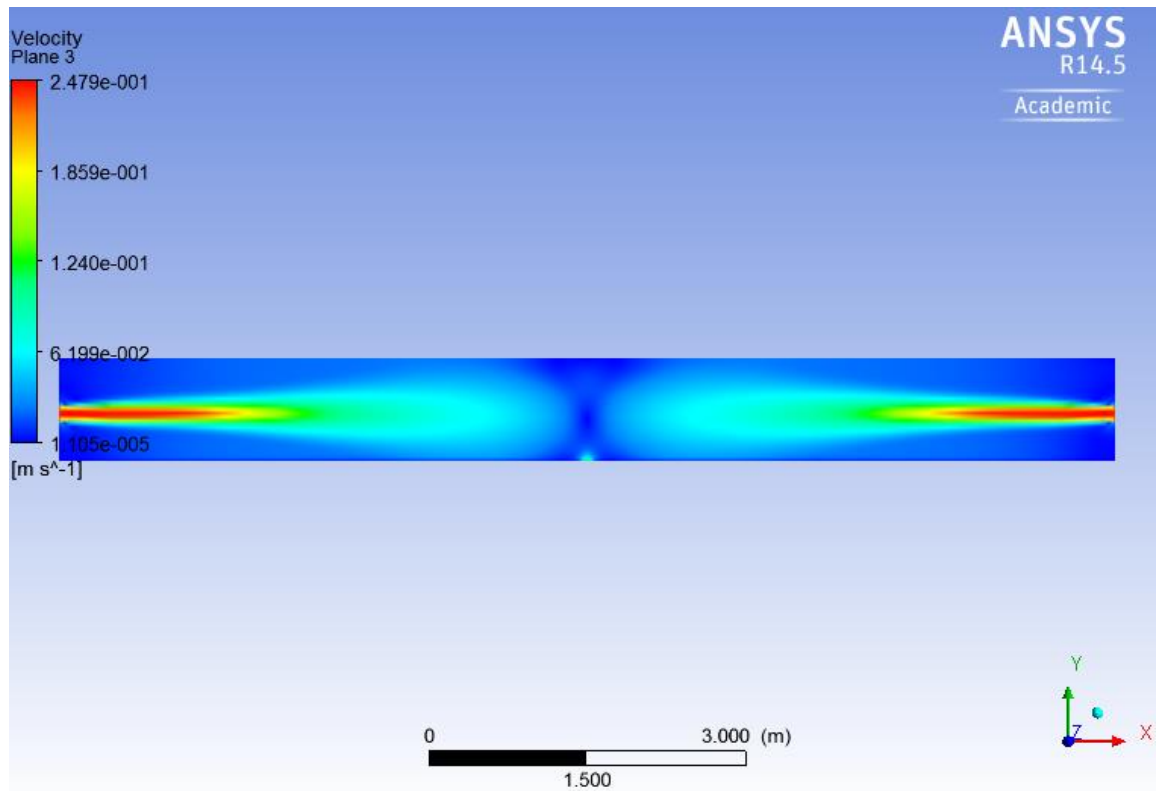
**Figure 4.3**: Velocity contours on plane 3 (z = 2.5 m); front view.

Figure 4.4: Stream lines starting from inlet distributed in the domain.

Figure 4.5: Stream lines in the domain, top view.

Figure 4.6 illustrates the concentration of hypochlorous acid at the surface ($y = 1$ m) after two hours. The average concentration at the surface was about 3.3 mg/L and the maximum concentration was 3.75 mg/L. Since volatilization and other chemical reactions were not considered in this study, in reality, the concentration is expected to be even less than the predicted values.
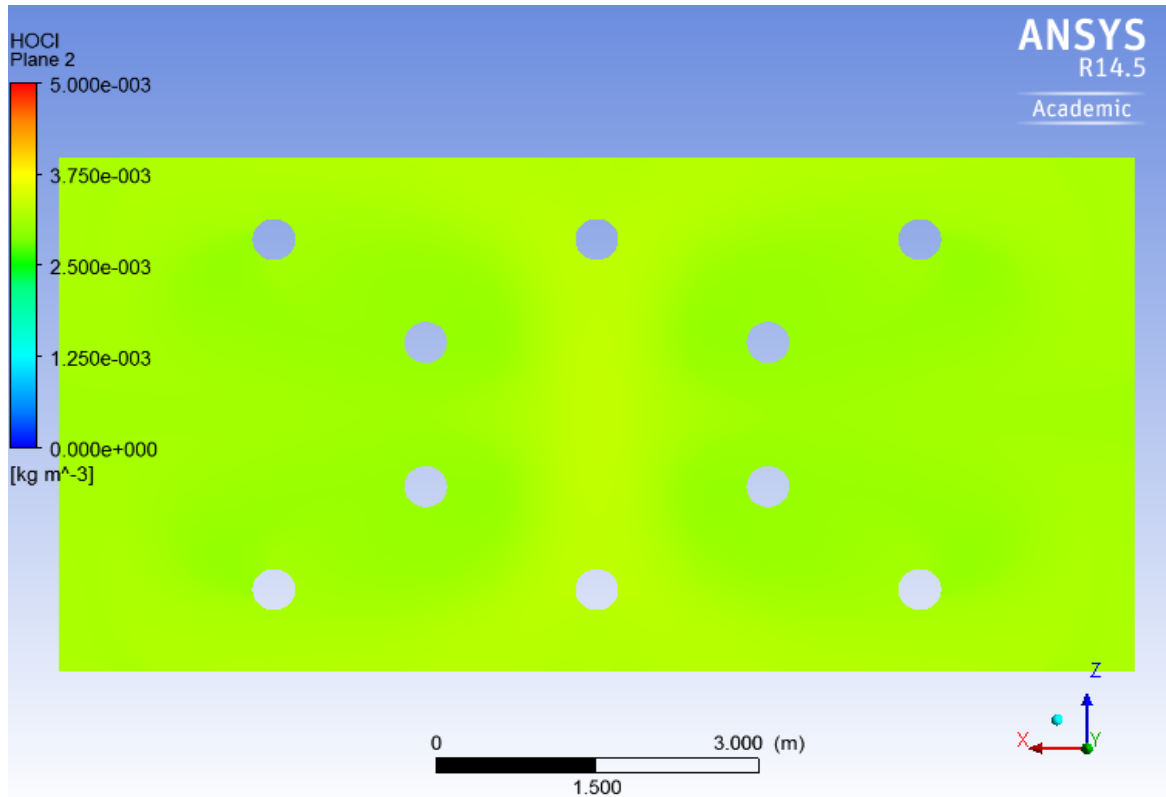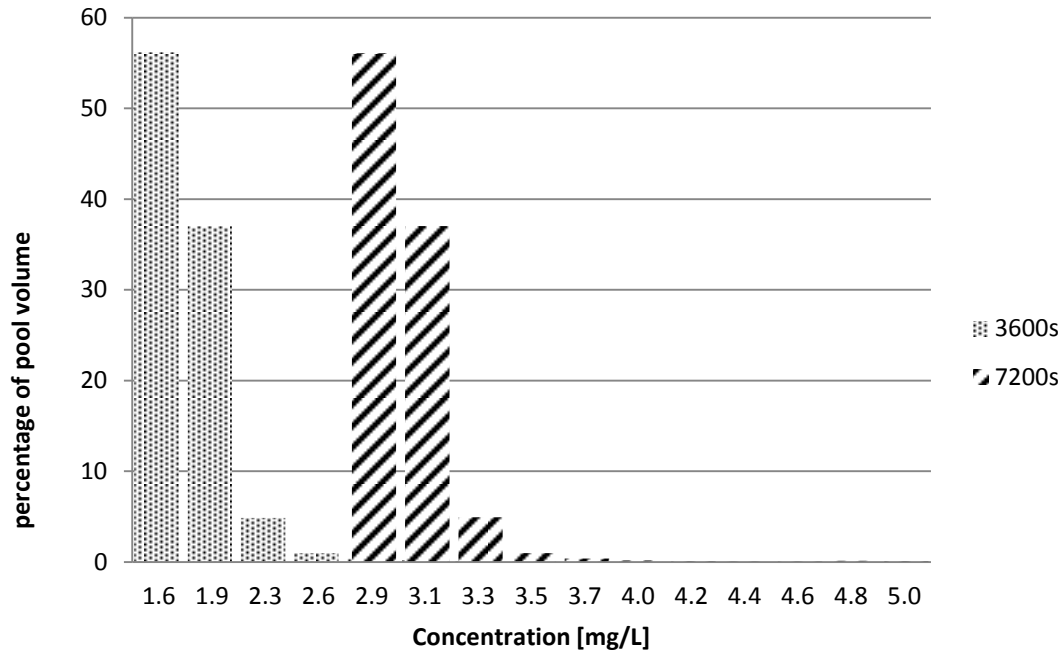
Figure 4.6: Hypochlorous acid concentration on plane 2 (elevation of y = 1 m) after 2 hours; concentration of chlorine is almost uniform on this plane which is about 3.7 mg/L.

Figure 4.7 shows the changes in hypochlorous acid concentration at different time steps on plane 1 (y = 0.45 *m*). After 2 hours, the average concentration of hypochlorous acid in the swimming pool was 3.1 *mg/L*, while hypochlorous acid was being injected into the domain at a continuous rate of 5 *mg/L*. After 2 hours, the average concentration of hypochlorous acid at plane 1 (y = 0.45 *m*) was 3.8 *mg/L*. This concentration was higher than the concentration at the surface of the swimming pool (plane 2) because plane 1 was at the same elevation as the inlets. Figure 4.8 shows that the minimum concentration of hypochlorous acid in the swimming pool after 2 hours is 2.9 *mg/L*, approximately 55% of the volume of swimming pool. Figure 4.9 shows that the concentration of hypochlorous acid increases exponentially over time to reach its upper limit which, in this study, was 5 *mg/L*. The concentration at the skimmers also increases according to this trend.
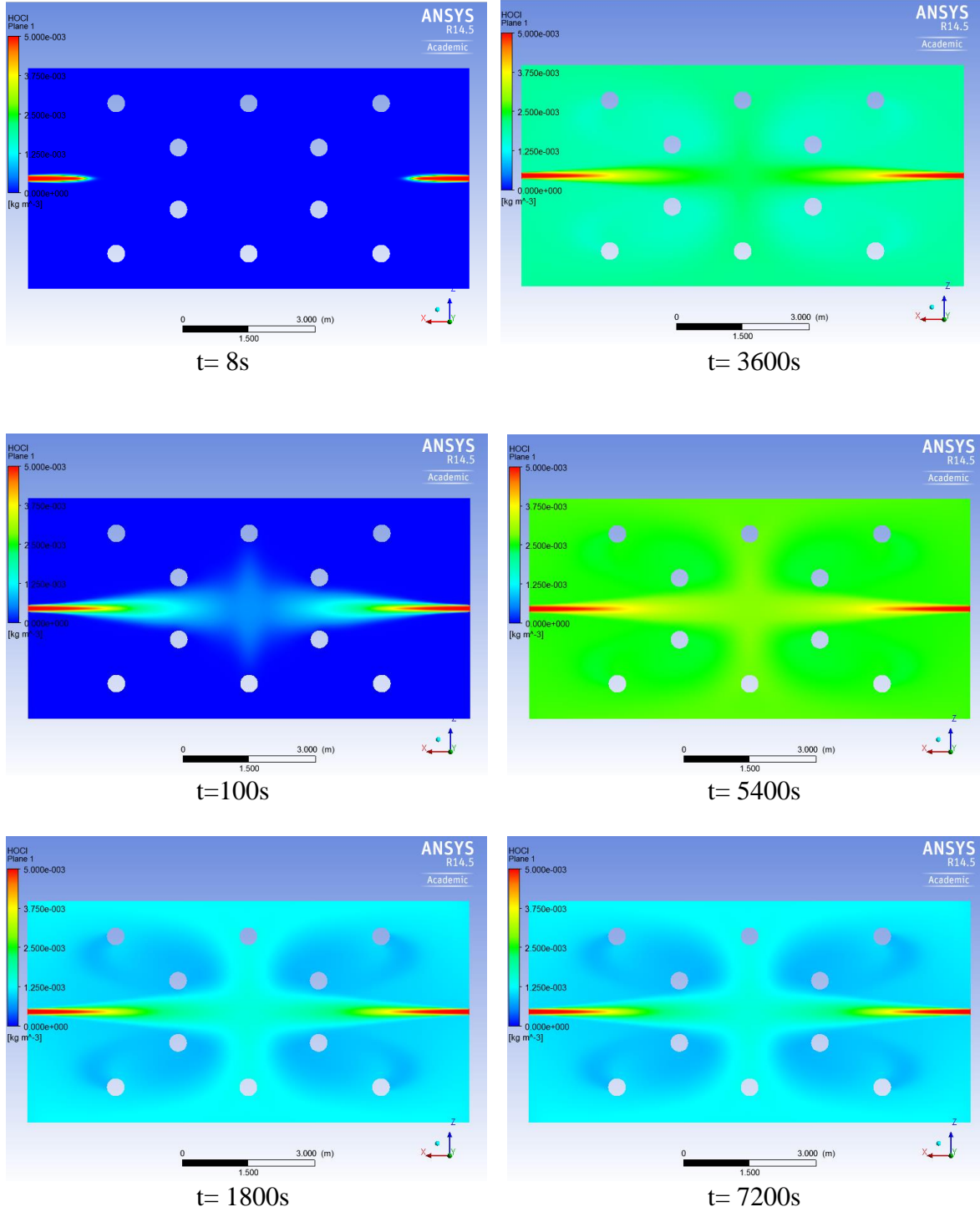
Figure 4.7: Hypochlorous acid concentration at plane 1 (elevation of y = 0.45); concentration gradually increases at different points in time.

Figure 4.8: Hypochlorous acid spatial distribution in the swimming pool after 3600 s and 7200 s
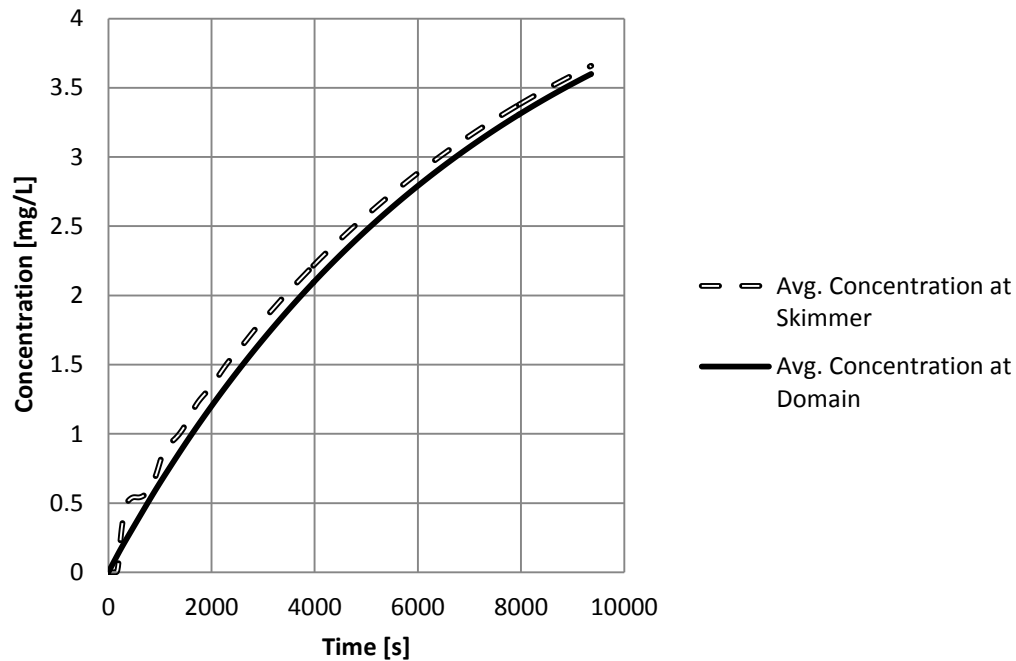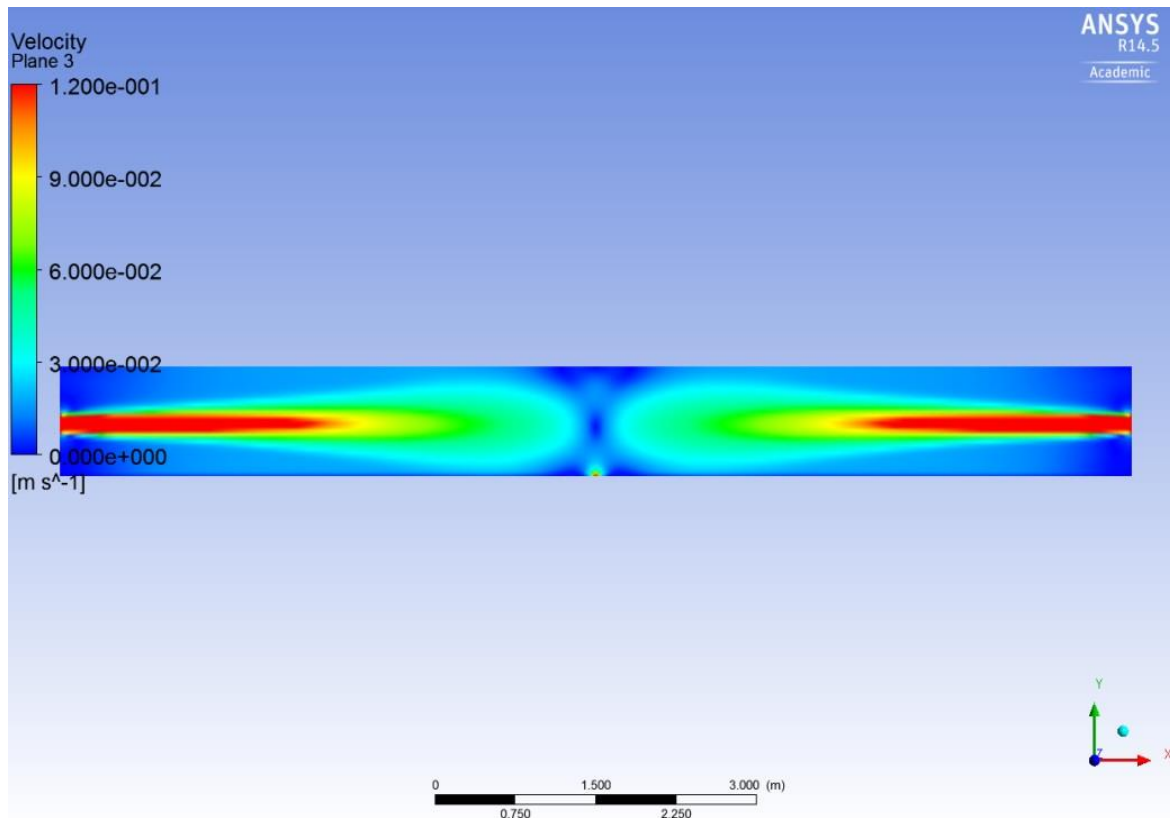

Figure 4.9: Average concentration of hypochlorous acid in the domain and at skimmers over 2 hour time period.

4.1.2 Scenario 2

In this scenario, the dimensions of the inlets are given as 0.15 $m \times 0.15$ m. Since the mass flow rate is the same, the velocity would be relatively lower. The maximum velocity at the inlets was 0.156 *m/s* and the average velocity was 0.142 *m/s*. Velocity contours at planes 1, 2, and 3 are illustrated in Figures 4.10 to 4.12. The average velocity in the entire domain was less than Scenario 1. Also, the ratio of (*ε/k*) is less, indicating that the mixing rate is better in Scenario 1.
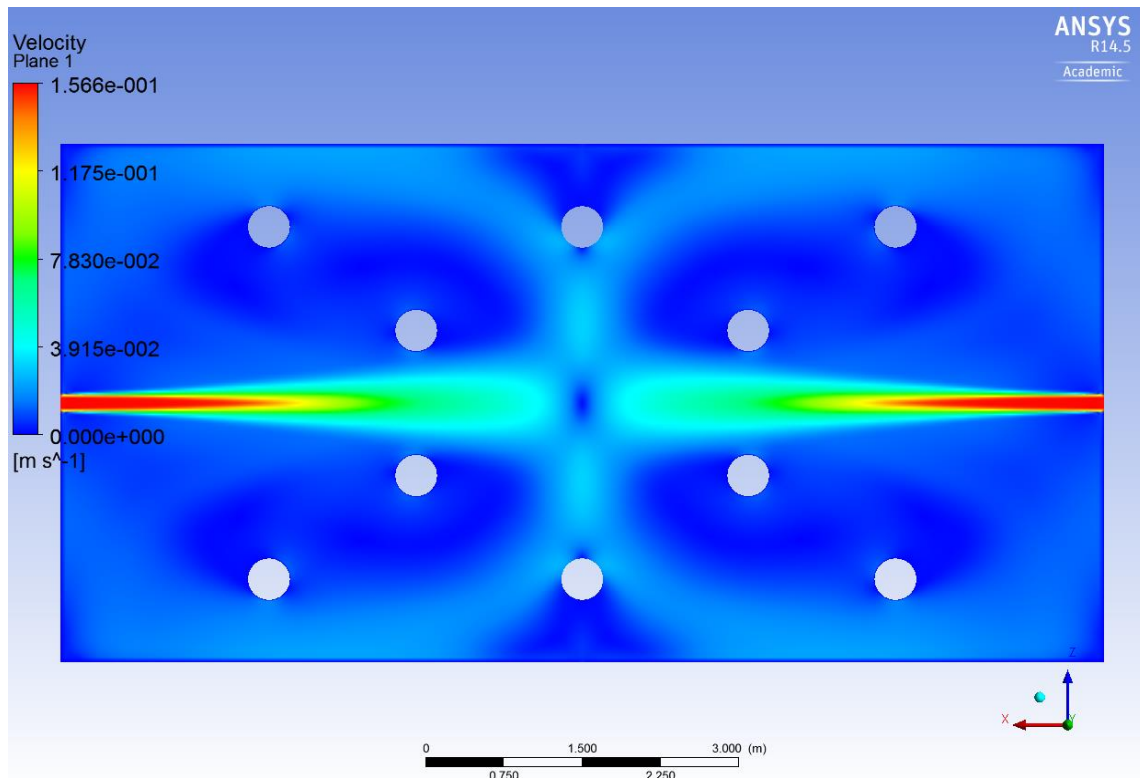
Figure 4.10: Velocity contours at plane 1 (elevation of y = 0.45 m), top view.

**Figure 4.11**: Velocity contours at plane 3 (z = 2.5), front view.
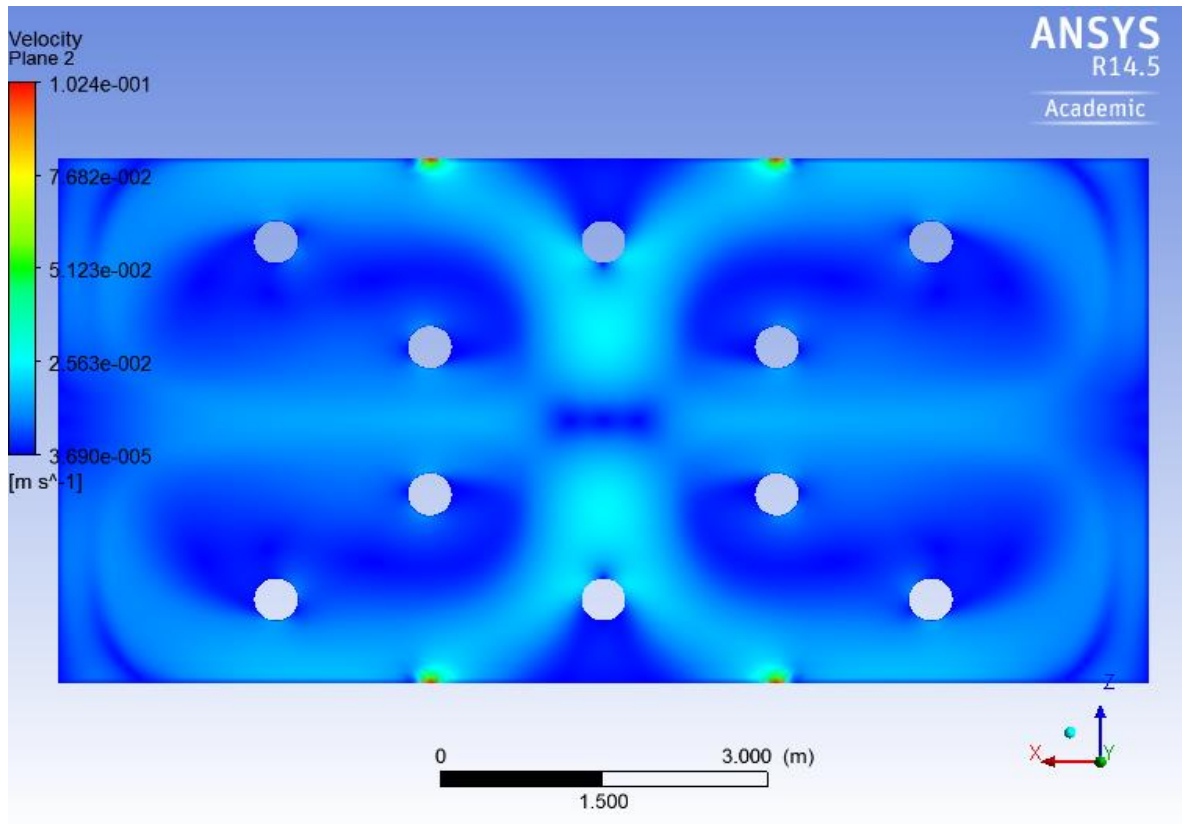
Figure 4.12: Velocity contours at plane 2 (elevation of y = 1 m), top view; dark blue regions have zero velocity while velocity is relatively higher near the skimmers

The average concentration of hypochlorous acid at the surface was 3.7 *mg/L* (Figure 4.13), which was higher than Scenario 1. Nevertheless, the total hypochlorous acid in the entire domain after 2 hours is the same as before (3.2 *mg/L*). Unlike in Scenario 1, 50% of the domain has an average concentration of 3 *mg/L*. Figure 4.14 shows the concentration at different time steps in plane 1. After 2 hours, the average concentration in plane 1 (y = 0.45 *m*) was 3.85 *mg/L*.

Comparing velocity contours against the concentration contours shows that regions with higher velocities have higher concentrations.
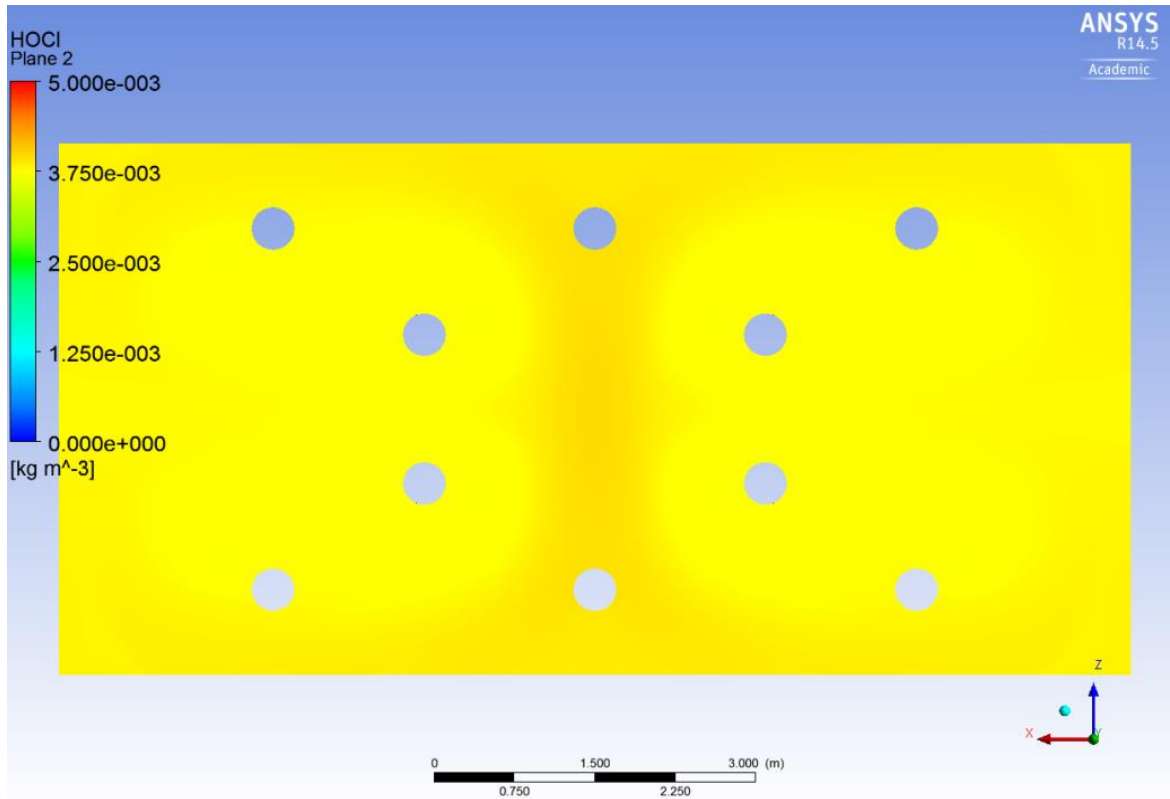
Figure 4.13: Hypochlorous acid concentration at plane 2 (elevation of y = 1 m) after 2 hours.
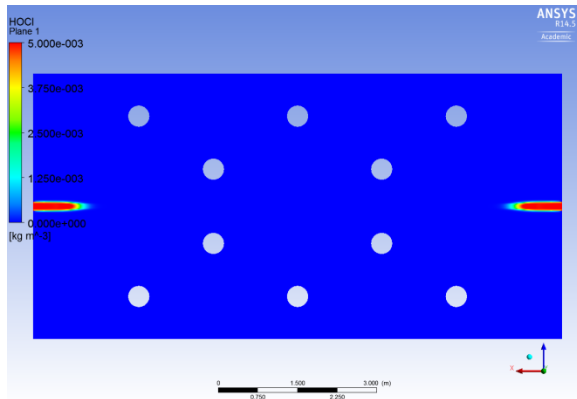
t= 8s
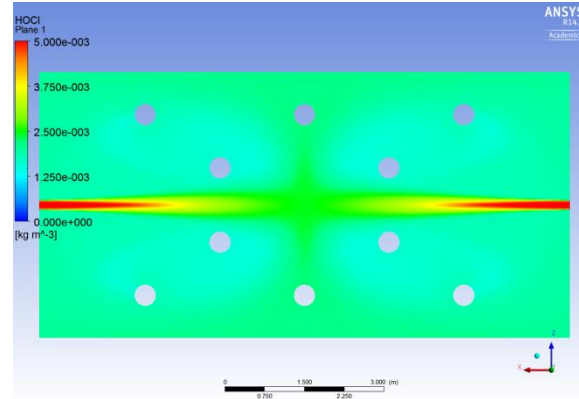
t= 3600s
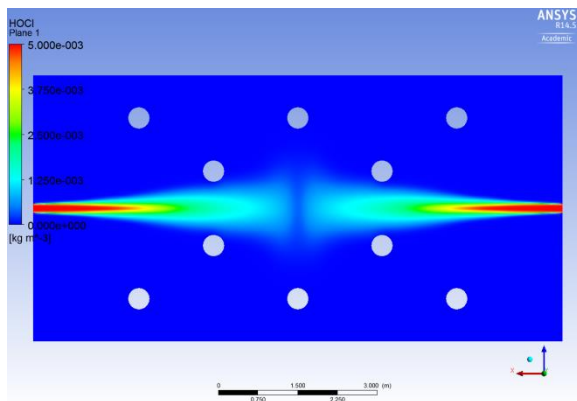
t= 100s
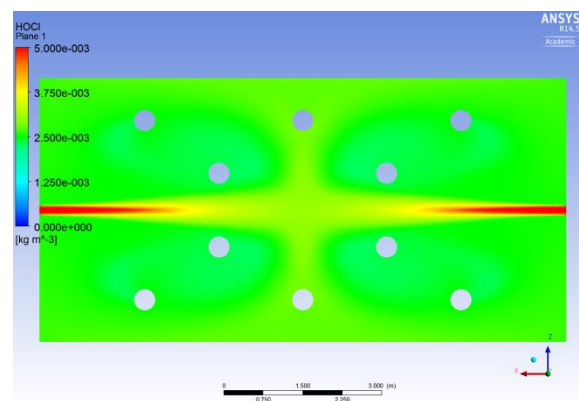
t= 5600s

t= 1800s

t= 7200s

Figure 4.14: Hypochlorous acid concentration at plane 1 (elevation of y = 0.45 m); concentration gradually increases at different points in time.
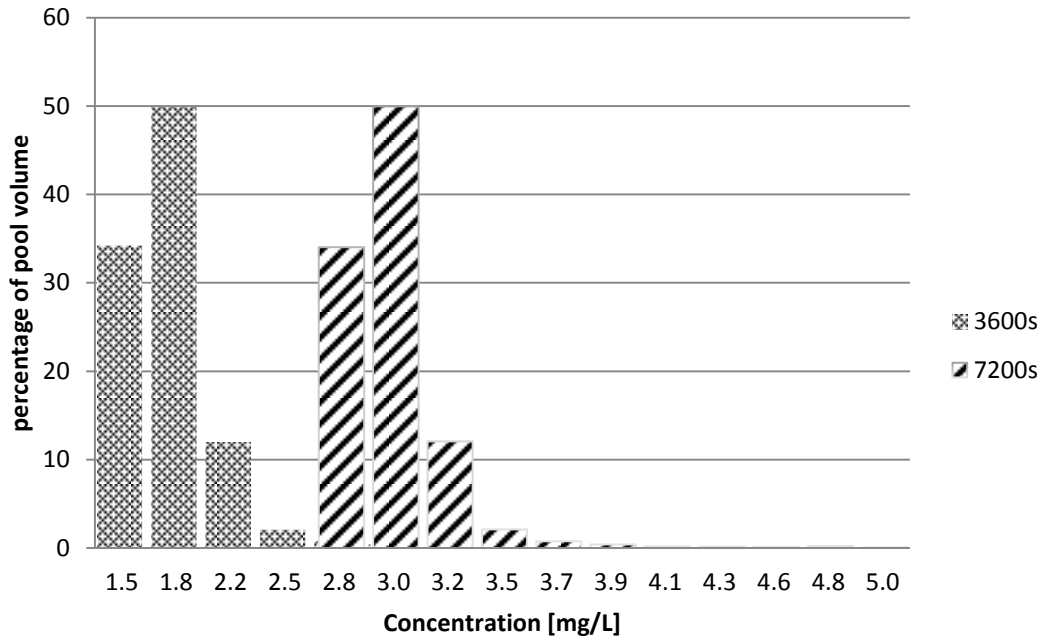
Figure 4.15: Hypochlorous acid spatial distribution in the swimming pool and skimmer after 3600 s and 7200 s.
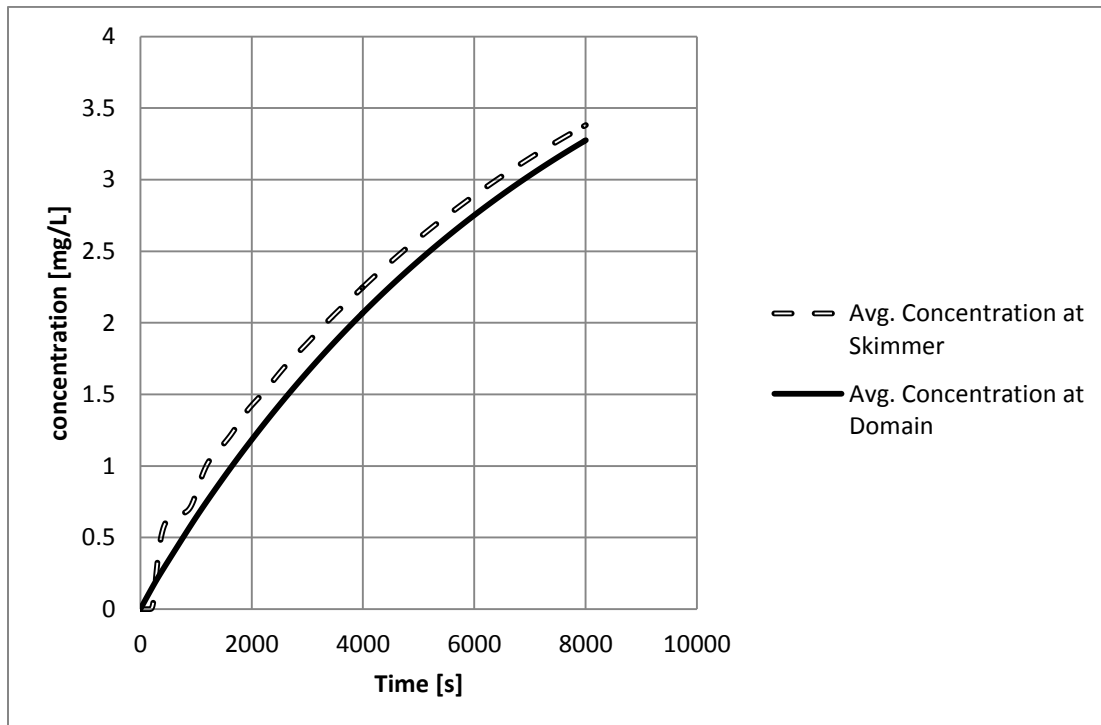
Figure 4.16: Average concentration of hypochlorous acid in the domain and skimmer over two hours

4.1.3 Scenario 3

In Scenario 3, it was assumed that the largest inlets would have dimensions of 0.17 $m \times$ 0.17 m resulting in a relatively lower velocity than in the previous scenarios. The maximum velocity at the inlets was 0.12 m/s and the average velocity was 0.10 m/s. Velocity contours at planes 1, 2, and 3 are illustrated in Figures 4.17 to 4.19. The velocity in the field is seen to be significantly lower in comparison to previous scenarios. In this scenario, the average concentration of hypochlorous acid in the domain reaches 2.1 mg/L in 3600 s, and reaches 3.2 mg/L in 7200 s. Figure 4.22 shows that 47% of the swimming pool has a hypochlorous acid concentration of 2.95 mg/L at 7200 s.
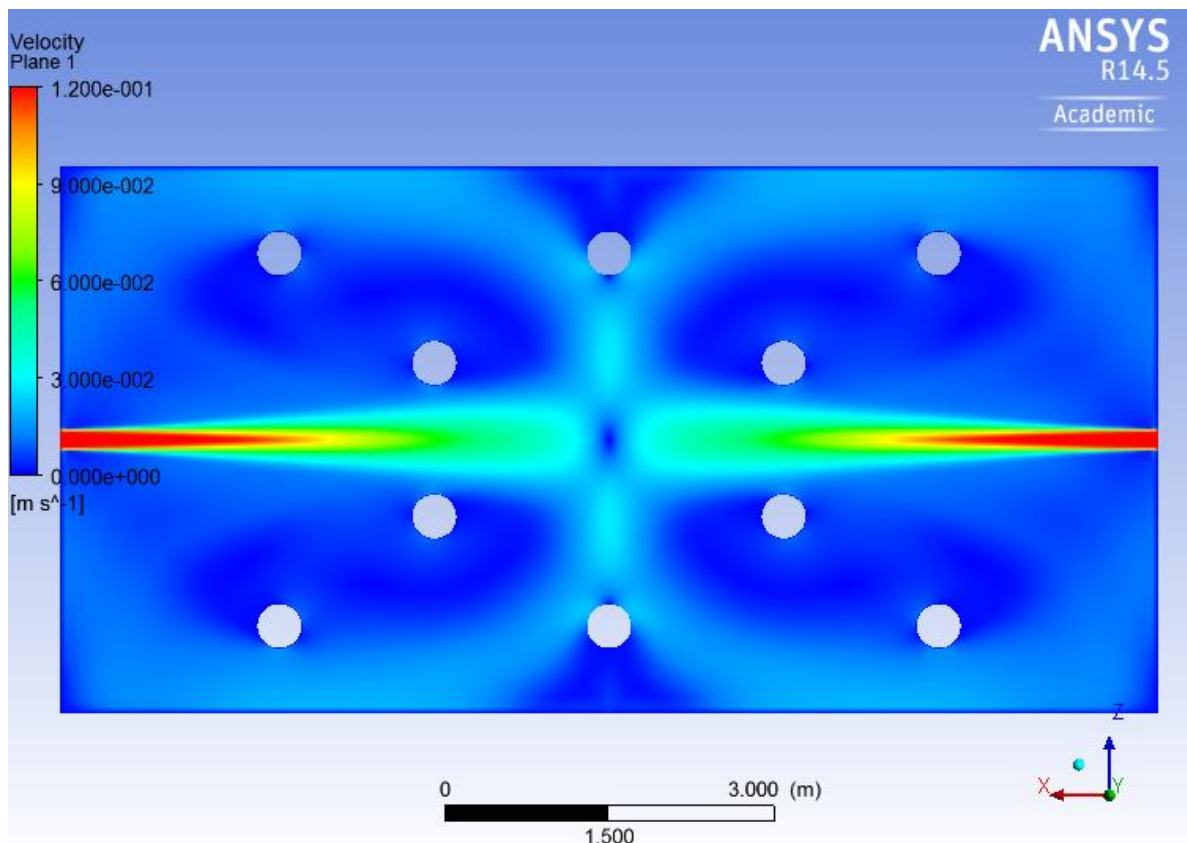
Figure 4.17: Velocity contours at plane 1 (elevation of y = 0.45 m), top view.

Figure 4.18: Velocity contours at plane 2 (elevation of y = 1 m), top view.
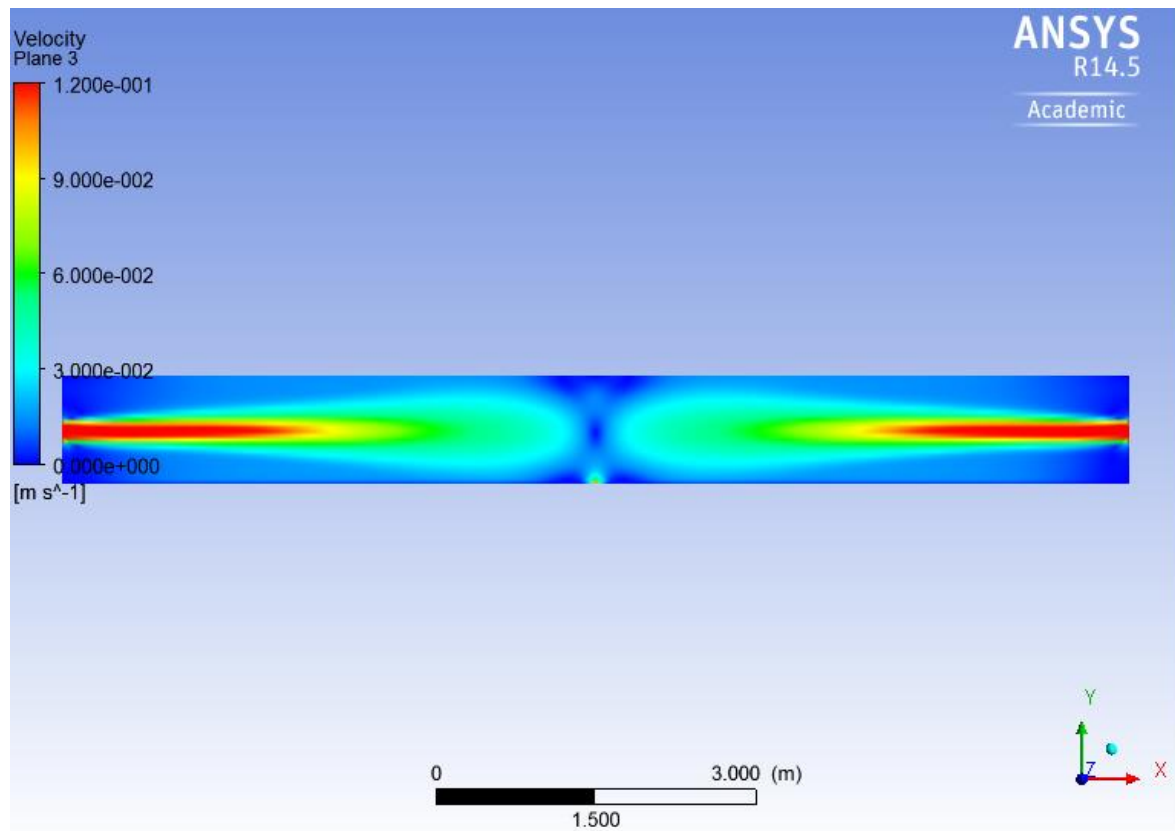
**Figure 4.19**: Velocity contours at plane 3 (z = 2.5 m), front view.
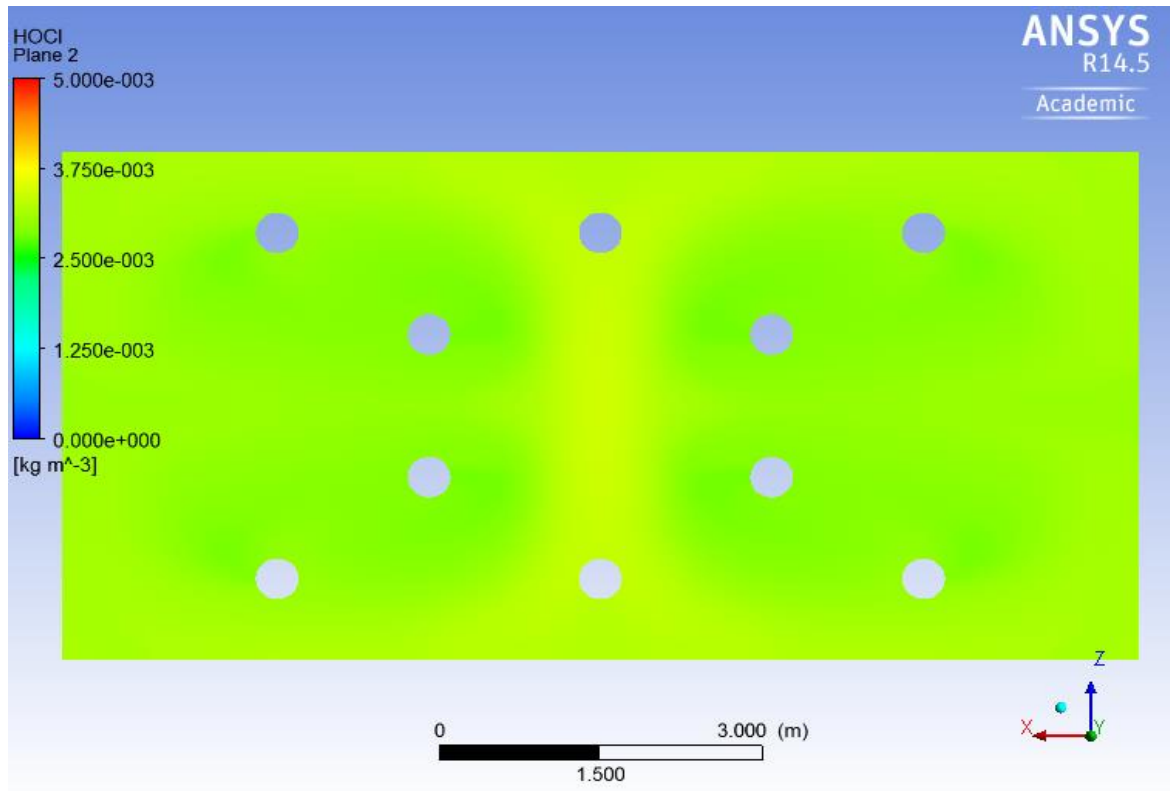
Figure 4.20: Hypochlorous acid concentration at plane 2 (elevation of y = 1 m) after 2 hours.

As illustrated in Figure 4.20, after 2 hours the surface of the pool has a concentration of 3.6 *mg/L* or less. Since volatilization is not considered in this simulation, the concentration at the surface, under realistic conditions, is expected to be even less. Figure 4.21 shows how the concentration of chlorine increases over time. After 1 hour, some locations in the domain have concentrations near zero, although the average concentration is 2.1 *mg/L*. Experimental samples from pool water are limited to certain locations near the edges of the pool, and hypochlorous acid is assumed to be uniformly distributed. This assumption may be misleading; however, as the previous figures indicate, CFD simulations show that the concentration of chlorine can vary from 0 to the maximum injected concentration of 5 *mg/L*.
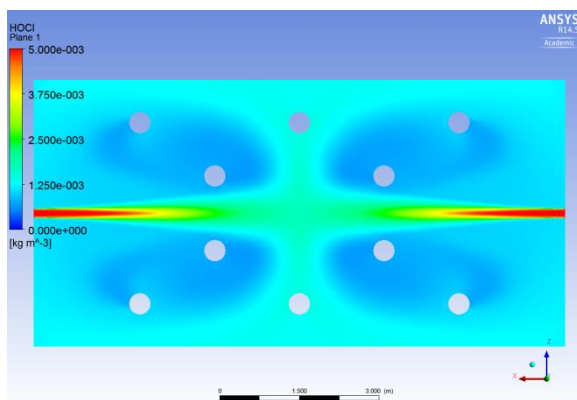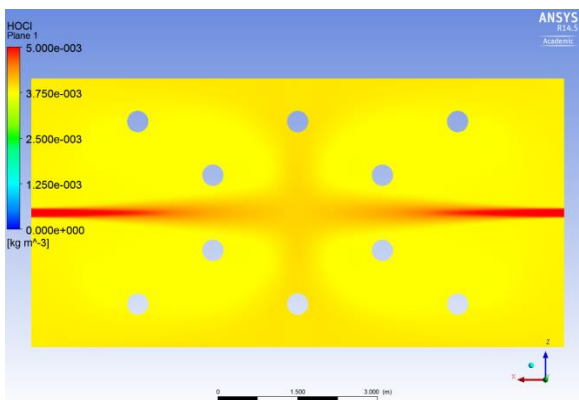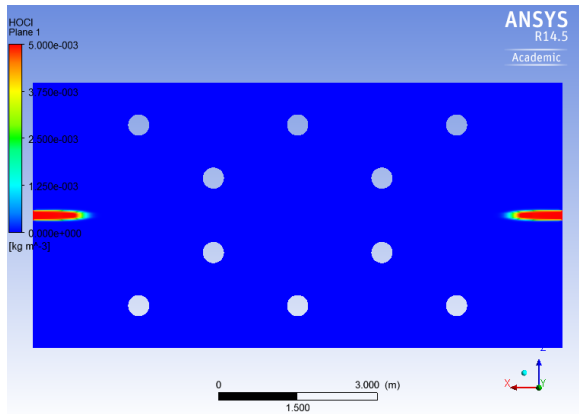
t= 8s
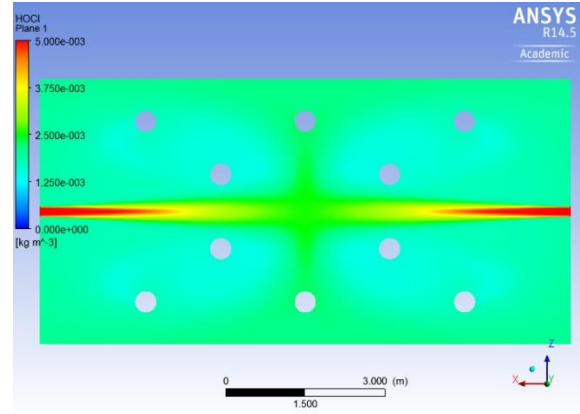
t=3600s
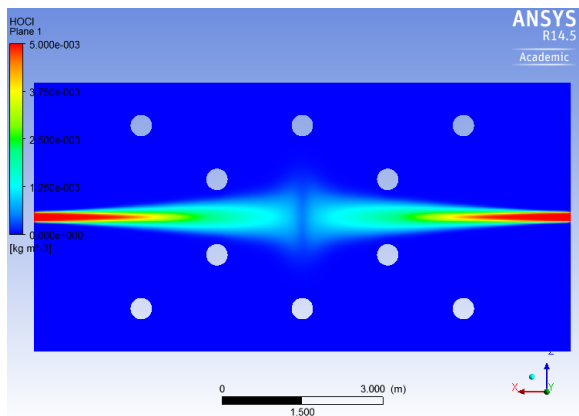
t= 100s
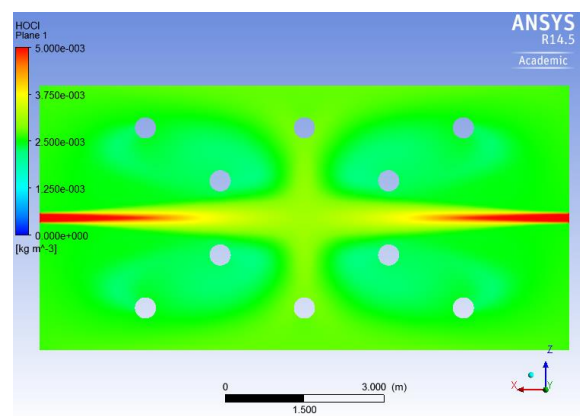
t=5400s
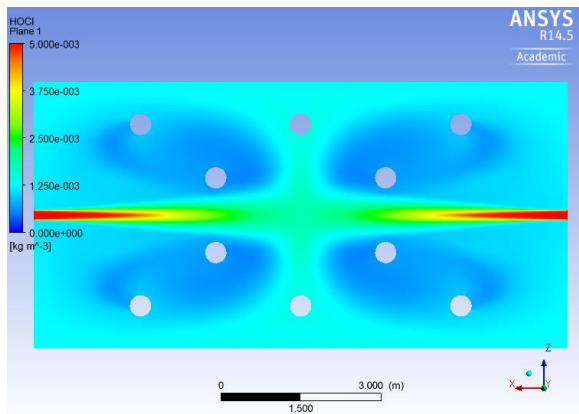
t= 1800s
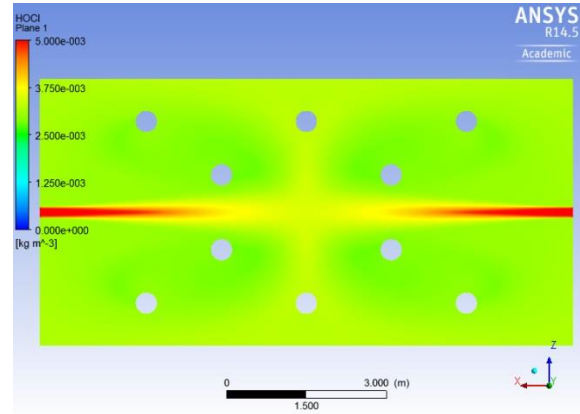
t=7200s

Figure 4.21: Hypochlorous acid concentration at plane 1 (elevation of y = 0.45 m); concentration gradually increases at different points in time.
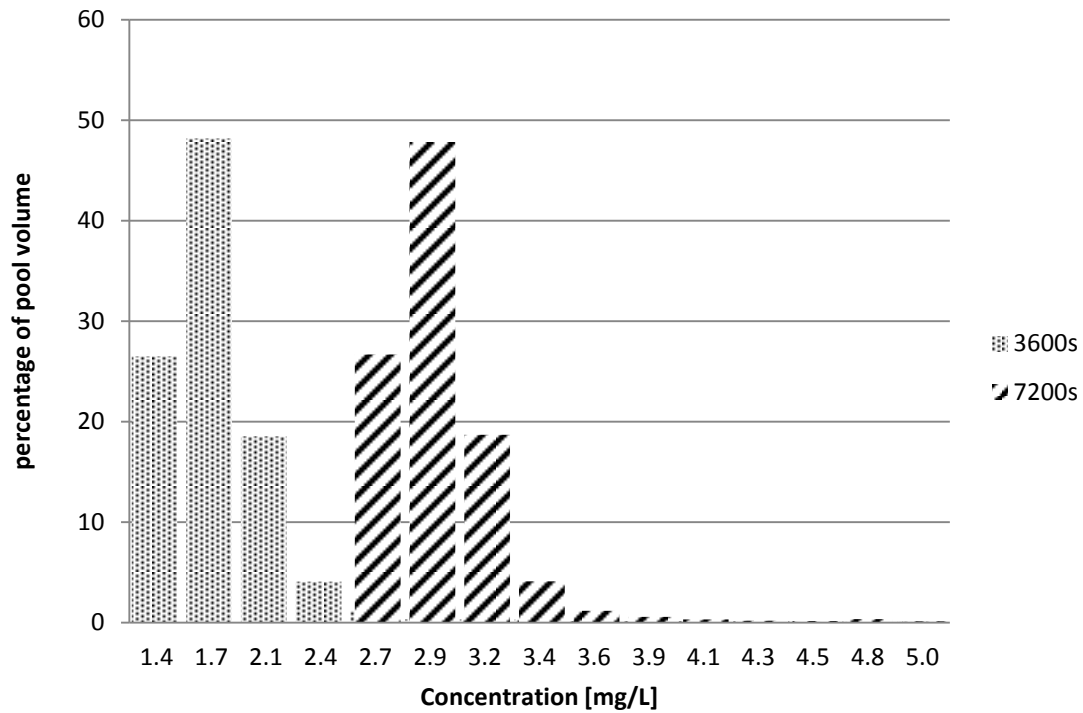
Figure 4.22: Hypochlorous acid spatial distribution in the swimming pool after 3600 s and 7200 s.

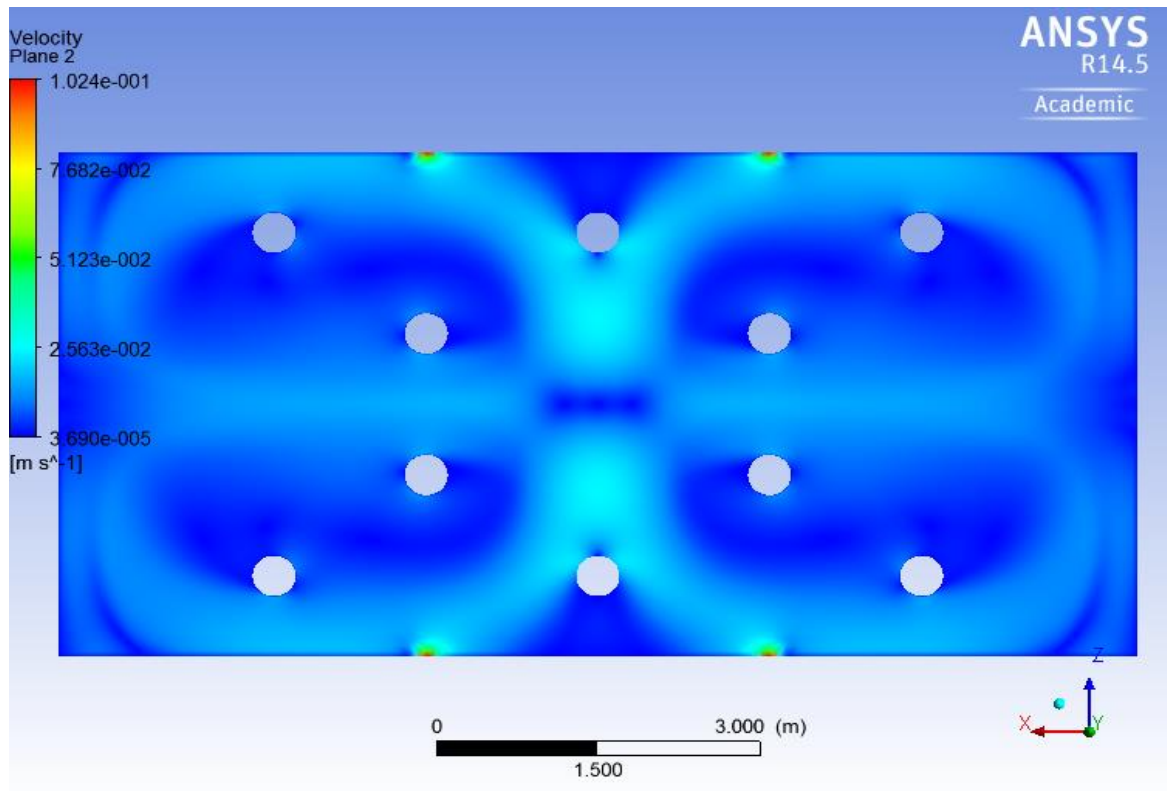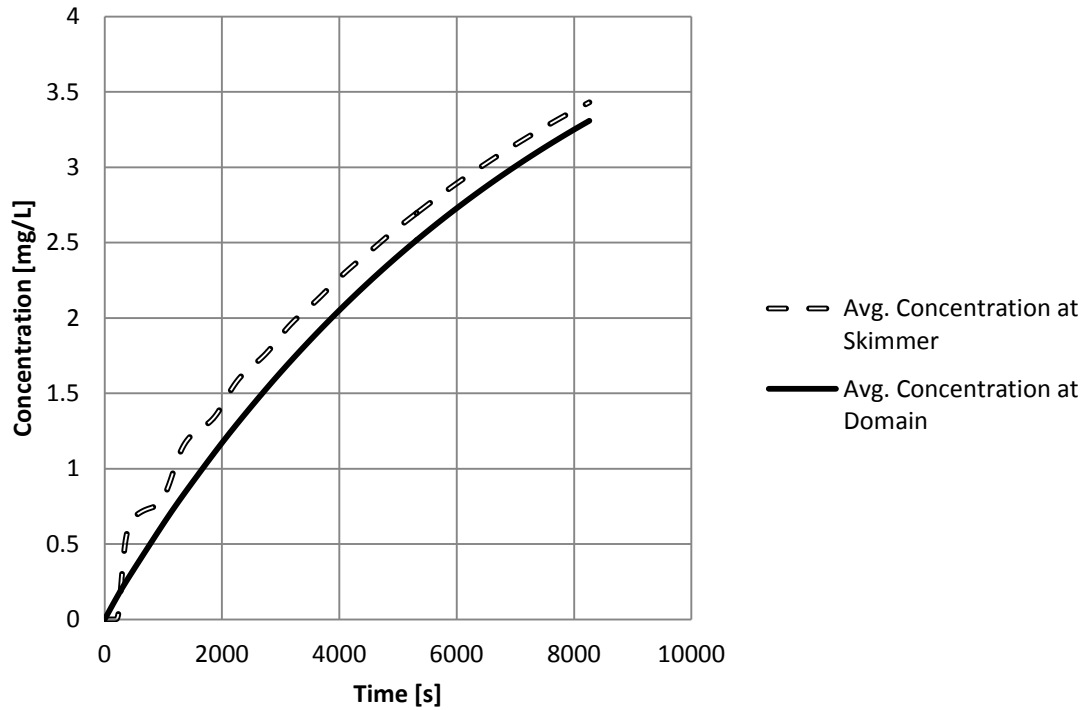**Figure 4.23**: Average concentration of hypochlorous acid in the entire domain over 2 hours.

In all three scenarios, 5 *mg/L* hypochlorous acid was introduced into the pool through the inlets while the average concentration of hypochlorous acid gradually increased at the same rate. After 1 hour, the average concentration of hypochlorous acid in the entire swimming pool reached 1.9 *mg/L* and, after 2 hours, it reached 3.1 *mg/L*. However, the distribution of hypochlorous acid is not the same: As expected, the maximum concentration (5 *mg/L*) is near the inlets and it occupies less than 1% of the volume of the entire domain in all three scenarios.

In Scenario 1, the minimum concentration across the domain was 2.9 *mg/L*, which occupied only 53% of the volume in the domain. The minimum concentration decreased to 2.8, and to 2.7 *mg/L* for Scenarios 2 and 3, respectively. In other words, the minimum concentration decreased as the size of the inlets increased. Furthermore, in Scenario 2, 34% of the domain had a concentration of 2.8 *mg/L*, while in Scenario 3, 26% of the domain had a concentration of 2.7 *mg/L*. Nevertheless, the average hypochlorous acid in the entire domain was almost the same in all three scenarios, even though the distribution was not uniform. The average mixing rate (ε/k) in all three scenarios was calculated to show values of 0.047/*s*, 0.034/*s*, and 0.028/*s* for Scenarios 1, 2 and 3 respectively. These results indicate that smaller inlet sizes allow improved distribution and higher mixing rates.

The following chapter will discuss the effects of chemical reactions in the case of a sudden release of urine contamination from bathers.

4.2   Chemical reactions

Bathers introduce both perspiration and urine into swimming pools, resulting in the presence of ammonia in the water where it can, in turn, react with chlorine to form chloramine. When a bather urinates in the swimming pool, a high concentration of ammonia will be released into the domain in a short period of time. For the purposes of this study, ammonia was injected into the domain for 21 *s* at a rate of 0.0013 *kg/s*, a flow rate which corresponds to the volume of the average human bladder, i.e., between 150 and 300 *cm³* (Hole, 1986). The initial concentration of ammonia in the domain before the injection is zero. The model simulates the two hours after the injection to find the decay rate of hypochlorous acid due to reaction with ammonia.

Although the primary component of urine is urea, ammonia was identified for the purposes of this study as the only component of urine as a precursor of chloramines. The reaction rate of both urea and hypochlorous acid is small, and the generation of trichloramine from urea over the period of 2 hours is relatively low (Schmalz et al., 2011). Furthermore, experimental samples demonstrate that a remarkable concentration of chloramines is derived from ammonia nitrogen rather than urea (WHO, 2006). On this basis, this study has elected to ignore the potential contribution of urea to the formation of chloramines. However, this strategy may result in an overestimation of the generation of chloramines.

The geometry of the pool, and the structure of the inlets used for the chemical reaction scenario were the same as Scenario 2, but due to computational limits, only a quarter of the complete domain was taken into account. This study worked with the assumption that no contamination is present in the re-circulated water as it entered the domain through the inlets. In reality, the recycled water may in fact contain some contamination. The presence of additional contamination will increase the decay rate of hypochlorous acid, and its final average concentration will be lower. It has been shown (above) that the average concentration of hypochlorous acid after 2 hours was approximately 3.2 *mg/L*. This it was taken to be the initial concentration for modelling the chemical reaction, although the initial concentration of ammonia is zero. At *t = 0 s* ammonia was injected into the swimming pool for 21 s.

Figure 4.24 shows the mass concentration of ammonia at three different points in time. Plane 4 is identified as the same elevation at which the urea discharge would occur. As seen in Figure 4.24, ammonia concentration tends to shift to the left side of the domain, due to the main water stream entering from the inlet at the right. This stream displaces the injected ammonia within the domain and, as the ammonia mixes with re-circulated water, it begins to react with the available free chlorine. The concentration of hypochlorous acid is much less than that of the ammonia; only a small portion of ammonia is possibly in contact with chlorine and involved in the reaction. Over a single turnover period (7200 *s*), the concentration of ammonia gradually decreases as it leaves the pool through the drain and the skimmers without reacting. Meanwhile, the concentration of free chlorine decreases dramatically. After an hour, the average concentration of hypochlorous acid is almost zero. Although hypochlorous acid is introduced continuously through the inlets, it reacts with the remaining ammonia instantaneously leaving the total

concentration of chlorine unchanged. Figure 4.25 illustrates the concentration of hypochlorous acid at different times: t = 3600 *s* and t = 7200 *s.* Ammonia at a high concentration is rapidly distributed over the whole domain and reacts with the hypochlorous acid. The available chlorine reacts instantaneously with ammonia and its average concentration remains close to zero. Therefore, after an hour, no change takes place in the average concentration of chlorine, although during this time the concentration of ammonia decreases, mainly by exiting the domain without a reaction (Figures 4.25 and 4.26). Weaver et al. (2009) studied chlorination in swimming pools and reported that, in 17% of the pools in which they had performed their experiment, the concentration of free chlorine was below the acceptable lower limit required for adequate disinfection.

Two hours after the injection of ammonia, we found a significant amount of ammonia still present in the domain. As well, high concentrations of hypochlorous acid can be found in some areas near the edges of the domain. As shown in Figure 4.27, the concentration of chloramines was initially limited to locations near the injected ammonia, but measurements at different points in time showed an increase in the concentration of monochloramine all over the domain.
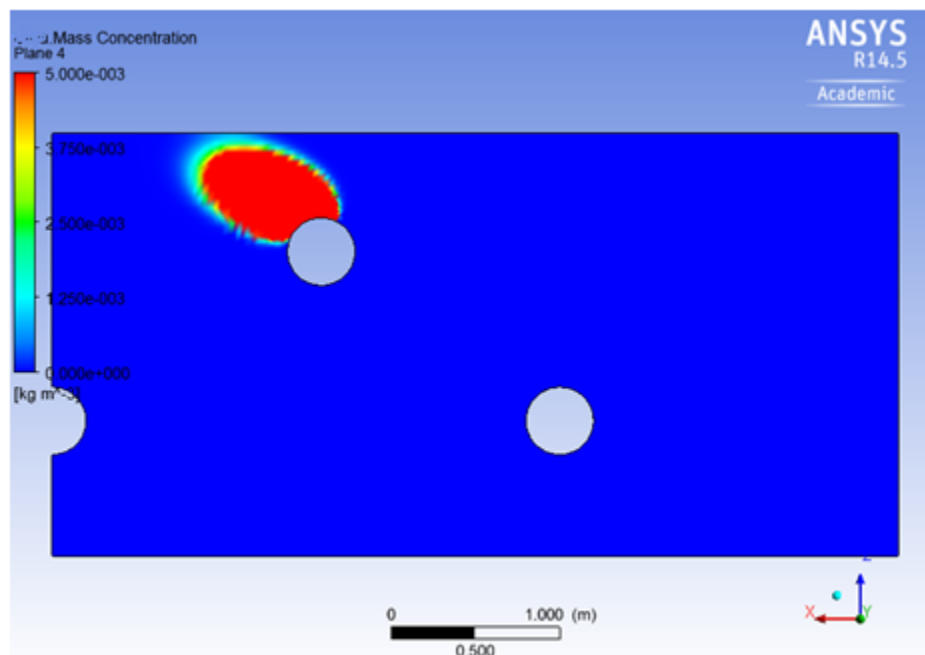
t = 21 s
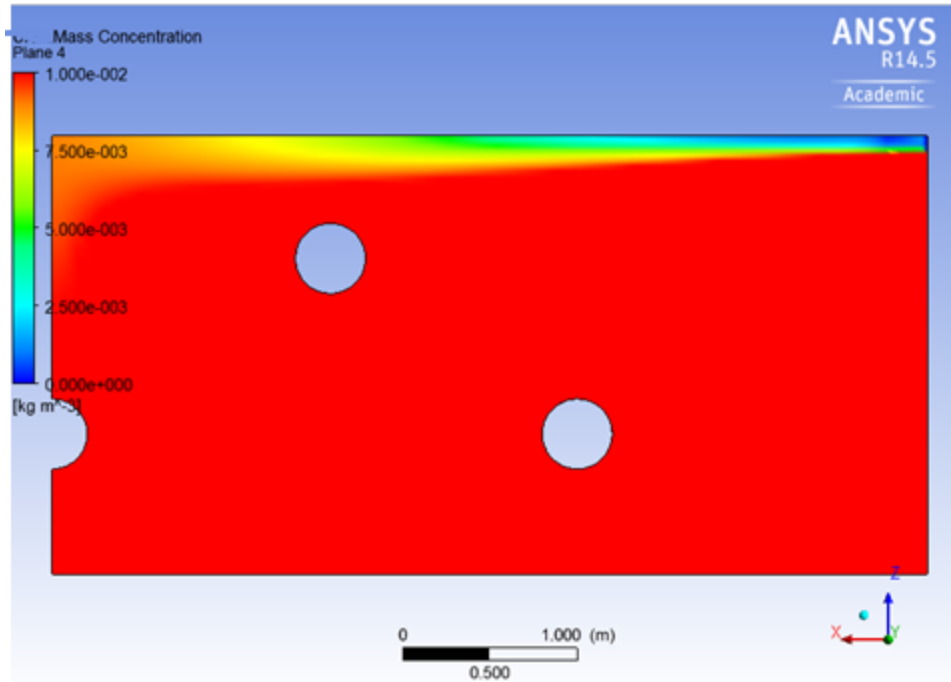
t = 3600 s
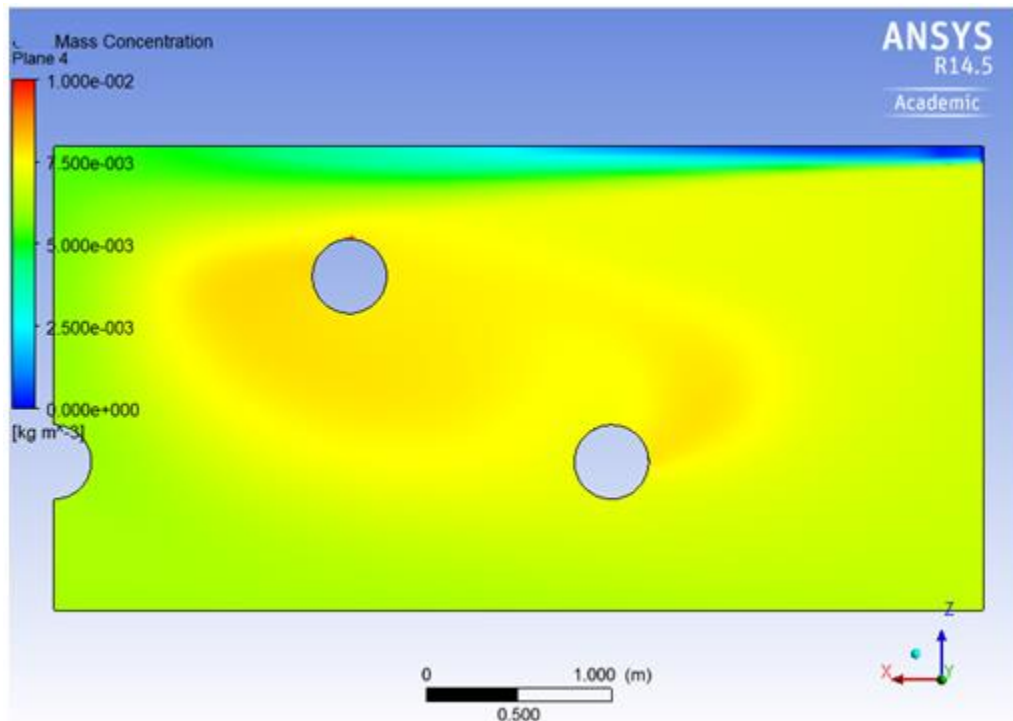
t = 7200 s

Figure 4.24: Mass concentration of ammonia at different points in time; at t=21 s ammonia is concentrated near injection point, at t=3600 s distributed all over the domain and at t= 7200 s still stays at domain.
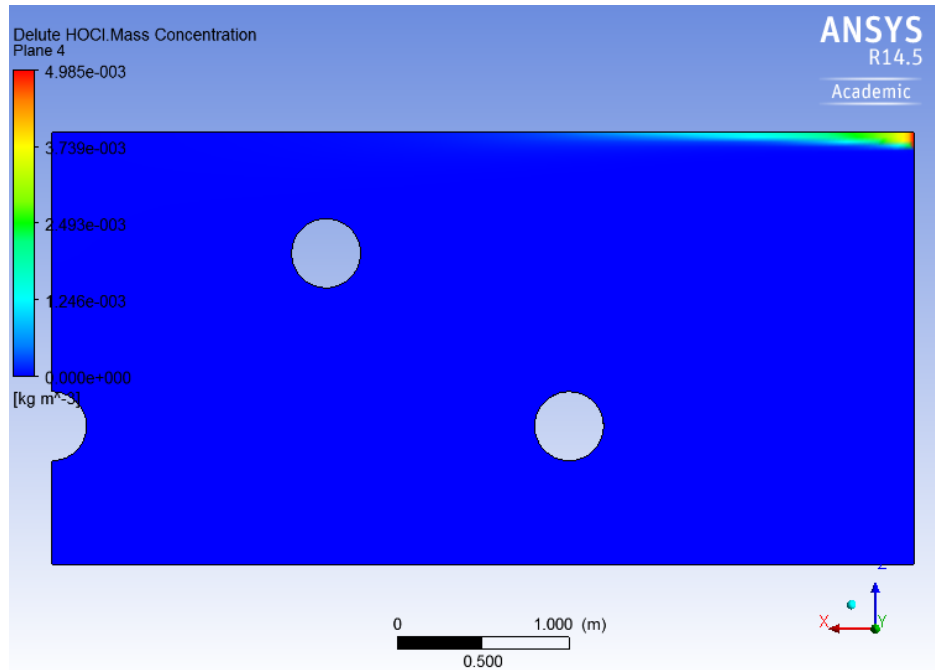
t = 3600 s
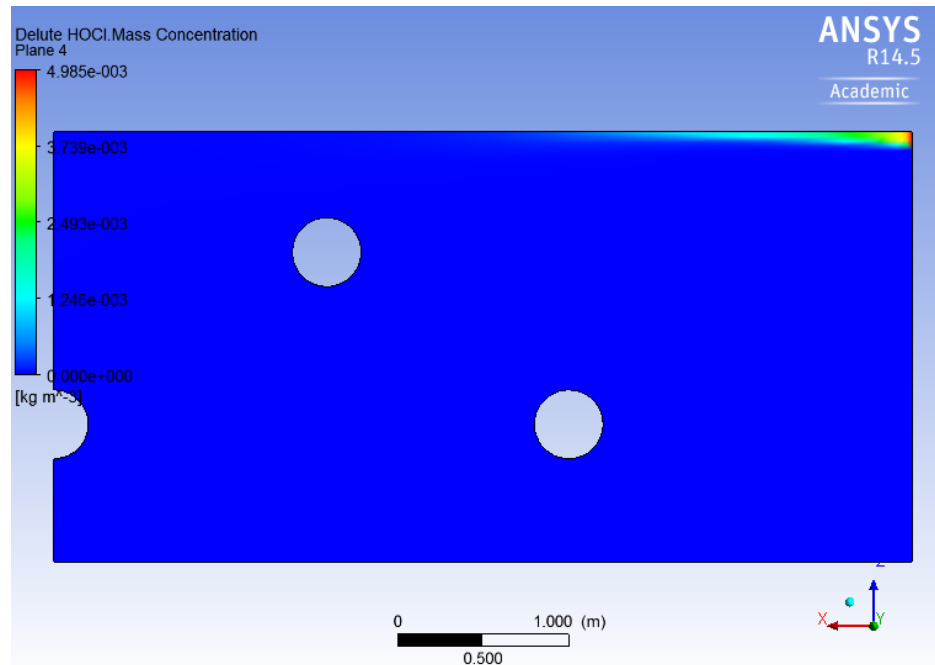
t = 7200 s

Figure 4.25: Mass concentration of chlorine at different points in time; concentration is not changed over time.

Spatial Distribution of HOCl

$t = 3600$ s

Spatial Distribution of HOCl
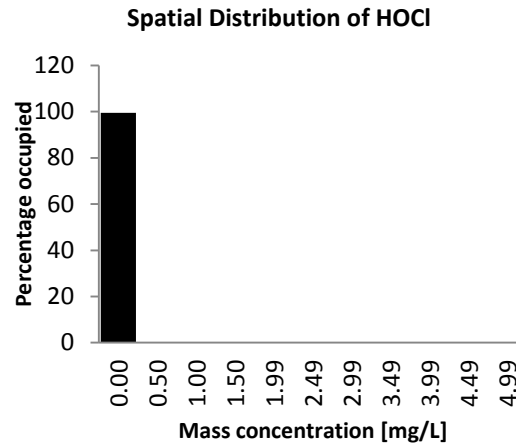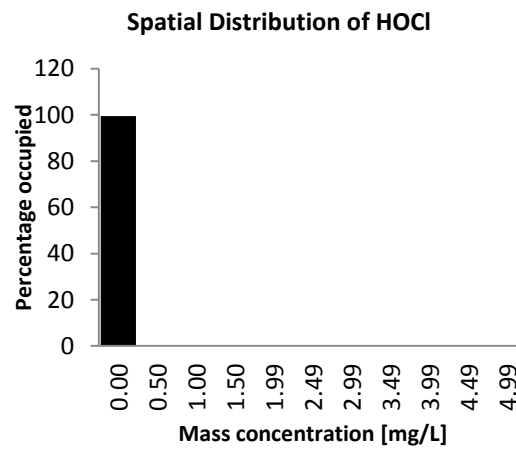
$t = 7200$ s

Figure 4.26: Spatial concentration of chlorine after 1 and 2 hours;
concentration still stay unchanged at t= 3600 s and t= 7200
s.

t = 21 s

t = 3600 s
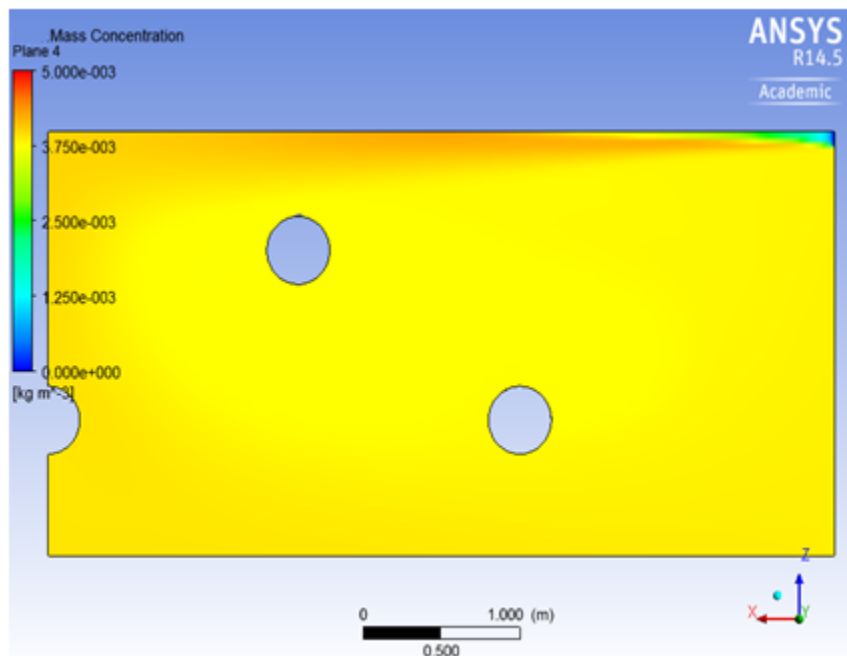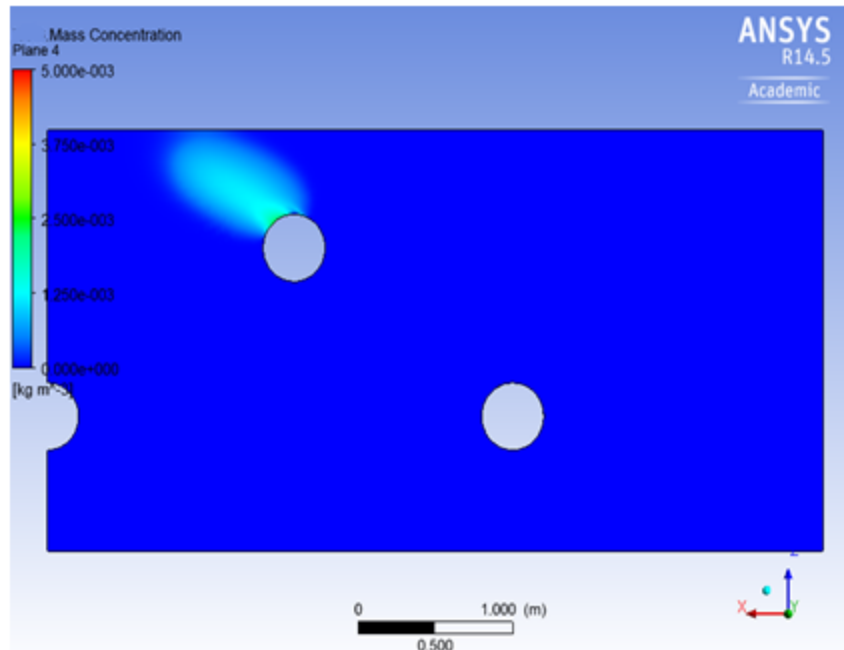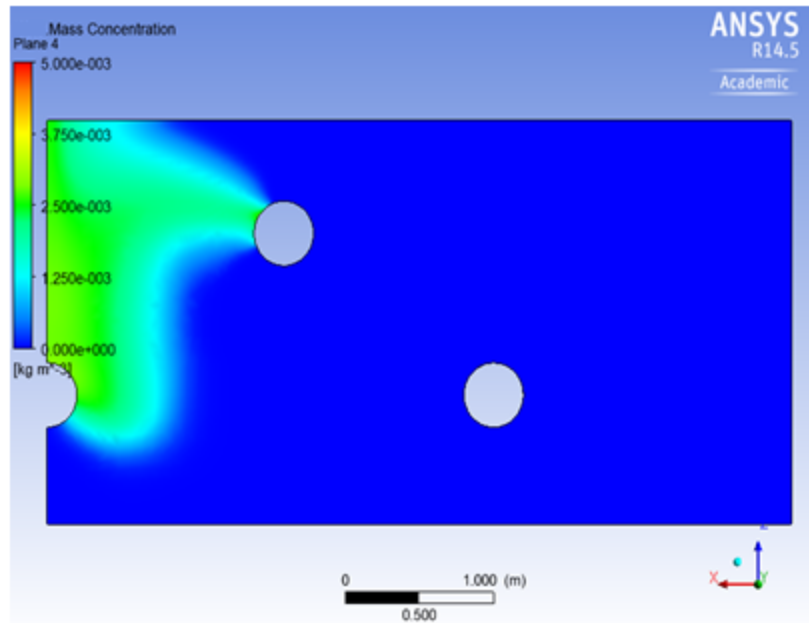
t = 100 s
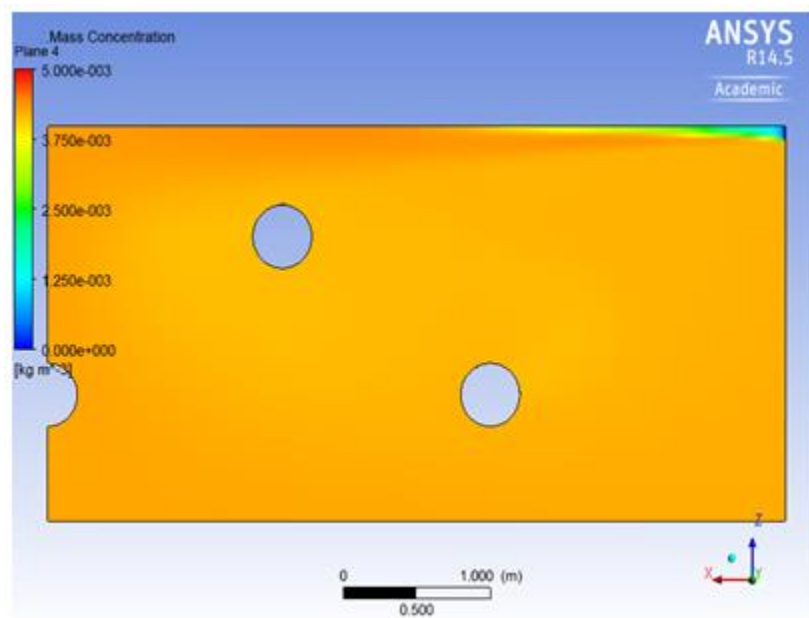
t = 7200 s

Figure 4.27: Mass concentration of chloramines at different points in time; concentration increases in time from zero to 3.9 mg/L.
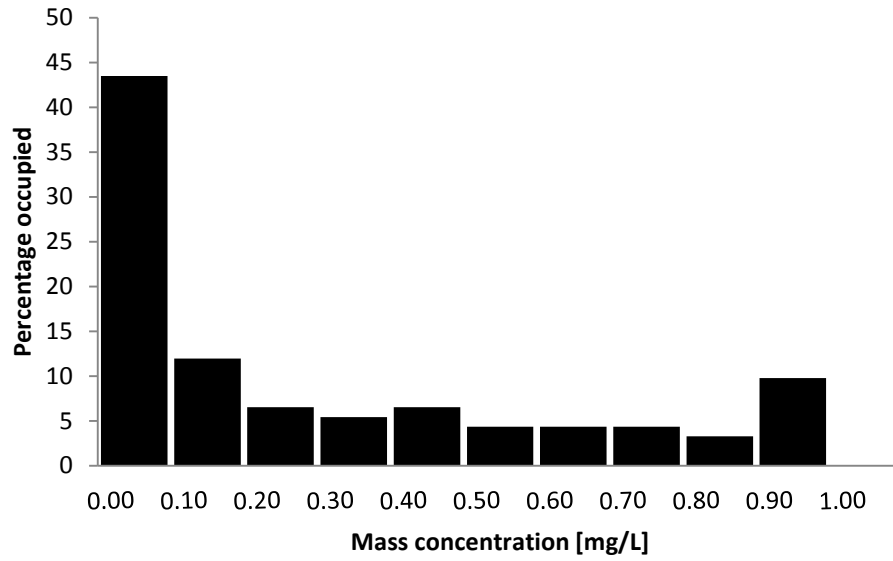
Figure 4.28: Spatial distribution of chloramines after 1 hour.
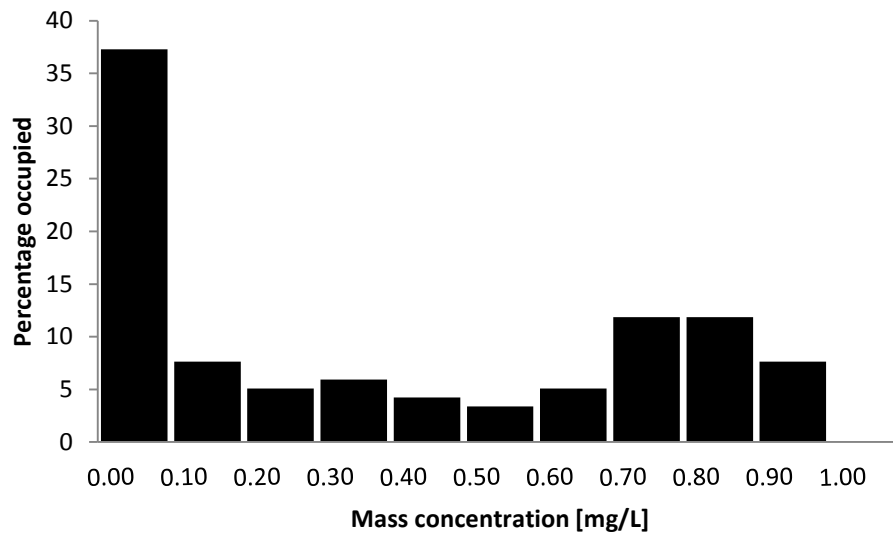
Figure 4.29: Spatial distribution of chloramines after 2 hours.

Figures 4.28 and 4.29 show the spatial distributions of the chloramines at two different time steps, 3600 *s* and 7200 *s*, respectively.
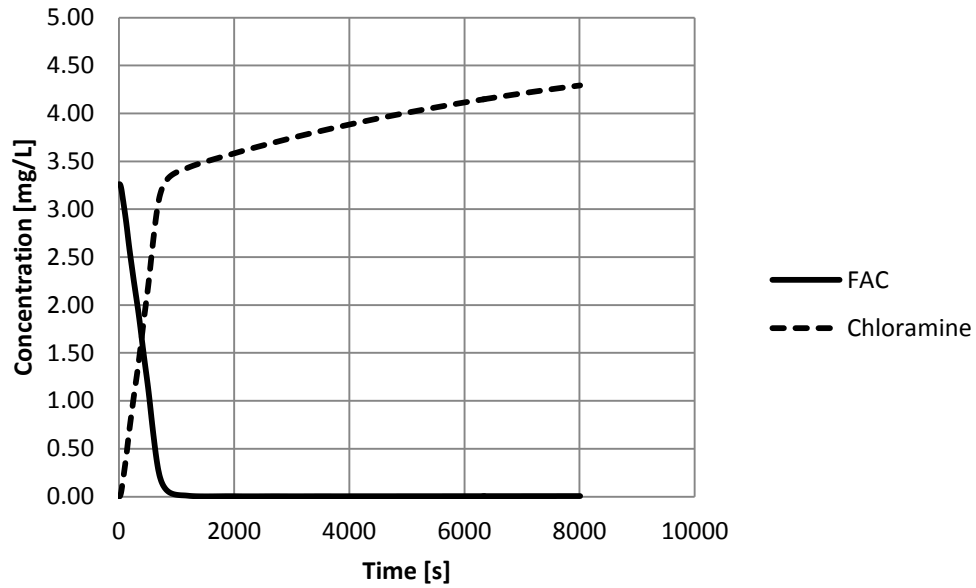
Figure 4.30: Rate of change of mass concentration of chlorine and chloramines; chlorine concentration merges to zero after 800 s while chloramines increase up to 4.3 mg/L.
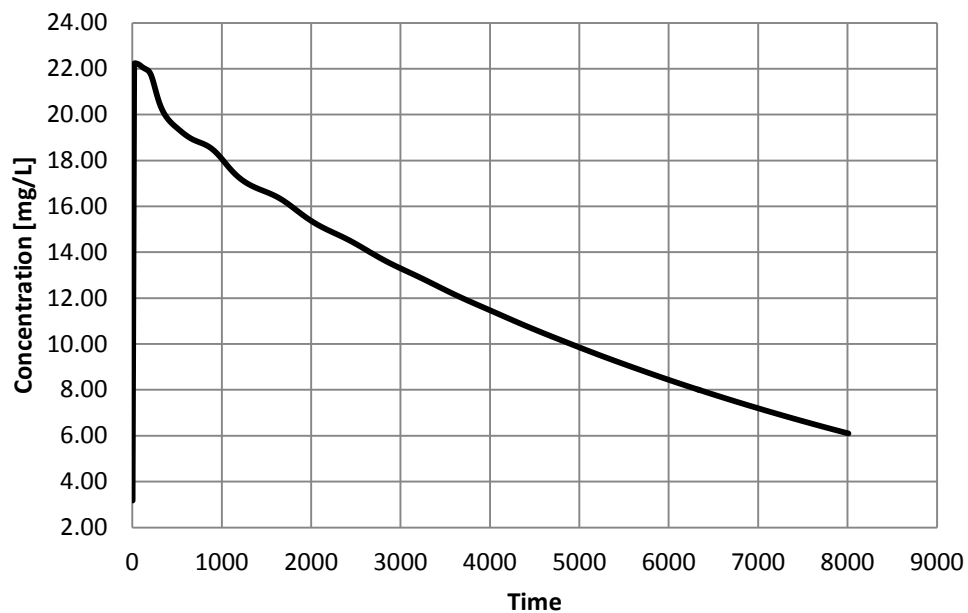
Figure 4.31: Rate of change of mass concentration of ammonia; decreases from 22 mg/L to 6 mg/L after two hours.

Figures 4.30 and 4.31 show the way in which the mass concentrations of chemical components change over time: The concentration of chloramine increased at a high rate in the first 800 s to the point where the average concentration of hypochlorous acid in the domain reached to zero. After this point, the generation rate of chloramines decrease in proportion to the injected hypochlorous acid.

4.3 Summary of results and verification

The results for all three scenarios are summarized in Table 4.1 which shows a comparison of the effects of inlet size. The ratio of turbulent eddy dissipation to turbulent kinetic energy *(ε/k)* is an important factor in determining the mixing rate, where a higher ratio indicates a higher mixing rate. Table 4.1 shows the average ratio, both at the inlet and the entire domain. Since the mass flow rate is constant in all three scenarios, a decrease in the size of the inlet results in an increase in the velocity. In Scenario 1, where the inlet size is the smallest, the *(ε/k)* ratio was significantly greater than in the other two scenarios (Scenario 3 has the smallest ratio).

Table 4.1: Summary of results.

Scenarios	Dimensions (m×m)	Inlet mass flow (kg/s)	Mean velocity (m/s)	(ε/k) Ratio at inlet (1/s)	Average (ε/k) ratio at domain (1/s)
1	0.12 × 0.12	3.4	0.22	1.42	0.047
2	0.15 × 0.15	3.4	0.14	0.84	0.034
3	0.17 × 0.17	3.4	0.11	0.44	0.028

In all selected scenarios, the average concentration gradually increases from zero to the upper limit of the concentration, i.e., the maximum concentration of introduced hypochlorous acid (5 *mg/L*). After that, the average concentration does not change with time. Plotting logarithmic values of time against logarithmic values of concentration, demonstrates a linear variation with $R^2 = 0.994$ (figure 4.32). This trend suggests an exponential decrease, represented by the following function:

$$C(t) = C_i + C_{max} \times (1 - \exp(-kt))$$ **Equation 4.1**

log time vs. log concentration

$R^2 = 0.9943$
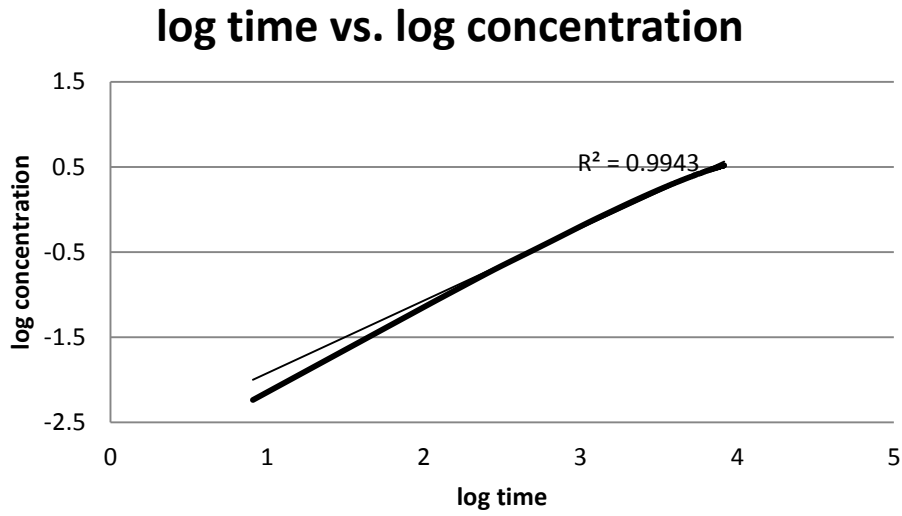
Figure 4.32: Regression of logarithmic values of time against concentration.

In Equation 4.1, C_{max} is the maximum concentration introduced, C_i is initial concentration which was also zero for this study, t is a time, and constant k can be found using a regression analysis, assigning the calculated average hypochlorous acid in the domain as the dependent variable and time as the independent variable. Analysis of Variance (ANOVA) can be summarized as follows:

$$\sum (y - y_m)^2 = \sum (y_i - y_m)^2 + \sum (y - y_i)^2 \qquad \textbf{Equation 4.2}$$

Here, the first term corresponds to the total variation in the response $C(t)$, the second term corresponds to the variation in the mean response, and the last term corresponds to error. Results from CFD modelling have been saved for every 6 seconds, so for period of 2 hours about 1200 dependent and independent variables have been saved for each scenario (Table 4.2).

Table 4.2: Summary of regression for first three scenarios.

	Scenario 1	Scenario 2	Scenario 3
Independent variable (Time, t)	t_j	t_j	t_j
Dependent variable calculated by CFD simulation (Concentration, C)	C_j	C_j	C_j
predicted value by regression (Concentration, C_j′)	$C_j' = 5(1 - \exp(-k_1 \times t_j))$	$C_j' = 5(1 - \exp(-k_2 \times t_j))$	$C_j' = 5(1 - \exp(-k_3 \times t_j))$
Constant calculated by regression(k)	K_1=0.000136	K_2= 0.000133	K_3=0.000133
Sum of concentration calculated by CFD modelling	2145	2150	2177
Sum of concentration predicted by regression	2131	2144	2174
Sum of error	0.0897	0.0286	0.0432

Hence, equation 4.1 can be written as follows:

$$C(t) = 5 \times (1 - \exp(-0.000133t)) \hspace{3cm} \textbf{Equation 4.3}$$

In order to compare these results with those produced by other studies, time and concentration can be normalized by dividing them into turnover time and C_{max} respectively:

$$\tau = \frac{t}{turnover\ period} \hspace{3cm} \textbf{Equation 4.4}$$

$$c = \frac{C(t)}{C_{max}}$$
Equation 4.5

Cloteaux et al. (2013) calculated RTD for Constant Stirred Tank Reactors (CSTRs) and compared their results with the Lagrangian approach to fluid flow for swimming pools. Figure 4.32 shows CFD Eulerian results plotted against this study.

A key factor observed in this study was the distribution of hypochlorous acid in the pool. Despite the continuous injection of chlorine, after 2 hours the average concentration of chlorine was still far less than the maximum introduced concentration. For all three inlet sizes, after 2 hours, the ratio of the average concentration to the maximum injected concentration (C_{ave}/C_{max}) = 0.6. In fact, the presence of chlorine in the swimming pool at the start-up may help to reach the desired maximum concentration more quickly. In addition, the spatial distribution of chlorine is not uniform, and it varies for different inlet sizes. After 2 hours, the minimum concentration for Scenario 1 was 2.9 g/m^3; for Scenario 2 it was 2.8 g/m^3, and for Scenario 3 it was 2.7 g/m^3.

However, the reported concentration for hypochlorous acid from experimental samplings may vary to a great extent from one study to another (Weaver et al., 2009). WHO (2006) recommends that samples should be taken from specific locations in the swimming pool each time. Usually samples are taken at the edges of the pool at a depth of 30 cm from the surface, and the assumption has been that concentration of hypochlorous acid is uniform. However, CFD simulations do not support this assumption, on the basis that the concentration of chlorine may vary significantly in different locations, even after a turnover cycle of 2 hours. In first three scenarios, the pool water is assumed to be free from contaminants other than ammonia. The presence of other chemical compounds and organic matter would be expected to reduce the average concentrations of chlorine
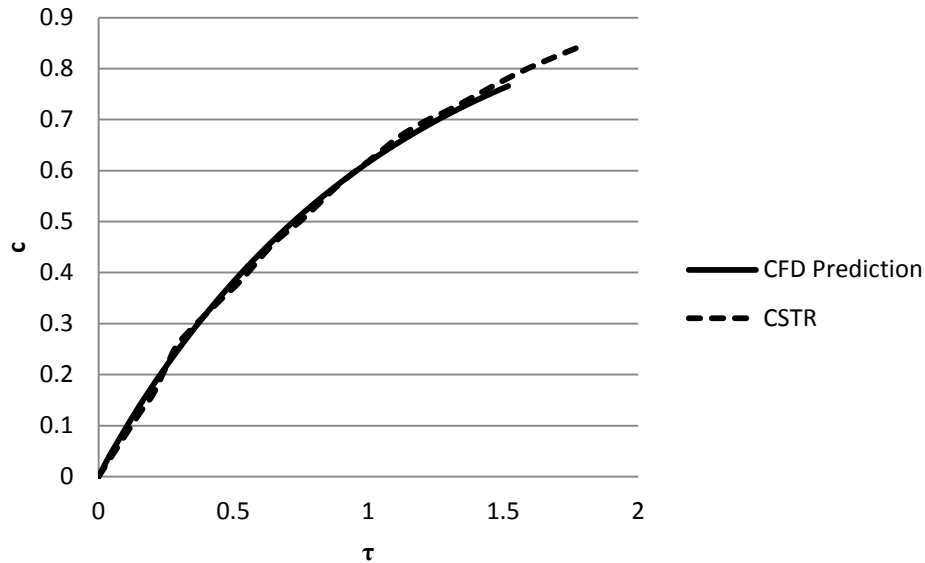
Figure 4.33: Comparison of concentration growth rate (CFD prediction) with CSTR based on results by Cloteaux et al. (2013)

Finally, the chemical reaction between hypochlorous acid and ammonia has been modelled to calculate the fate of chlorine. During the first 1000 s, the rate of change in the hypochlorous acid mass concentration is equal to the changes of chloramine (see Figure 4.30). When the mass concentration of hypochlorous acid becomes zero, the rate of change of the product decreases and becomes proportional to the rate of injected chlorine, which is 5 *mg/L*. Meanwhile, the concentration of ammonia decreases with time. The rate of change of ammonia is much higher than both hypochlorous acid and chloramines, since large amounts of ammonia exit the domain without reacting (see Figure 4.31). However, in reality contaminants would not be completely removed from the water and may partially re-enter the pool from the inlets. Therefore, it is likely that part of the ammonia may return into the domain during re-circulation. During the 2 hours period of simulation monochloramine was the only generated chloramine.

Recalling Reaction 2.3 from Chapter 2 ($HOCl + NH_3 \rightarrow NH_2Cl + H_2O$) for the complete reaction, the stoichiometric ratio of hypochlorous acid to ammonia should be ($HOCl/NH_3$) = 3.1. Accordingly, for the generation of dichloramine and trichloramine, a higher concentration of hypochlorous acid is required. In other words, when the ratio of concentration of available chlorine to ammonia is less than one, all of the free available chlorine is consumed to form

monochloramine (Benjamin and Lawler, 2013). Table 4.3 summarizes the theoretical weight
ratio for chlorine and ammonia according to the American Water Works Association [AWWA]
and American Society of Civil Engineers [ASCE] (1990).

Table 4.3: Required Cl_2/NH_3 ratio for reaction and
generation of chloramines.

Reaction	mg Cl_2 /mg NH_3
Monochloramine (NH_2Cl)	4.2
Dichloramine ($NHCl_2$)	8.4
Trichloramine (NCl_3)	12.5

Ratios in Table 4.3 in terms of hypochlorous acid to ammonia ($HOCl/ NH_3$) are 3.1, 6.2 and 9.3,
respectively. In the present study, the ratio of free available chlorine to ammonia nitrogen
($HOCl/ NH_3$) is 0.12 following the sudden release of ammonia. Almost all of the available
chlorine reacts with ammonia instantaneously to form monochloramine, and the chance of
reactions forming $NHCl_2$ and NCl_3 is significantly low. Although hypochlorous acid was
introduced into the domain continuously, the average concentration of chlorine would not change
significantly, since the available ammonia is much higher than the available chlorine for the
reaction. Therefore, for a molar ratio ($HOCl/ NH_3$) of one or less than one, monochloramine
(NH_2Cl) is the only observed chloramine (Health Canada, 2001). The mean concentration of
FAC and chloramines from seven different pools in the experimental study of Weaver et al.
(2009) is summarized in Table 4.4. This study showed that the concentration of trichloramine is
significantly less than monochloramine and dichloramine. This table also can be used to verify
numerical simulations. Free available chlorine measured in different pools varies from 0.6 mg/L
to 2.08 mg/L. Although these sampling were collected over long period (6 month) they confirm
findings from current study that concentration of chlorine may vary to high extent and in some
cases it may not be sufficient.

Table 4.4: Mean concentration of chloramines and FAC from experimental samples (after Weaver et al, 2009).

Compounds (*mg/L*)	Pool 1	Pool 2	Pool 3	Pool 4	Pool 5	Pool 6	Pool 7
FAC	1.48	1.16	1.25	1.46	2.51	0.603	2.08
NH_2Cl	0.24	0.194	0.151	0.13	0.186	0.167	0.492
$NHCl_2$	0.053	0.616	0.05	0.042	0.098	0.048	0.188
NCl_3	0.05	0.632	0.045	0.04	0.014	0.01	0.154
Total Chloramine	0.343	1.442	0.246	0.212	0.298	0.225	0.834

Even in the worst case scenario, some areas in the pool may have a high chlorine concentration, even though the average concentration in the entire domain would be almost zero. These areas are more likely to be situated closer to the edges of the domain and in the vicinity of the inlets. In order to monitor the available chlorine, British Columbia Guidelines for Pool Operations has regulated that sampling should be done twice a day (British Columbia Ministry of Health, 2014). This means that any temporal fluctuations in the available chlorine will be neglected between the two samplings, which may take place anywhere between 4 to 8 hours apart. The CFD simulations in the scenarios presented here indicate that at least 8 hours are required in order to reach the desirable maximum concentration—without taking into consideration the loss of hypochlorous acid due to reactions with other contaminants. Ignoring these variations over time can lead to serious risks to human health.

This study proposes that pool managers should collect water samples from the swimming pool more frequently and not just from areas near the edges or corners of the pool. Improved sampling methods can greatly improve the accuracy of the data, especially with respect to monitoring the concentration of DBPs and free chlorine. Reliable data are vital for more accurate assessments of human exposure to health risks.

4.4 Exposure assessment

Research indicates that some DBPs in swimming pools may be toxic or even carcinogenic, and therefore pose serious risks to human health. The results from this research will help to identify some of the potential risks to bathers and will contribute to improved risk management plans for indoor swimming pools. As a result of reaction between ammonia and chlorine, trichloramine may be generated, which is highly volatile and has been linked to respiratory issues, including asthma (WHO, 2006; Carbonnelle et al., 2002; Thickett et al., 2002; Bernard et al., 2003). Richardson et al. (2010) reported average concentration of 0.17–0.43 mg/m^3 of trichloramine in the air at indoor swimming pools.

In this study, for the two-hour period, monochloramine was the only chloramine generated. The formation of trichloramine in swimming pools depends on many factors, especially when found in a higher ratio of chlorine to nitrogen, which produces more trichloramine. This study showed that, following the injection of ammonia, the ratio of (HOCl/ NH_3) decreased suddenly in the first few moments, after which it gradually began to increase (Figure 4.32). This trend will continue until all of the injected ammonia exits the domain, a period that would take over two hours. However, the exponential trend show in Figure 4.32 reveals that after 14 hours, the ratio of (HOCl/ NH_3) reaches to 9, where generation of trichloramine can be significant. Concentration of ammonia after 14 hours is about 0.0005 *mg/L* and concentration of hypochlorous acid is 0.0046 *mg/L*, therefore it is expected to generate 0.003 *mg/L* of trichloramine. Schmaltz et al. (2011) calculated the trichloramine flux from water to air and reported 1.8×10^{-3} g/$h\,m^2$, 7×10^{-3} g/$h\,m^2$, and 12.6×10^{-3} g/$h\,m^2$ for quiescent, rippled, and rough water surfaces respectively. Considering quiescent for this study, where surface area is $12.5m^2$, flux rate from water to air would be 22.5 g/h . Concentration of trichloramine in air depends on so many factors such as air volume and ventilation rate etc.

Under real conditions in swimming pools, where heavy loads of contaminants may be introduced to water continuously over a longer period of time, rate of generation of trichloramine may be higher. Weng and Blatchley (2011) measured concentration of chloramines and chlorine over ten days in a swimming pool. They have reported that concentration of trichloramine increased from

0.2 *mg/L* to 0.8 *mg/L.* Meanwhile concentration of monochloramine and dichloramine were reported as 0.2 *mg/L* and 0.1 *mg/L* respectively.

The focus of this study was specifically to look at the generation of chloramines from ammonia, without taking into account other precursors (such as urea). Schmalz et al. (2011) reported that for (Cl/N) =1, less than 1% of urea nitrogen will be converted to trichloramine over a period that could take up to 72 hours.

Exposure to chlorine and chlorination by-products in swimming pools can occur by way of ingestion, inhalation, or contact with the skin. As noted above, trichloramine is volatile and may pose adverse health effects if inhaled. However, for the period of two hours and given ratios generation of trichloramine is unlikely. In addition to trichloramine, there are three other potentially harmful components available in pool water; chlorine, monochloramine and dichloramine. Chlorine concentration up to 5 *mg/L* is permitted according to the WHO (2006) guidelines for drinking water. The ingestion of chlorination by-products considered in our study, according to the calculations set out above, are not likely to have adverse health effects. Additionally, there are no reports in the research literature to date with respect to potential toxic effects from the ingestion of monochloramine and dichloramine (Florentin et al., 2011).
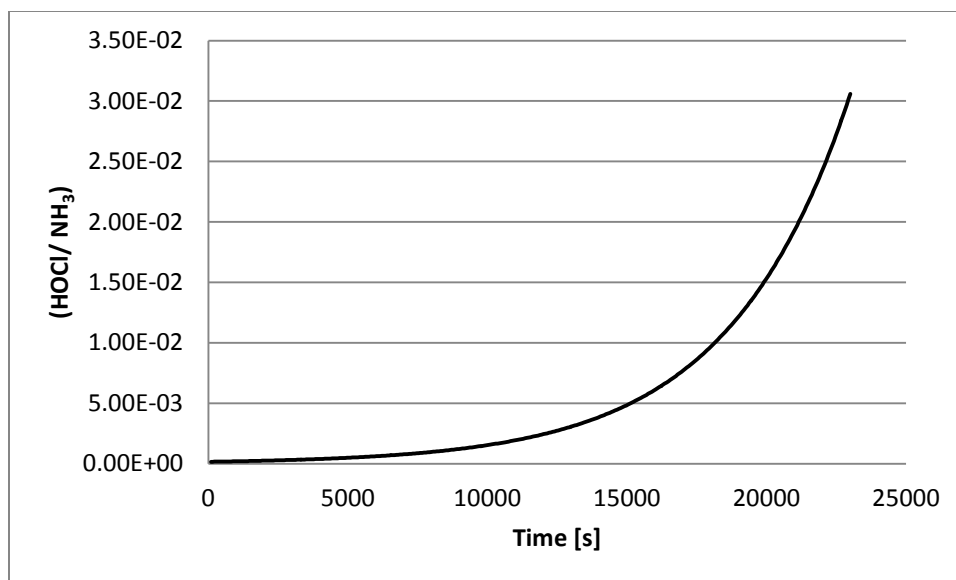
Figure 4.32: Average ratio of (HOCl/ NH₃); ratio increase exponentially over time.

It is important to note that, in the time frame established for the purposes of this study, a significant amount of ammonia remains in the domain, unchanged by chemical reactions—an amounts that indicates a potential hazard (ATSDR 2004). The concentration contours in Figures 4.24, 4.25, and 4.26 indicate that the minimum concentration of hazardous components is near the inlets and that the concentration of ammonia and its by-products increase in the vicinity of the outlets.

4.4.1 Potential application to TTHM

The focus of this study was on the fate of chlorine and the generation of chloramine in swimming pools. The method presented here can also be applied to study formation and fate of regulated DBPs, provided the chemical reaction rate is less than mixing rate *(ε/k)*. Trihalomethanes (THM) are of particular interest due to their relatively high concentration in

swimming pools (Richardson et al., 2010) and their potential to cause health effects (Zwiener et al., 2007).

In a recent study, Angeloudis et al. (2014) applied CFD method to calculate generation of the Total Trihalomethane (TTHM)[1] as the reaction between chlorine and Total Organic Carbons (TOC). They borrowed the mathematical model of Singer (1994) to calculate formation of TTHM in chlorine contact tanks. Singer (1994) predictive model was based on UV radiation, concentration of bromide, temperature and pH (Equation 4.6).

$$TTHM = 0.00306 \times [(TOC)(UV_{254})]^{0.44} \times (C_{cl})^{0.409} \times (Te)^{0.665}$$
$$\times (pH - 2.6)^{0.715} \times (Br + 1)^{0.036} \times t^{0.265}$$

Equation 4.6

In a similar way, a TTHM formation model could be coupled with the CFD model presented in this thesis to evaluate the fate of TTHM in swimming pools. For this purpose, predictive model of Chang et al. (1996) was applied. This predictive model is simple and robust (Sadiq and Rodriguez, 2004) as it is merely a function of TOC and chlorine. This model can be written as following:

$$TTHM = 12.7 \times (TOC)^{0.291} \times t^{0.271} \times D^{-0.072}$$

Equation 4.7

where (TOC) is concentration of total organic carbon (*mg/L*), *t* is time in hours, *D* is concentration of hypochlorous acid (*mg/L*) and concentration of TTHM is in (*µg/L*). Decay rate of TOC and hypochlorous acid were calculated in CFD model and inserted in Equation 4.6 to

---

[1] Total trihalomethanes (TTHM) is the combined total of the concentrations of chloroform, bromodichloromethane, dibromochloromethane and bromoform. Most drinking water regulations for THMs are expressed as TTHM.

find TTHM. Initial concentration of TOC and chlorine assumed to be 4.5 (*mg/L*) and 3.2 (*mg/L*) respectively. Figure 4.34 shows concentration of TTHM.
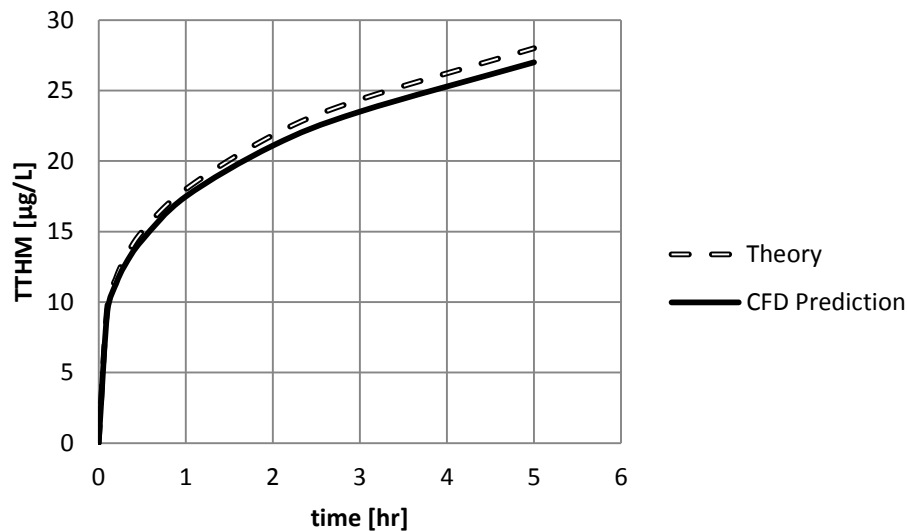
Figure 4.34: Concentration of TTHM calculated by CFD modelling

Figure 4.34 above demonstrates that CFD prediction is slightly lower than the original prediction, since concentration of chlorine and TOC were changing with time. As compared to the results reported by Angeloudis et al. (2014), less TTHM was predicted in this study. It can be explained by the basic differences between predictive models of Chang et al. (1996) and Singer (1994) which have limited accuracy depending on site specific data. For example, in the later model, additional control variables such as UV radiation, bromide concentration were used to predict TTHM concentration.

Chapter 5: Conclusions and Recommendations

5.1   Major findings and conclusions

This research has numerically modelled the fate of chlorine in an indoor swimming pool using computational fluid dynamics (CFD). The effect of inlet size on the chlorination process was examined and the chemical reaction between chlorine and ammonia was analyzed. In order to have a more realistic simulation Eulerian approach has been applied to model fate of chlorine and associate DBPs. This research has demonstrated that more frequent water samples should be taken in the indoor swimming pools as well as sampling locations should represent the complete geometry of the pool not just close to the edge, which is a current practice. The specific outcomes of the research are summarized as following:

- The distribution of chlorine in the pool has been found to be non-uniform. In addition, this study found that the concentration profile of the chlorine varies significantly at different depths in the swimming pool.

- The effect of inlet size on the hydraulic behavior of swimming pools was investigated. Smaller inlet sizes allow improved distribution and higher mixing.

    - In order to predict the average available chlorine in the entire domain, a simple regression equation, as a function of time and injected chlorine concentration, has been proposed.

- After two hours (turnover period) average concentration of chlorine in the domain is 60% of the maximum injected chlorine. In order to reach desired concentration about 5 hours is required. After 5 hours concentration of chlorine reaches to its highest level and would not change afterward (in absence of chemical reactions)

- Based on chemical reaction between ammonia and chlorine (a sudden release of ammonia into the water), this research demonstrated that the maximum allowable chlorine might be insufficient in the short term (<2 hours).

- Sampling conducted every 4-8 hours may not necessarily reflect the variation in concentration over time (at least 8 hours are required to reach desirable maximum concentration).

- Eddy Dissipation Concept for micromixing reaction can also be used to improve predictive models for TTHM and other DBPs.

The results of this research have the potential to assist pool managers to minimize some of the potential health risks associated with exposure to the water in swimming pools. These results will also contribute in shaping guidelines for design engineers; as an example it may be suggested that:

- Sampling period should be defined as function of turnover period; at least one sample is required per turnover period. For example if turnover period is two hours, sampling may be conducted every two hour. More frequent turnover requires more sampling. Additional sampling may give a greater scope of chlorination process.

- Although there is a greater cost in additional injection ports the increased numbers of inlets will result in a more effective distribution of chorine, and can help to increase the efficiency of chlorination process.

- At this study only formation of chloramines have been considered. Generated amount chloramines at given scenario could not expose any risk to bathers. However, available chlorine may not be sufficient to react with other contaminants.

- As it is recommended in some guidelines (Chapter 2) It may be helpful to increase concentration of chlorine to higher levels at least once a day in the absence of swimmers.

5.2   Limitations

- This study has been limited by the assumption of negligible volatilization of chemical components in the CFD analysis. This could lead to an overestimation of the chemical components present in water.

- This study was also limited by the necessity to reduce the CPU time which consequently restricted modelling of only one quarter of the domain. This could have caused an overestimation of the concentration of ammonia.

- This study did not consider the effects of a possible re-circulation of ammonia, and subsequent reactions with other components in pool water which can be subjected to further research. Evaporation of chemicals was ignored this could have caused an overestimation of the concentration in the water.

5.3   Recommendations

There have been limited research done that may allow comprehensive understanding of chlorination process in swimming pools and related health consequences effects due to exposure to chlorination and its DBPs. Future research should
- investigate the effects of inlet and outlet positions in the flow regime
- consider the effect of volatilization
- model the chemical reaction for the entire geometry of the pool
- model the hydraulic behavior of non-symmetrical pool designs (e.g., pools with varying depths)
- consider chemical components other than ammonia
- study the fate of other DBPs, such as HAAs, etc.; and
- perform a detailed human exposure and health risk assessment.

References

American Institute of Aeronautics and Astronautics [AIAA]. (1998). Guide for the Verification and Validation of Computational Fluid Dynamics Simulations (G-077-1998e).

American Water Works Association [AWWA] & American Society of Civil Engineers [ACSE]. 1990. *Water Treatment Plant Design* (2nd ed.). New York: McGraw-Hill Inc.

Angeloudis, A., Stoesser, T., & Falconer, R. (2014). Predicting the disinfection efficiency range in chlorine contact tanks through a CFD-based approach. *Water Research, 60*, 118-129.

ANSYS, C.F.X. (2012). Release 14.5. *ANYSYS CFX-Solver Theory Guide*. ANYSIS.

Baldyga, J., & Pohorecki, R. (1995). Turbulent micromixing in chemical reactors: A review. *The Chemical Engineering Journal and the Biochemical Engineering Journal, 58*(2), 183-195.

Baldyga, J., Bourne, J.R., & Hearn, S.J. (1997). Interaction between chemical reactions and mixing on various scales. *Chemical Engineering Science, 52*(4), 457-466.

Bardina, J. E., Huang, P. G., & Coakley, T. J. (1997). Turbulence modeling validation. *NASA Technical Memorandum 110446*. Retrieved from http://ntrs.nasa.gov/archive/nasa/casi.ntrs.nasa.gov/19970017828.pdf

Benjamin, M. M., & Lawler, D. F. (2013). *Water quality engineering: physical/chemical treatment processes*. John Wiley & Sons.

Bernard, A., Carbonnelle, S., de Burbure, C., Michel, O., & Nickmilder, M. (2006). Chlorinated pool attendance, atopy, and the risk of asthma during childhood. *Environmental Health Perspectives, 114*(10), 1567-1573.

Bernard, A., Carbonnelle, S., Michel, O., Higuet, S., De Burbure, C., Buchet, J.P., Hermans, C., Dumont, X., & Doyle, I. (2003). Lung hyperpermeability and asthma prevalence in schoolchildren: Unexpected associations with the attendance at indoor chlorinated swimming pools. *Occupational and Environmental Medicine, 60*(6), 385-394.

Bernard, A., Nickmilder, M., & Voisin, C. (2008). Outdoor swimming pools and the risks of asthma and allergies during adolescence. *European Respiratory Journal, 32*(4), 979-988.

Blatchley, E.R., & Cheng, M. (2010). Reaction mechanism for chlorination of urea. *Environmental Science & Technology, 44*(22), 8529-34. doi:10.1021/es102423u

British Columbia Ministry of Health. (2011). *B.C. Guidelines for Swimming Pool Design* (April 2011).

Carbonnelle, S., Francaux, M., Doyle, I., Dumont, X., de Burbure, C., Morel, G. Michel, O., & Bernard, A. (2002). Changes in serum pneumoproteins caused by short-term exposures to nitrogen trichloride in indoor chlorinated swimming sools. *Biomarkers: Biochemical Indicators of Exposure, Response, and Susceptibility to Chemicals, 7*(6), 464-78.

Catto, C., Sabrina, S., Ginette, C. T., Manuel, R., & Robert, T. (2012). Occurrence and spatial and temporal variations of disinfection by-products in the water and air of two indoor swimming pools. *International journal of environmental research and public health*, 9(8), 2562-2586.

CDC (Centers for Disease Control and Prevention). (2001). Model Aquatic Health   Code (MAHC) Retrieved from http://www.cdc.gov/healthywater/swimming/pools/mahc/structure-content/index.html

Chang, E. E., Chao, S. H., Chiang, P. C., & Lee, J. F. (1996). Effects of chlorination on THMs formation in raw water. *Toxicological & Environmental Chemistry*, 56(1-4), 211-225.

Chao, M.S. (1968). The diffusion coefficients of hypochlorite, hypochlorous acid, and chlorine in aqueous media by chronopotentiometry. *Journal of the Electrochemical Society*, *115*(11),1172-1174.

Chowdhury, S., Al-Hooshani, K., & Karanfil, T. (2014). Disinfection byproducts in swimming pool: Occurrences, implications and future needs. *Water Research, 15*(53), 68-109.

Cimbala, J,. & Cengel, Y. (2006). Fluid mechanics: Fundamentals and applications. Columbus, OH: McGraw-Hill Education.

Cloteaux, A., Gérardin, F., & Midoux, N. (2013). Influence of swimming pool design on hydraulic behavior: A numerical and experimental study. *Engineering, 5*(5), 511-524.

Deborde, M., & von Gunten, U. (2008). Reactions of chlorine with inorganic and organic compounds during water treatment: Kinetics and mechanisms: A critical review. *Water Research, 42*(1-2), 13-51. doi:http://dx.doi.org/10.1016/j.watres.2007.07.025

Dyck, R., Sadiq, R., Rodriguez, M. J., Simard, S., & Tardif, R. (2011). Trihalomethane exposures in indoor swimming pools: A level III fugacity model. *Water Research*, *45*(16), 5084-5098.

Erdinger, L., Kuhn, K. P., Kirsch, F., Feldhues, R., Frobel, T., Nohynek, B., & Gabrio, T. (2004). Pathways of trihalomethane uptake in swimming pools. *International Journal of Hygiene and Environmental Health*, *207*(6), 571-575.

Florentin, A., Hautemaniere, A., & Hartemann, P. (2011). Health effects of disinfection by-products in chlorinated swimming pools. *International Journal of Hygiene and Environmental Health, 214*(6), 461-469.

Greene, D.J., Farouk, B., & Haas, C.N. (2004). CFD design approach for chlorine disinfection processes. *Journal - American Water Works Association, 96*(8), 138-150.

Hannon, J., Hearn, S., & Marshall, L. (1998). *Assessment of CFD Approaches to Predicting Fast Chemical Reactions*. American Institute of Chemical Engineers.

Health Canada. (2001). Chemistry of chlorine formation. Retrieved from http://www.hc-sc.gc.ca/ewh-semt/pubs/contaminants/psl2-lsp2/inorg_chloramines/index-eng.php#a212

Health Canada. (2006/2009). *Guidelines for Canadian Drinking Water Quality: Guideline Technical Document: Trihalomethanes* (with April 2009 addendum). Retrieved from http://www.hc-sc.gc.ca/ewh-semt/alt_formats/pdf/pubs/water-eau/trihalomethanes/trihalomethanes-eng.pdf

Hjertager, L.K., Hjertager, B.H., & Solberg, T. (2002). CFD modelling of fast chemical reactions in turbulent liquid flows. *Computers & Chemical Engineering, 26*(4), 507-515.

Hole, J. W. (1986). *Essentials of human anatomy and physiology.* Dubuque, Iowa: W.C. Brown Co.

Isaac, R.A., & Morris, J.C. (1983). Transfer of active chlorine from chloramine to nitrogenous organic compounds. 1. Kinetics. *Environmental Science & Technology* 17(12): 738-742.

Jafvert, CT, & Valentine, RL. (1992). Reaction Scheme for the Chlorination of Ammoniacal Water. *Environmental Science & Technology, 26*(3), 577-586. doi:10.1021/es00027a022 http://pubs.acs.org/doi/abs/10.1021/es00027a022

Jones, W.P. & Launder, B. (1972). The prediction of laminarization with a two-equation model of turbulence. *International Journal of Heat and Mass Transfer, 15*(2), 301-314.

Launder, B.E., & Sharma, B.I. (1974). Application of the energy-dissipation model of turbulence to the calculation of flow near a spinning sisc. *Letters in Heat and Mass Transfer, 1*(2), 131-137.

Launder, B.E., & Spalding, D.B. (1974). The numerical computation of turbulent flows. *Computer Methods in Applied Mechanics and Engineering, 3*(2), 269-289.

Levesque, B., Duchesne, J.F, Gingras, S., Lavoie, R., Prud'Homme, D., Bernard, E., Boulet, L.P., & Ernst, P. (2006). The determinants of prevalence of health complaints among young competitive swimmers. *International Archives of Occupational and Environmental Health, 80*(1), 32-39.

Lian, L., Li, J., & Blatchley III, E. R. (2014). Volatile Disinfection Byproducts Resulting from Chlorination of Uric Acid: Implications for Swimming Pools. *Environmental science & technology,* 48(6), 3210-3217.

Liu, C.H., & Barkelew, C.H. (1986). Numerical analysis of jet-stirred reactors with turbulent flows and homogeneous reactions. *AIChE Journal, 32*(11), 1813-1820.

Liu, Y., & Ducoste, J. (2006). Numerical simulation of chloramines formation in turbulent flow using a multi-fluid micromixing model. *Environmental Modelling & Software, 21*(8), 1198-1213.

Magnussen, B.F., & Hjertager, B.H. (1976). On mathematical modeling of turbulent combustion with special emphasis on soot formation and combustion. *Sixteenth Symposium (International) on Combustion* (pp. 719-729)*.* Pittsburgh: The Combustion Institute.

National Aeronautics and Space Administration [NASA]. (2008) CFD analysis process. Retrieved from http://www.grc.nasa.gov/WWW/wind/valid/tutorial/process.html

National Collaborating Centre for Environmental Health [NCCEH | CCNSE]. (2014). Pool chlorination and closure guidelines. Retrieved from http://ncceh.ca/en/professional_development/practice_questions/pool_chlorination

Nemery, B., Hoet, P. H. M., & Nowak, D. (2002). Indoor swimming pools, water chlorination and respiratory health. *European Respiratory Journal*, *19*(5), 790-793.

Pohorecki, R., & Bałdyga, J. (1983). The use of a new model of micromixing for determination of crystal size in precipitation. *Chemical Engineering Science, 38*(1), 79-83.

Pope, S.B. (2000). *Turbulent Flows*. New York: Cambridge University Press.

Qiang, Z., & Adams, C.D. (2004). Determination of monochloramine formation fate constants with stopped-flow spectrophotometry. *Environmental Science & Technology, 38*(5), 1435-1444. doi:10.1021/es0347484 http://dx.doi.org/10.1021/es0347484

Richardson, S. D., DeMarini, D. M., Kogevinas, M., Fernandez, P., Marco, E., Lourencetti, C., & Villanueva, C. M. (2010). What's in the pool? A comprehensive identification of disinfection by-products and assessment of mutagenicity of chlorinated and brominated swimming pool water. *Environmental Health Perspectives, 118*(11), 1523-1530. doi: 10.1289/ehp.1001965

Richardson, S. D., Plewa, M. J., Wagner, E. D., Schoeny, R., & DeMarini, D. M. (2007). Occurrence, genotoxicity, and carcinogenicity of regulated and emerging disinfection by-products in drinking water: A review and roadmap for research. *Mutation Research/Reviews in Mutation Research, 636*(1), 178-242.

Rook, J. J. (1977). Chlorination reactions of fulvic acids in natural waters. *Environmental Science & Technology, 11*(5), 478-482.

Sadiq, R., & Rodriguez, M.J. (2004). Disinfection by-products (DBPs) in drinking water and predictive models for their occurrence: A review. *The Science of the Total Environment, 321*(1-3), 21-46. doi:10.1016/j.scitotenv.2003.05.001

Sagaut, P. (2000). *Large Eddy Simulation for Incompressible Flows* (3rd ed.). Berlin: Springer.

Schmalz, C., Frimmel, F.H, & Zwiener, C. (2011). Trichloramine in swimming pools: Formation and mass transfer. *Water Research, 45*(8), 2681-2690.

Singer, P. C. (1994). Control of disinfection by-products in drinking water. *Journal of environmental engineering*, 120(4), 727-744.

Statistics Canada. (2013). *Sport Participation 2010, Research Paper.* Statistics Canada Catalogue no. CH24-1/2012E. Ottawa, Ontario.

Thickett, K.M., McCoach, J.S., Gerber, J.M., Sadhra, S., & Burge, P.S. (2002). Occupational asthma caused by chloramines in indoor swimming-pool air. *European Respiratory Journal, 19* (5), 827-832. doi:10.1183/09031936.02.00232802

US Department of Health and Human Services. (2004). Toxicological profile for ammonia. Public Health Service Agency for Toxic Substances and Disease Registry.< http://www. atsdr. cdc. gov/toxprofiles/tp126. pdf.

Versteeg, H.K., & Malalasekera, W. (1995). *An Introduction to Computational Fluid Dynamics.* Harlow, England: Pearson Education Limited.

Vikesland, P.J., Ozekin, K., & Valentine, R.L. (2001). Monochloramine decay in model and distribution system waters. *Water Research, 35*(7), 1766-1776. Retrieved from http://www.ncbi.nlm.nih.gov/pubmed/11329679

Wang, H., & Falconer, R.A. (1998). Simulating disinfection processes in chlorine contact tanks using various turbulence models and high-order accurate difference schemes. *Water Research, 32*(5), 1529-1543.

Weaver, W.A., Li, J., Wen, Y., Johnston, J. Blatchley, M.R, & Blatchley, E.R. (2009). Volatile Disinfection by-product analysis from chlorinated indoor swimming pools. *Water Research, 43*(13), 3308-3318.

Weng, S.C. and Blatchley III, E.R., (2011) "Disinfection by-product dynamics in a chlorinated, indoor swimming pool under conditions of heavy use: National swimming competition." *Water Research* 45(16), 5241-5248.

White, G. C. (1986). *Handbook of Chlorination* (2nd ed.). New York: Van Nostrand Reinhold Company.

Wilcox, D.C. (1998). *Turbulence Modeling for CFD* (2nd ed.). La Canada, CA: DCW Industries Inc.

World Health Organization [WHO]. (2006). *Guidelines for Safe Recreational Water Environments: Vol. 2. Swimming Pools and Similar Environments*. Geneva: World Health Organization. Retrieved from http://apps.who.int/iris/handle/10665/43336#sthash.ApTFIPsW.dpuf

Yakhot, V., Orszag, S.A., Thangam, S., Gatski, T.B., & Speziale, C.G. (1992). Development of turbulence models for shear flows by a double expansion technique. *Physics of Fluids A (Fluid Dynamics), 4*(7): 1510-1520.

Yang, P.J., Pham, J.C., Choo, J., & Hu, D.L. (2013). Law of urination: All mammals empty their bladders over the same duration. Preprint retrieved from arXiv:1310.3737 [physics.flu-dyn]

Zwiener, C., Richardson, S.D., De Marini, D.M. Grummt, T., Glauner, T, & Frimmel, F.H. (2007). Drowning in disinfection byproducts? Assessing swimming pool water. *Environmental Science & Technology, 41*(2), 363-372.

Appendix A: Turbulence modeling

The k-ε model was originally proposed to improve the algebraic mixing length model (Bardina et al., 1997). Two major formulations that can represent the k-ε model are Standard and RNG k-ε. The Standard model was developed and studied by Jones and Launder (1972) and later developed by Launder and Sharma (1974), and Launder and Spalding (1974). For a high Reynolds number, Launder and Spalding (1974) suggested using the equation of transport for variables k and ε, such as:

$$\frac{D(\rho k)}{Dt} = \frac{\partial}{\partial x_k}\left(\frac{\mu_t}{\sigma_k}\frac{\partial k}{\partial x_k}\right) + \mu_t \frac{\partial U_i}{\partial x_k}\left(\frac{\partial U_i}{\partial x_k} + \frac{\partial U_k}{\partial x_i}\right) - \rho\varepsilon \qquad \text{Equation A .1}$$

$$\frac{D(\rho \varepsilon)}{Dt} = \frac{\partial}{\partial x_k}\left(\frac{\mu_t}{\sigma_\varepsilon}\frac{\partial \varepsilon}{\partial x_k}\right) + C_1\,\mu_t\frac{\varepsilon}{k}\,\frac{\partial U_i}{\partial x_k}\left(\frac{\partial U_i}{\partial x_k} + \frac{\partial U_k}{\partial x_i}\right)$$

$$-\rho C_2\,\frac{\varepsilon^2}{k} \qquad \text{Equation A.2}$$

Turbulent viscosity can be found as:

$$\mu_t = \frac{\rho C_\mu k^2}{\varepsilon} \qquad \text{Equation A.3}$$

Suggested constants for the k-ε model are shown in Table A.1 (Versteeg & Malalasekera, 1995).

Table A.1: Constants for the standard k-ε model.

C_μ	σ_k	σ_ε	C_1	C_2
0.09	1	1.3	1.44	1.92

For a low Reynolds number, the effects of wall and viscous sub-layer that dampen turbulent shear stress must be considered (Versteeg & Malalasekera, 1995). Launder and Spalding (1974) suggested using a modified transport equations, such as:

$$\frac{d(\rho\varepsilon)}{dt} = \frac{\partial}{\partial x_i}\left[\left(\frac{\mu_t}{\sigma_\varepsilon}+\mu\right)\frac{\partial\varepsilon}{\partial x_i}\right] + C_1\frac{\varepsilon}{k}\mu_t\frac{\partial U_i}{\partial x_i}\left(\frac{\partial U_i}{\partial x_j}+\frac{\partial U_j}{\partial x_i}\right)$$
$$-\rho\frac{C_2'\varepsilon^2}{k}-\rho\phi_1$$

<div align="right">Equation A.4</div>

$$\frac{d(\rho k)}{dt} = \frac{\partial}{\partial x_j}\left[\left(\frac{\mu_t}{\sigma_k}+\mu\right)\frac{\partial k}{\partial x_j}\right] + \mu_t\frac{\partial U_i}{\partial x_j}\left(\frac{\partial U_i}{\partial x_j}+\frac{\partial U_i}{\partial x_i}\right) - \rho\varepsilon$$
$$-\rho\phi_2$$

<div align="right">Equation A.5</div>

where,

$$\phi_1 = \frac{2\,\upsilon\mu_t}{\rho}\left(\frac{\partial^2 U_i}{\partial x_j\,\partial x_i}\right)^2$$

<div align="right">Equation A.6</div>

$$\phi_2 = 2\,\upsilon\left(\frac{\partial k^{\frac{1}{2}}}{\partial x_j}\right)^2$$

<div align="right">Equation A.7</div>

$$C_2' = C_2\left(1.0 - 0.3\exp - R_t^2\right)$$

<div align="right">Equation A.8</div>

$$C_\mu' = C_\mu\exp\left(-\frac{2.5}{\left(1+\dfrac{R_t}{50}\right)}\right)$$

<div align="right">Equation A.9</div>

R_t is the turbulent Reynolds number. Turbulent viscosity can also be found from:

$$\mu_t = \frac{\rho\,C_\mu'\,k^2}{\varepsilon}$$

<div align="right">Equation A.10</div>

And, by definition, the kinetic turbulent viscosity is:

$$\upsilon_t = \frac{\mu_t}{\rho}$$

<div align="right">Equation A.11</div>

from which the specific Reynolds stress tensor can be calculated:

$$-\tau_{ij,\,turbulent} = \upsilon_t\left(\frac{\partial U_i}{\partial x_j}+\frac{\partial U_j}{\partial x_i}\right) - \frac{2}{3}\delta_{ij}k$$

<div align="right">Equation A.12</div>

where δ_{ij} is the delta function.

The Standard k-ε model is popular in industrial applications. Moreover, wall-bounded and free shear flows can be modelled, with reasonable agreement with experimental studies. Nevertheless, according to Bardina, Huang, and Coakley (1997), this method is only accurate for small pressure gradients, and is not accurate in predicting high pressure gradients and mixing layers according to Versteeg and Malalasekera (1995).

To account for the effects of small-scale motions of flow, Yakhot, Orszag, Thangman, Gatski, & Speziale, (1992) developed a new model by applying the Re-Normalization Group (RNG) method. This approach improves the k-ε model and enables the turbulent viscosity term to include contributions from turbulent diffusion at different scales. The mean strain is introduced to simplify the formulations:

$$S_{ij} = \frac{1}{2} \left(\frac{\partial U_i}{\partial x_j} + \frac{\partial U_j}{\partial x_i} \right)$$

Equation A.13

The RNG k-ε transport equation can be represented as (Yakhot et al., 1992; Versteeg & Malalasekera, 1995):

$$\frac{D(\rho k)}{Dt} = \frac{\partial}{\partial x_k} \left(\alpha_k \mu_{eff} \frac{\partial k}{\partial x_k} \right) + \tau_{ij} . S_{ij} - \rho \varepsilon$$

Equation A.14

$$\frac{D(\rho \varepsilon)}{Dt} = \frac{\partial}{\partial x_k} \left(\alpha_\varepsilon \mu_{eff} \frac{\partial k}{\partial x_k} \right) + C_1^* \frac{\varepsilon}{k} \tau_{ij} . S_{ij} - \rho C_2 \frac{\varepsilon^2}{k}$$

Equation A.15

where effective viscosity, μ_{eff}, is the sum of turbulent viscosity and laminar viscosity:

$$\mu_{eff} = \mu + \mu_t$$

Equation A.16

and C_1^* is calculated as:

$$C_1^* = C_1 - \frac{\eta \left(1 - \frac{\eta}{\eta_o} \right)}{1 + \beta \eta^3}$$

Equation A.17

where

$$\eta = \frac{k}{\varepsilon} \sqrt{2 S_{ij} S_{ij}}$$

Equation A.18

Imperial constants are defined in Table A.2.

Table A.2: Constants for the RNG k-ε model.

C_μ	$\alpha_k = \alpha_\varepsilon$	C_1	C_2	η_0	β
0.0845	1.39	1.42	1.68	4.377	0.012